THE THERMODYNAMICS OF IONIC AMPHIPHILE-WATER SYSTEMS, A THEORETICAL ANALYSIS

Bengt Jönsson

Lund 1981

THE THERMODYNAMICS OF IONIC AMPHIPHILE-WATER SYSTEMS.

A THEORETICAL ANALYSIS.

BENGT JÖNSSON
FIL. KAND., HELSINGKRONA NATION

AVHANDLING FÖR TEKNOLOGIE DOKTORSEXAMEN

AVHANDLINGEN KOMMER ATT FÖRSVARAS VID EN OFFENTLIG DISPUTATION I SAL D, KEMICENTRUM, LUND LÖRDAGEN DEN 16 MAJ 1981, KL. 10.15

THE THERMODYNAMICS OF IONIC AMPHIPHILE-WATER SYSTEMS, A THEORETICAL ANALYSIS

BY

BENGT JÖNSSON
DEPARTMENT OF PHYSICAL CHEMSITRY 2
CHEMICAL CENTER, P.O.B. 740
S-220 07 LUND 7, SWEDEN

LUND 1981

UNIV.
LEIDEN
BIBL.

Organization
LUND UNIVERSITY
Department of Physical Chemistry 2
Chemical Center, P.O.B. 740
S-220 07 Lund 7
SWEDEN

Document name
DOCTORAL DISSERTATION
Date of issue
25/4 1981
CODEN:

Author(s)
Bengt Jönsson

Sponsoring organization

Title and subtitle

THE THERMODYNAMICS OF IONIC AMPHIPHILE - WATER SYSTEMS, A THEORETICAL ANALYSIS.

Abstract

A thermodynamic model of the amphiphile association behaviour in ionic amphiphile-water systems is presented. The treatment is based on model expressions for the free energy contributions. The contributions are 1. a hydrophobic energy 2. a surface free energy of the aggregates 3. an electrostatic free energy 4. an entropy of mixing for the micellar aggregates and 5. an energy that limits the aggregate size in at least one dimension to the length of an extended amphiphile molecule. In particular the electrostatic contributions are treated in detail using both the Poisson-Boltzmann equation and a modified Poisson-Boltzmann equation where the effect of the pair correlation between the mobile ions is included. From the expression of the free energy the chemical potentials of the different components are determined by calculating $(\partial G/\partial b)$ directly. The calculations are restricted to three aggregate geometries: spheres as in normal and reversed micellar solutions, infinite cylinders as in normal and reversed hexagonal phases and lamellae as in lamellar liquid crystalline phases. For each type of aggregate the optimal aggregate dimensions is determined by requiring that $(\partial G/\partial b)=0$. By using the expression for the chemical potentials, the stability regions of the different phases, including two and three phase regions, are determined for several soaps.

Key words

Classification system and/or index terms (if any)

Supplementary bibliographical information

Language
English

ISSN and key title

ISBN

Recipient's notes

Number of pages
118

Price

Security classification

DOKUMENTDATABLAD enl SIS 61 41 21

Distribution by (name and address)
Bengt Jönsson, Department of Physical Chemistry 2, Chemical Center, P.O.B. 740, S-220 07 Lund 7, Sweden

I, the undersigned, being the copyright owner of the abstract of the above-mentioned dissertation, hereby grant to all reference sources permission to publish and disseminate the abstract of the above-mentioned dissertation.

Signature Bengt Jönsson Date 12/3 1981

TABLE OF CONTENTS

1. INTRODUCTION 1

2. IONIC AMPHIPHILE-WATER SYSTEMS 3

3. THERMODYNAMIC MODEL 7
   3.1 Subsystems 7
   3.2 Gibbs´free energy for a subsystem 9
   3.3 The hydrophobic interaction 11
   3.4 The interfacial energy 13
   3.5 The constraint that no charged groups or water molecules are located in the interior of the aggregates 14
   3.6 The electrostatic free energy 18
   3.7 Dispersion forces 24
   3.8 The free energy of an ionic amphiphile-water system 25

4. THE POISSON-BOLTZMANN EQUATION 27

5. CHEMICAL POTENTIALS 30

6. ION DISTRIBUTIONS 38

7. NUMERICAL SOLUTIONS OF THE POISSON-BOLTZMANN EQUATION 47

8. AGGREGATE SIZE 51

9. PHASE EQUILIBRIA 62

10. MULTICOMPONENT SYSTEMS 69

11. SYSTEMS OF THE REVERSED TYPE 81

CONCLUDING REFLECTIONS 87

REFERENCES 88

Digitized by the Internet Archive
in 2026

https://archive.org/details/IA41553424_0015

APPENDIX

Appendix I: The contribution to the free energy from the pair correlation between the ions.

Appendix II: Calculus of variations.

Appendix III: Energy calculations for normal systems.

Appendix IV: The solution to the Poisson-Boltzmann equation for a system with cylindrical symmetry and no salt present.

Appendix V: Energy calculations for reversed systems.

Appendix VI: The solution to the Poisson-Boltzmann equation for the reversed cylindrical system, when no salt is present.

1. INTRODUCTION

The main purpose of this work is to present a thermodynamic model for the description of the amphiphile association behaviour in ionic amphiphile-water systems. The treatment is based on model expressions for the main contributions to the systems free energy G, because a full description of the molecular interactions in an ionic amphiphile-water system is at present not feasible.

To pick out the dominating contributions to the free energy G is of course very difficult; it is important to have as few contributions as possible, to be able to work with the total expression for the free energy G, and at the same time not to simplify the model so much that it can't describe the system.

The properties that the model shall describe are

1. The association process of amphiphilic molecules to micellar aggregates and at higher amphiphile concentrations to lyotropic liquid crystalline phases.

2. The chemical potentials of the components.

3. The aggregate dimensions.

4. The composition in different parts of the system.

The calculations will in some parts be rather involved because of the complexity of the systems and I will therefore present the work in such a way that the theory is an independent part where no experimental tests of the equations occur, all the tests are in the later chapters.

Here follows a short description of the main parts of the work:

1. A short summary of experimental observations from different ionic amphiphile-water systems.

2. The contributions to the free energy within the model.

3. The Poisson-Boltzmann equation.

4. Differentiation of G to obtain expressions for the chemical potentials.

5. Ion distributions in amphiphilic systems calculated from the thermodynamic model.

6. Aggregate sizes.

7. Phase equilibria in two component-systems.

8. Multicomponent systems.

9. Reversed systems.

2. IONIC AMPHIPHILE-WATER SYSTEMS

Amphiphilic substances have one hydrophobic part (for instance a hydrocarbon chain) and one hydrophilic part (a polar, for example a charged group).

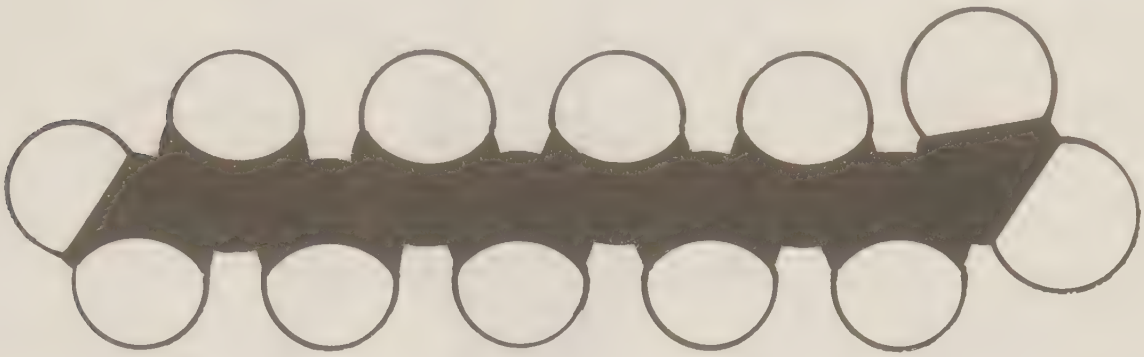

Figure 1. Space filling molecular model of decanoate.

The association of amphiphilic molecules in an aqueous medium typically occurs in a stepwise manner as the amphiphile concentration is increased. In a sufficiently dilute solution there are only surfactant monomers. As the concentration is increased these often associate to form micellar aggregates which still exist in an isotropic solution.

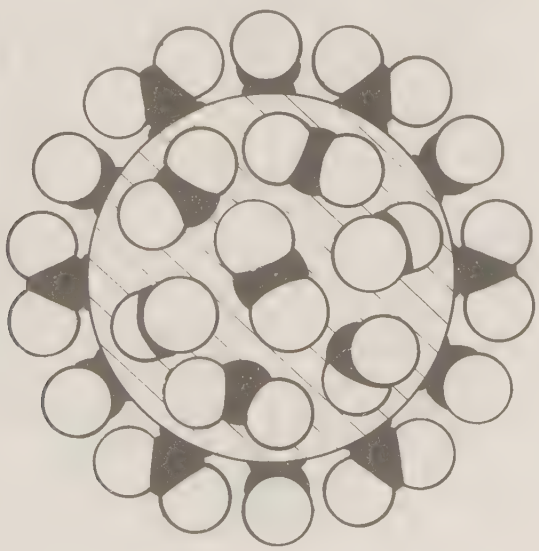

Figure 2. Schematic representation of a spherical micell.

At still higher amphiphile concentrations lyotropic liquid crystalline phases are formed. For simple soaps the phase formed first is the normal hexagonal phase, consisting of cylindrical aggregates packed in an hexagonal array.

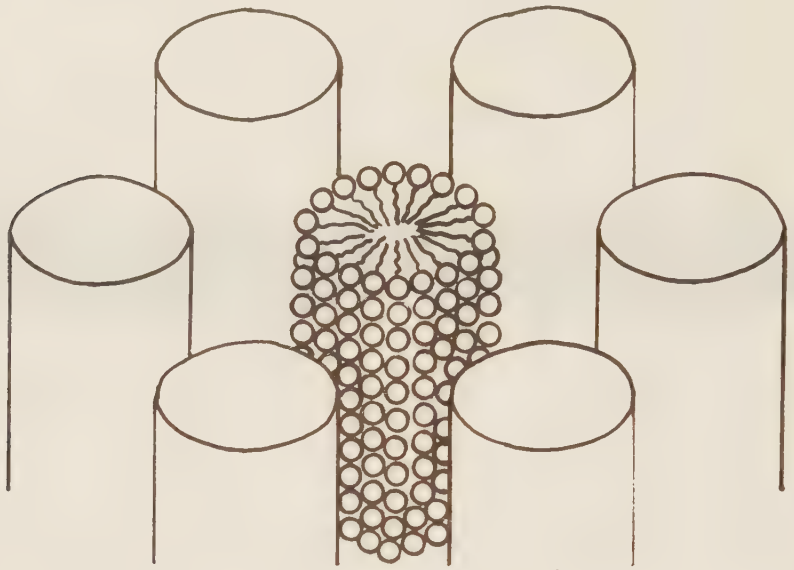

Figure 3. Schematic representation of a hexagonal mesophase.

At very high amphiphile concentrations a lamellar phase can appear.

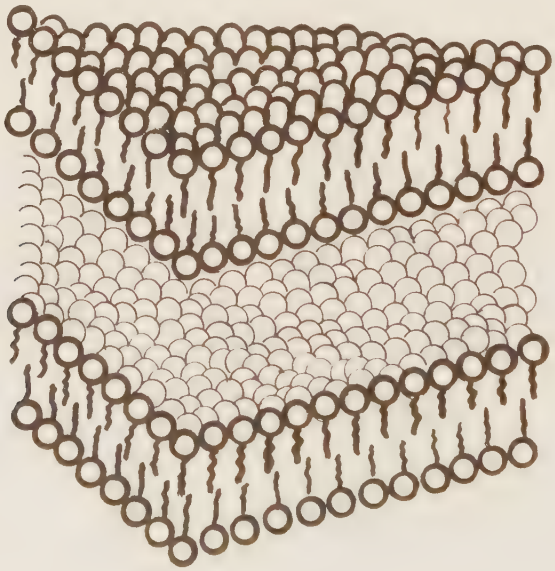

Figure 4. Schematic representation of a lamellar mesophase.

When a third, weakly polar compound is added to the system the phase behaviour becomes even more complex. At high concentrations of this third component the reversed phases appear. The reversed hexagonal phase

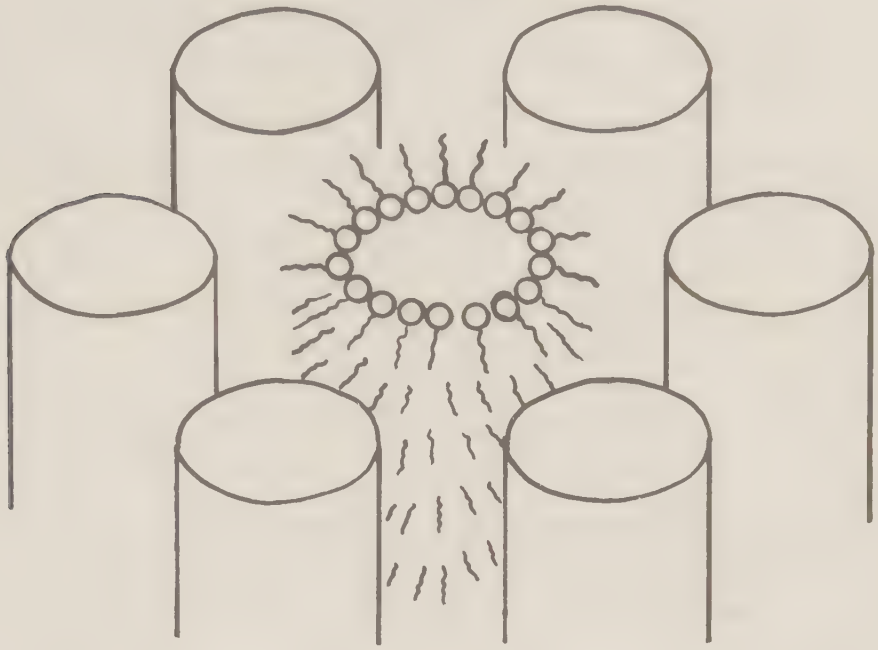

Figure 5. Schematic representation of the reversed hexagonal mesophase.

and the reversed micellar phase.

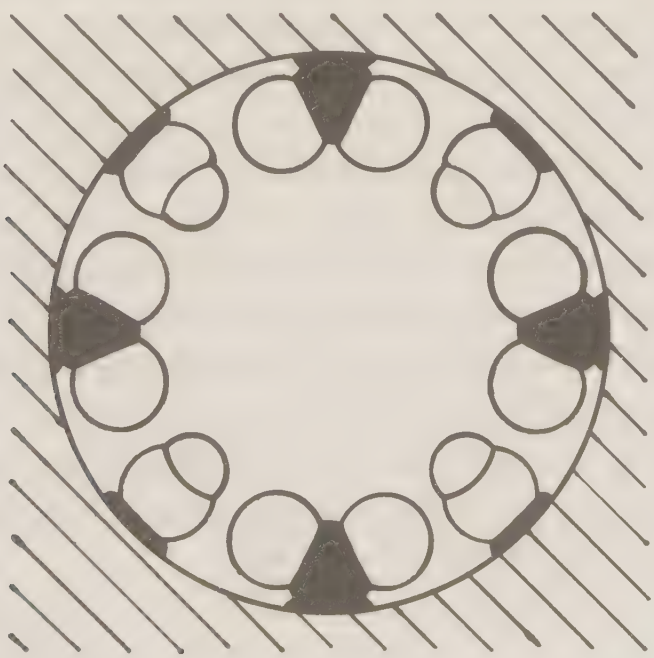

Figure 6. Schematic representation of a reversed micelle.

A number of other phase structures such as cubic phases can also be formed. For reviews of phase diagrams in amphiphile-water sytems, see refs. (1-4).

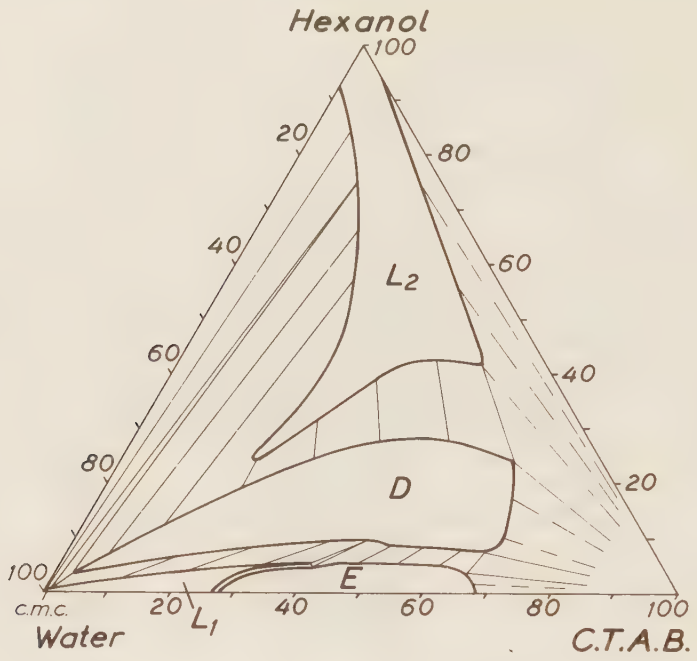

Figure 7. The ternary system water-cetyltrimethylammonium bromid (CTAB) -hexanol. From the work by Ekwall et al. (56).

The diversity of the phase behaviour and thus of the preferred aggregate structure is in sharp contrast to the variations in molecular properties. As a rule these change very little with composition (5-9). Apparently the local molecular environment is rather independent of aggregate shape and/or phase structure. This shows that there is a strong similarity between the different phases and that the formation of micelles is only a first step in a continuing association process (10-11). It also indicates that the changes in the stability of different phase structures for a given amphiphile is not primarily caused by changes in local molecular properties but rather in interactions associated with the aggregates themselves.

In later chapters the variation of structural and thermodynamic parameters in different systems is further discussed and experimental values is compared against theoretical calculations.

3. THERMODYNAMIC MODEL

3.1 SUBSYSTEMS

The association of amphiphilic molecules in an aqueous solution into aggregates leads to a distribution of aggregate dimensions.

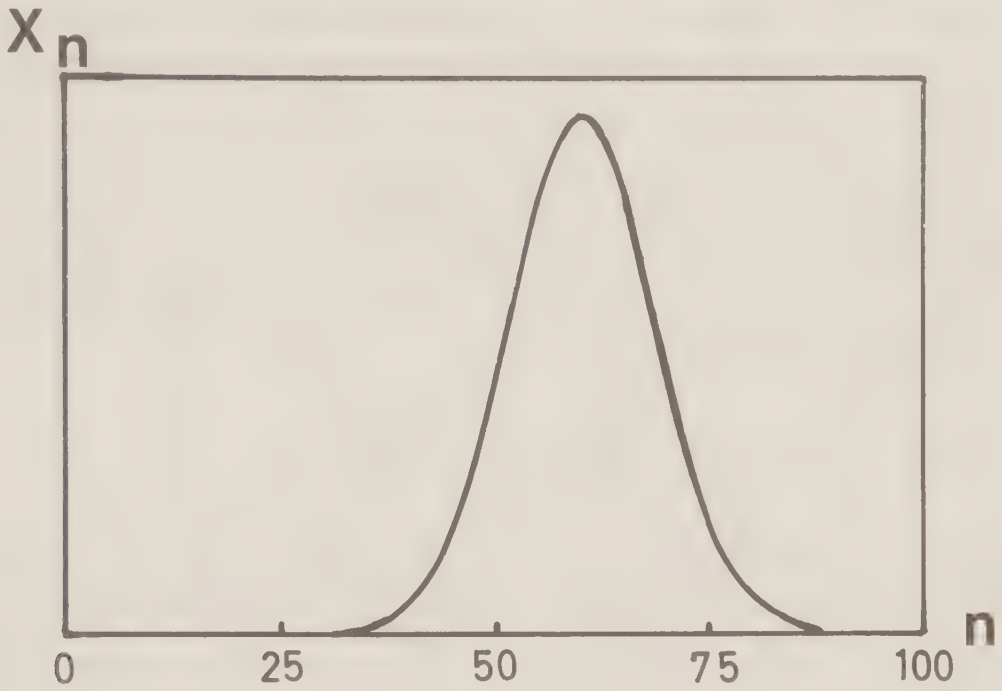

Figure 8. Schematic picture of the aggregate size distribution for dodecyl sulfate well above the CMC.

To simplify the calculations this distribution is ignored and it is assumed that all aggregates have the same dimensions. The calculations are also possible for a polydisperse system, see ref. (12).

The interactions between different aggregates are for the lyotropic liquid crystalline phases of such an order that an ordering of the aggregates are attained. It is therefore possible for these systems to divide the total system into a number of subsystems, all with the same dimensions (the cell model ref. (13)). The Gibbs free energy for such a system will be

$$G = N \cdot G_0 \qquad (1)$$

where N is the number of subsystems and G_0 is the free energy of a subsystem.

For micellar systems the cell model will cause problem, because the interactions between the micellar aggregates are not big enough to order the aggregates. This means that the division of the total system into subsystems can't be done in such an easy way as for the lyotropic liquid crystals. One way to overcome this trouble is to divide the total system into equivalent subsystems as before but to allow the aggregate to move in a part of the subsystem (free volume) see ref. (13). The size of this free volume will of course depend on the volumes of the aggregate and the subsystem as well as the strength of the interactions between the aggregates. To get an equation for the size of the free volume is of course very difficult but when the micelle concentration is low or when the aggregate interactions are small the free volume will be approximately the same as the cell volume. In that case there is ideal mixing and the Gibbs'free energy for the total system may be written

$$G = N \cdot G_0 + kT \cdot N \cdot (\ln X_m - 1) \qquad (2)$$

where k is the Boltzmann constant, T the absolute temperature and X_m the mole fraction of micelles in the solution. For simplicity eq. (2) will be used for all micelle concentrations. This is reasonable because the term $kT \ln(X_m-1)$ is much less than G_0 for high micelle concentrations and the introduced error will therefore not be disturbing.

Another simplification must also be introduced, namely the choice of cell geometries. The equations that will appear for the electrostatic contributions to the free energy can only be solved if one of the following five geometries is used.

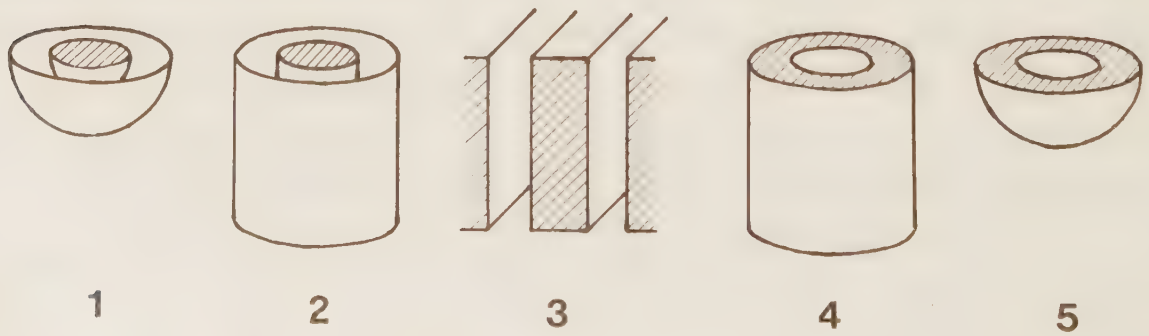

Figure 9. Schematic representation of five geometries: 1. spherical 2. cylindrical 3. lamellar 4. reversed cylindrical and 5. reversed spherical. Hatching represents the regions of nonpolar material.

With these geometries predestinated the choice of geometry that will represente the different phases must be the following

1. micellar systems (LI)
2. hexagonal systems (E)
3. lamellar systems (D)
4. reversed hexagonal systems (F)
5. reversed micellar systems (L2)

The designations in the brackets are the symbols used by Ekwall (2) to represent the different structures. Because the cubic phase (see fig. 10) can't be represented by any of the geometries in fig. 9 it will not appear in the following chapters.

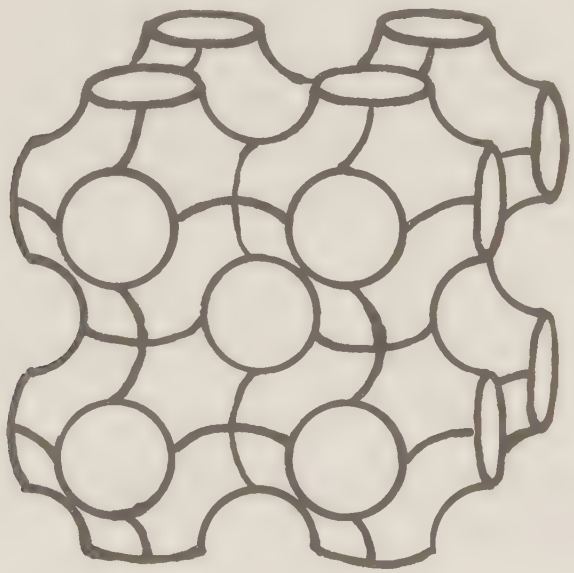

Figure 10. Proposed model for the cubic mesophase. The Schwarz´minimal surface model.

3.2 GIBBS´FREE ENERGY FOR A SUBSYSTEM

The problem of determining the free energy of an ionic amphiphile-water system was in the previous chapter simplified to the determination of the free energy of a subsystem and in this chapter this determination will be done. A full description of the molecular interactions in an ionic amphiphile-water subsystem is however at present not feasible. Instead one can make

use of the fact that the amphiphilic aggregates contain sufficiently many molecules so that the properties of the aggregates approach those of a macroscopic system, i.e. the effects of the complex molecular interactions can be described with a few parameters due to the averaging effects. It is then of great importance to note that the molecular properties are largely independent of the type of aggregate. This applies to the surfactant (5,7,9,14), to the solubilized molecules (15) and also to the counterions (6,16) and the water (17). It is also significant that the changes in partial molar enthalpies are small at phase boundaries (8,18).

On the basis of these observations the amphiphile-water system is characterized as having an apolar hydrocarbon region of fully fluid character (9,10,14), an aqueous region with the properties of a bulk aqueous solution (17,19) and an interface between these two regions. It is assumed that no water molecules or charged groups can be located in the interior of the aggregates (20,21). The counterions will reside entirely in the aqueous region, while the amphiphile is distributed between the aggregates and the aqueous region. Within this model the important contributions to the free energy of a subsystem are due to

1. A free energy difference between an uncharged amphiphile molecule in the aqueous medium and in the aggregate (the hydrophobic interaction $\Delta\mu^{o}_{am}$).

2. An interfacial energy due to the interface between the aggregates and the aqueous medium.

3. A constraint that no charged groups or water molecules are located in the interior of the aggregate.

4. Entropy contributions due to the ideal mixing of the components in the aqueous region.

5. An electrostatic free energy.

6. The van der Waals´interaction between the aggregates.

These contributions will in the following chapters be discussed one by one and equations for their dependence on different parameters will be obtained.

3.3 THE HYDROPHOBIC INTERACTION

The hydrophobic free energy may be defined as the difference between the standard chemical potentials of an apolar solute at infinite dilution in a hydrocarbon solvent μ^o_{HC} and in water μ^o_{aq} (see ref. (22)).

$$\mu^o_{HF} = \mu^o_{HC} - \mu^o_{aq} \tag{3}$$

The hydrophobic interaction has been extensively studied (23) especially for homologous series. In a majority of cases there is a constant increment of μ^o_{HF} in a homologous series. The increment is furthermore roughly independent of the functional group so that similar values apply to alcohols, carboxylic acids and pure hydrocarbons (24-26). Thus for an homologous series of compounds.

$$\mu^o_{HF} = (a - b \cdot n_c) \cdot kT \tag{4}$$

where a and b are constants and n_c is the number of carbon atoms. The value of a and b are tabulated for some compounds in table 1.

Table 1. Values of the constants a and b at 298 K from refs. (24-26).

Compounds	a	b
$CH_3(CH_2)_{n-2}CH_3$	- 4.11	1.49
$CH_3(CH_2)_{n-1}OH$	1.40	1.39
$CH_3(CH_2)_{n-2}COOH$	7.18	1.39

A further insight into the nature of the hydrophobic effect is obtained by separating the free energy into enthalpic and entropic parts.

$$\mu^o_{HF} = h^o_{HF} - T \cdot s^o_{HF} \tag{5}$$

A characteristic feature of the hydrophobic interaction is that it is dominated by entropy effects. Calorimetric measurements show that h^o_{HF} is close to zero at room temperature (ref. (27)). Ref. (28) found that for short alkyl chains

$$c_p^{HF} \simeq 90 \text{ J/mol}\cdot\text{K} \quad \text{per } CH_2\text{-group} \tag{6}$$

It was also concluded that c_p^{HF} seems independent of temperature.

The question is if these μ^o_{HF} values from calorimetric measurements may be used for $\Delta\mu^o_{am}$, although the motion of the hydrocarbon chains within the aggregates are restricted by the polar head at the surface of the aggregate? One way to answer the preceding question is to test critical micelle concentrations CMC against theoretical calculations where eq. 4 is used. This has been done by ref. (29). As seen in fig. 11 there is indeed a linear relation between $\Delta\mu^o_{am}$ and n_c. The slope of the line is -1.31 kT (29), a value rather close to the values in table 1.

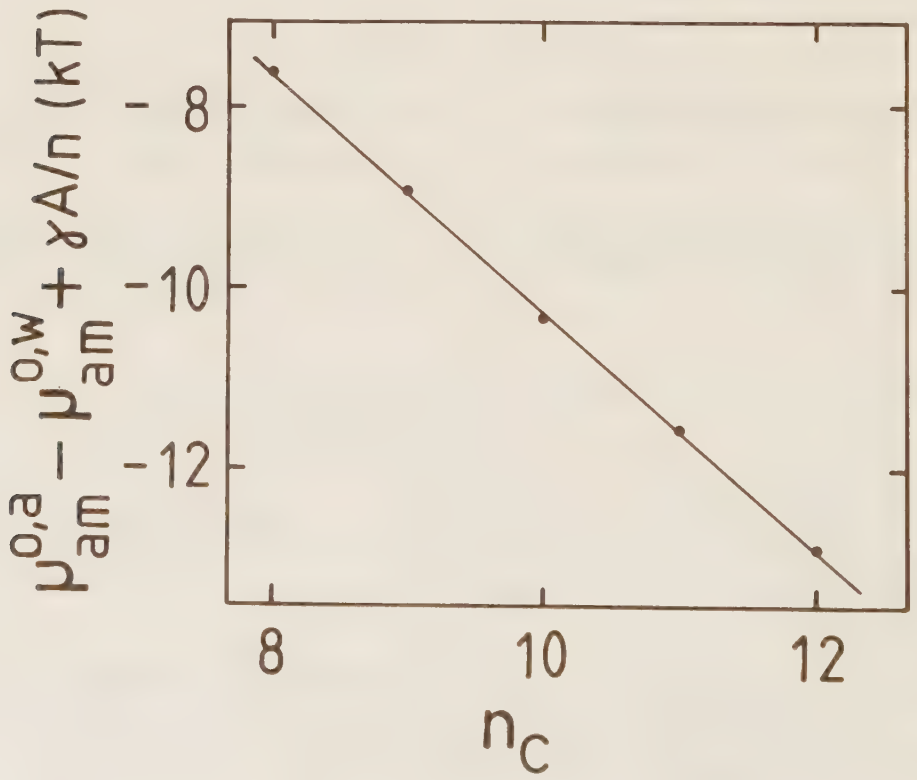

Figure 11. Calculated $\Delta\mu^o_{am}$ values for n-alkyl sulfates plotted versus alkyl chain length, from ref. (29).

3.4 THE INTERFACIAL ENERGY

A complete removal of all contact between the alkyl chains and the water is not achieved when an amphiphilic molecule is placed in an aggregate. To be able to account for these effects an energy G_s, proportional to the surface area of the aggregate, is introduced.

$$G_s = \gamma \cdot A \tag{7}$$

where γ is a proportionality constant and A is the area of the aggregates.

The reason why G_s can be written as γA and not as $\gamma(A-n_a \cdot A_p)$, where $n_a \cdot A_p$ is the area of the hydrophilic heads on the amphiphile molecules, is that the term γA_p is a constant and may be added to the standard chemical potential μ_a^o of an amphiphilic molecule in an aggregate.

If the molecules in the aggregate had been pure aliphatic hydrocarbons the value of γ had been around $50 \cdot 10^{-3}$ J/m^2 ($51 \cdot 10^{-3}$ J/m^2 is the interfacial tension between water and octane according to ref. (30)). There are at least two important differences between an octane-water interface and an amphiphile-water interface.

1. The lateral mobility of the hydrophilic groups at the surface are often strongly reduced by their mutual interactions.

2. The mobility of the hydrocarbon chains in the interior of the aggregate will be affected by the fact that the headgroups are anchored at the surface.

which means that it would not be surprising if the amphiphile-water value is quite different from the octane-water value.

Another important question is if the γ value is dependent on parameters as the aggregate dimensions or the aggregate geometry.

The only possibility to answer these questions is to test the assumed G_s dependence (eq. (7)) against experimental values. This is done in chapter 8 where the γ value is further discussed. Concerning the definition of the surface area see the next chapter.

3.5 THE CONSTRAINT THAT NO CHARGED GROUPS OR WATER MOLECULES ARE LOCATED IN THE INTERIOR OF THE AGGREGATES

It is from an energy point of view very unfavourable to take a charge from a medium with high to one with low dielectric constant. The difference in energy for an ion with the charge e and radius a in two media with dielectric constants ε_{r1} and ε_{r2} is

$$\Delta E = \frac{e^2}{8\pi \cdot \varepsilon_o \cdot a} \left(\frac{1}{\varepsilon_{r1}} - \frac{1}{\varepsilon_{r2}} \right) \qquad (8)$$

where ε_o is the permittivity of vacuum. Typical values for an ion in a water respectively a hydrocarbon medium: ε_r(water) $\simeq$ 80, ε_r(hydrocarbon) $\simeq$ 3, the radius of the ion a = 2 Å and the temperature T = 298 K, gives $\Delta E \simeq 45$ kT.

Recent studies (31, 32) of partial molar volumes and partial molar compressibilities give very good evidence for the absence of any appreciable water penetration into the micelles.

What is then the interior of an aggregate, how much of for example a micelle shall be counted to the interior? From a dynamic point of view there is always a dynamic protrusion of methylene groups from the hydrocarbon core (33) which meansthat the aggregate surface always is very rough and can only be defined as a mean value. The contact between the alkyl chain and the water certainly varies from system to system but may typically be around 50 % or less for the α-CH_2 group and below 20 % for the β-CH_2. It diminishes then rapidly as one moves away from the polar head (20).

Different surfaces have in this and in the preceding chapters been defined (surface of tension, surface of hydrophobic core) and in the following chapters the surface of charges and surface of closest approach for the counterions will be defined.

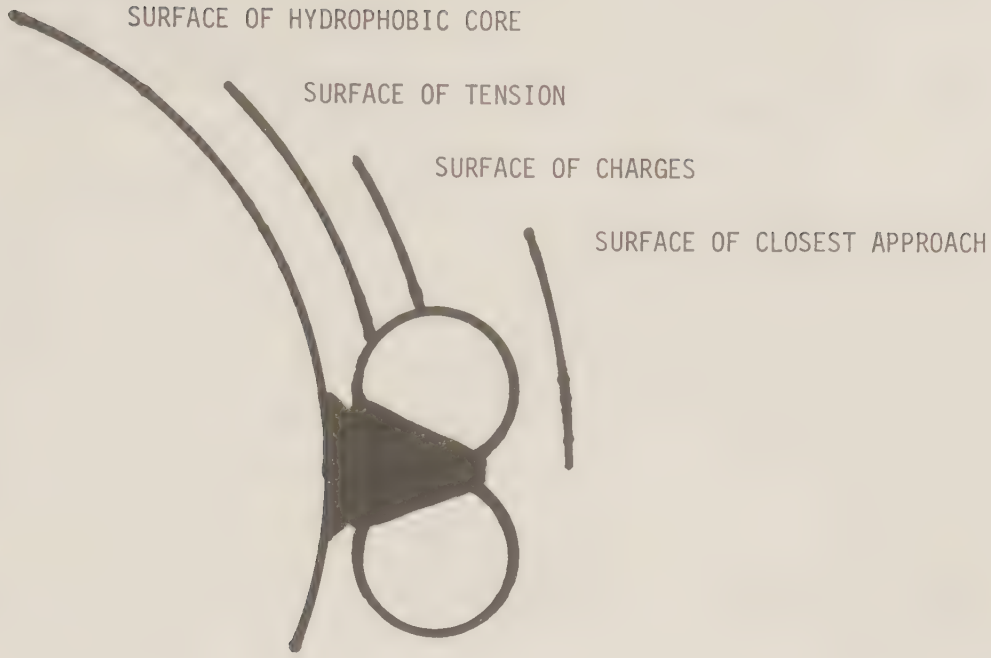

Figure 12. Schematic representation of the location of the different interfaces.

To get as simple calculations as possible all these surfaces have been merged into one, the mean charge surface, which is defined as the surface characterized by the mean distribution of the charges on the aggregate. This will of course introduce errors in the calculations but they will probably not be important since the difference between the different surfaces is often small.

The volume enclosed by the aggregate surface may be written

$$V = \sum_i n_i \cdot V_i \qquad (9)$$

where the sum is over all types of molecules in the aggregate, n_i is the number of and V_i is the volume of molecule i.

For simplicity the V_i-values are assumed to be independent of the dimensions and geometry of the aggregate. The reason for this is that the differences in V_i between different aggregate geometries are rather small (34). It has been shown from experiments (35) that V_i may be written in the form of eq. 10 for molecules containing one alkyl chain.

$$V_i = V(CH_3) + n \cdot V(CH_2) + V(x) \qquad (10)$$

where n is the number of CH_2-groups and x stands for -OH, COO^- or $-CH_3$. At 25 ^oC the values of the group contributions are

Table 2. Group contributions to the volume of an amphiphile molecule at 298 K.

$V(CH_3)$	=	49 $Å^3$
$V(CH_2)$	=	28 $Å^3$
V(-OH)	=	17 $Å^3$
$V(-COO^-)$	=	35 $Å^3$

The three first values are approximatively the same as the values used by (35-36). The $V(-COO^-)$ value has been calculated according to fig. 13.

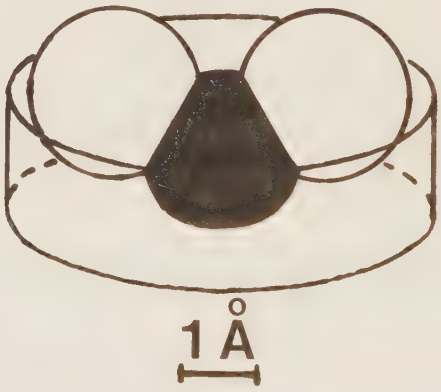

Figure 13. Model used to calculate the volume of a $-COO^-$ group.

The choice of the V(-OH) and $V(-COO^-)$ values can of course be criticized, but the total volume of an amphiphile molecule is often much bigger than V(x) so the errors introduced with the V(-OH) and $V(-COO^-)$ values can be

neglected. To be able to calculate molecular volumes at other temperatures than 25 ^{o}C the following expressions from the temperature dependences for liquid hydrocarbons was used (30).

$$V_i(T) = V_i(298) \cdot (1 + 8 \cdot 10^{-4} \cdot (T - 298)) \qquad (11)$$

The constraint that no charged groups are allowed to be in the interior of an aggregate prevents the aggregates from growing without limit in all directions. The parameter b characterizing the aggregate size (see fig. 12) is thus limited to a maximum value b_{max} which is assumed to be the length of a fully extended amphiphile molecule.

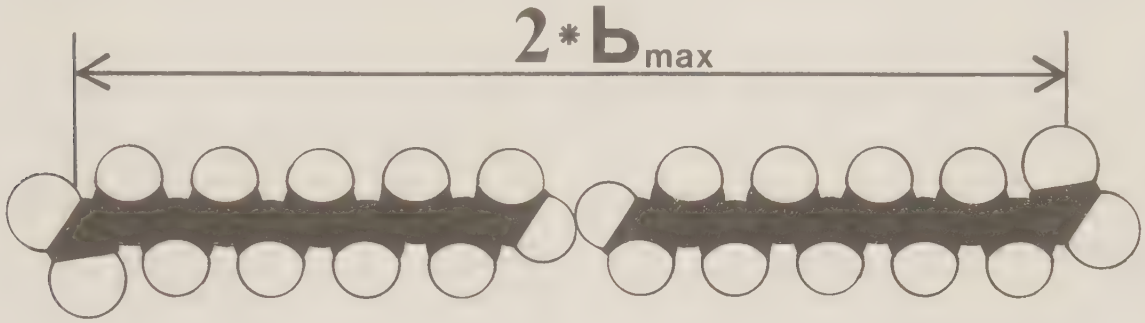

Figure 14. Schematic representation of a lamellar system where b is equal to b_{max}.

Expressed in terms of a free energy there is a contribution G_c such that

$$\begin{aligned} G_c &= 0 \qquad & b \leq b_{max} \\ G_c &= \infty \qquad & b > b_{max} \end{aligned} \qquad (12)$$

The assumption of a step-function behaviour of G_c is of course an idealization and the transition should be smooth in a more realistic model.

3.6 THE ELECTROSTATIC FREE ENERGY

To permit the electrostatic interactions to be treated in a simple way it is assumed that the solvent, water in this case, may be represented by a continuous medium of uniform dielectric constant ε_r. It is in this model possible to calculate the partition function Z only referring to the energy of the ion-ion interactions.

$$Z = \int \ldots \int e^{-U_{el}/kT} \, d\vec{r}_1 \ldots d\vec{r}_N \tag{13}$$

where

$$U_{el} = \frac{1}{2} \cdot \frac{1}{4\pi \cdot \varepsilon_o \varepsilon_r} \cdot \sum_{\substack{ij \\ i \neq j}} \frac{q_i q_j}{|\vec{r}_i - \vec{r}_j|} \tag{14}$$

Helmholtz´electrostatic free energy A_{el} may then be calculated from Z according to

$$A_{el} = - kT \ln Z \tag{15}$$

Gibbs´electrostatic free energy may also be calculated because

$$G_{el} = A_{el} + P \cdot \Delta V_{el} \tag{16}$$

where ΔV_{el} is the volume change during the charging process. To simplify the calculations it is assumed that $P \cdot \Delta V_{el}$ is so small that it may be neglected and eq. (16) becomes

$$G_{el} \simeq A_{el} \tag{17}$$

It is important to point out that the mean value $\langle U_{el} \rangle$ only constitutes a part of the electrostatic energy E. This is due to the representation of the water as a continuous medium of dielectric constant ε_r. The connection between E and $\langle U_{el} \rangle$ may according to ref. (37) be written

$$E = \langle U_{el} \rangle \cdot \left(1 + \frac{T}{\varepsilon_r} \cdot \frac{d\varepsilon_r}{dT}\right) \tag{18}$$

The entropy change associated with the charging process can now also be calculated, because

$$A_{el} = E - TS \tag{19}$$

and if Z is known then A_{el} can be calculated from eq. (15). To obtain an analytic equation that describes the partition function Z´s dependence of parameters as temperature, ion concentrations and cell dimensions is at present not possible. An approximative solution to the problem is therefore presented below, but it is of course always difficult to estimate the errors made in such approximations. The only guidance is to test the obtained results against experiments and this is done in later chapters.

The definition of the electrostatic potential in the point r_j from all ions except ion j located in r_j is

$$\Psi_j(r_j) = \frac{1}{4\pi \cdot \varepsilon_o \varepsilon_r} \cdot \sum_{i \neq j} \frac{q_i}{|\vec{r}_i - \vec{r}_j|} \tag{20}$$

U_{el} may be expressed as

$$U_{el} = \frac{1}{2} \cdot \sum_j q_j \Psi_j(r_j) \tag{21}$$

From the canonical ensemble average of $\Psi_j(r_j)$

$$\langle \Psi_j \rangle = \frac{\int \ldots \int \Psi_j(r_j) \cdot e^{-U_{el}/kT} \, d\vec{r}_1 \ldots d\vec{r}_N}{\int \ldots \int e^{-U_{el}/kT} \, d\vec{r}_1 \ldots d\vec{r}_N} \tag{22}$$

the following equation can be obtained

$$\left(\frac{\partial A_{el}}{\partial q_j}\right)_{VT} = \langle \Psi_j \rangle_{\text{all } j} \tag{23}$$

and the total differential of A_{el} becomes

$$dA_{el} = \sum_j \langle \Psi_j \rangle \cdot dq_j \qquad (24)$$

Equation (24) is the starting-point when calculating free energies in homogeneous ion systems but offers often difficulties when used in inhomogeneous systems. The proceeding calculations are therefore performed in a slightly different manner. Instead of a straight forward charging process it is assumed that a hypothetic two step process is taking place, that begins with an uncharged system and ends in a charged system.

1. In the first step the system is anticipated to be uncharged. The uncharged molecules is however affected by a hypothetic force in such a way that the average concentration of the different components will be the same as in the charged system. The pair correlation function between the uncharged ions is constant and equals unity during this first step. The free energy change in this process may be written

$$A_1 = W + N_A \cdot kT \cdot \sum_i \int c_i \left(\ln \frac{c_i(r)}{c_o} - \ln \frac{\overline{c_i}}{c_o} \right) dV \qquad (25)$$

where W is the energy from the interactions between the uncharged ions and the hypothetic force. In eq. (25) it is also assumed that water is present in excess in the aqueous region and the total concentration c_o is in that case approximately constant (55 M). $\overline{c_i}$ is the average concentration of component i, N_A is Avogadros number.

2. The system will in step two become charged but in the same time as the charges of the ions increase, the strength of the hypothetic force diminishes in such a way that the average concentration will remain the same during the whole charging process. The free energy change during this process may be obtained from a modified eq. (24)

$$dA_2 = \sum_j \langle \Psi_j - V_j \rangle dq_j \qquad (26)$$

where V_j is the potential of the hypothetic force and the negative sign comes from the fact that the strength of the force diminishes when the charge increases. Because the average concentrations are the same during this step the free energy change owing to the removal

of the hypothetic force becomes

$$\sum_j \int_0^1 \langle - V_j \rangle q_j \, d\lambda = - W \tag{27}$$

where λ is a charging parameter.

$$dq_j = q_j \cdot d\lambda \qquad 0 \leq \lambda \leq 1 \tag{28}$$

Ψ_j may then be divided into two parts according to

$$\Phi(r) = \langle \Psi(r) \rangle \tag{29}$$

$$\hat{\Psi}_j(r_j) = \Psi_j(r_j) - \Phi(r_j) \tag{30}$$

and the change in the free energy during the charging process becomes

$$A_2 = - W + \frac{1}{2} \cdot \int \rho(r) \cdot \Phi(r) \cdot dV + \sum_j q_j \int_0^1 \langle \hat{\Psi}_j \rangle \, d\lambda \tag{31}$$

where $\rho(r)$ is the charge density at r. The summation in eq. (31) may also be written as an integral

$$\sum_j q_j \int_0^1 \langle \hat{\Psi}_j(\lambda) \rangle \, d\lambda = \int \rho(r_j) \int_0^1 \langle \hat{\Psi}_j(\lambda) \rangle \, d\lambda \, dV \tag{32}$$

The free energy of process 1. and 2. becomes

$$A_{el} = N_A \, kT \sum_j \int c_j \left(\ln \frac{c_j(r)}{c_o} - \ln \frac{\overline{c_j}}{c_o} \right) dV + \frac{1}{2} \cdot \int \rho(r) \, \Phi(r) \, dV +$$

$$+ \int \rho(r_j) \int_0^1 \langle \hat{\Psi}_j(\lambda) \rangle \, d\lambda \, dV \tag{33}$$

The problem that remains is to calculate $\langle \hat{\Psi}_j(\lambda) \rangle$, but this can only be done in an approximative way. Here follows the calculations.

Let $\langle \Psi(r, r_j) \rangle$ be the canonical average of $\Psi(r)$, keeping one particle, in this case j, fixed at r_j. If the same procedure is done with $\hat{\Psi}$ the result becomes

$$< \hat{\Psi}(r,r_j) > = < \Psi(r,r_j) > - \Phi(r) \tag{34}$$

Taking the Laplacian of both sides of eq. (34) with respect to the variable r gives

$$\nabla^2 < \hat{\Psi}(r,r_j) > = - \frac{1}{\varepsilon_o \varepsilon_r} \{< \rho(r,r_j) > - < \rho(r) >\} \tag{35}$$

The Poisson equation has here been used to evaluate $\nabla^2 \cdot \Psi(r,r_j)$ and $\nabla^2 \cdot \Phi(r)$.

$$\nabla^2 \cdot \Psi(r,r_j) = - \frac{\rho(r,r_j)}{\varepsilon_o \varepsilon_r} \tag{36}$$

and

$$\nabla^2 \cdot \Phi(r) = - \frac{\rho(r)}{\varepsilon_o \varepsilon_r} \tag{37}$$

But $< \rho(r,r_j) >$ may be written in terms of distribution functions according to

$$< \rho(r,r_j) > = \sum_i N_A \cdot e \cdot z_i \cdot c_i \cdot g_{ij}(r,r_j) \tag{38}$$

and equation (35) becomes

$$\nabla^2 (< \hat{\Psi}(r,r_j) >) = - \frac{\sum_i N_A \cdot e \cdot z_i \cdot c_i}{\varepsilon_o \varepsilon_r} \{g_{ij}(r,r_j) - 1\} \tag{39}$$

g_{ij} may as an approxiamtion be written

$$g_{ij}(r,r_j) = \exp\{- q_i < \hat{\Psi}(r,r_j) > / kT\} \tag{40}$$

It is also assumed that $< \hat{\Psi}(r,r_j) >$ only depends on $|r - r_j|$ and that $c_i(r)$ can be replaced by $c_i(r_j)$. These approximations are reasonable if $g_{ij}(r,r_j)$ differs from one only in the vicinity of r_j. Equation (39) will now become

$$\frac{1}{x^2}\,\frac{d}{dx}(x^2 \cdot \hat{\Psi}(x)) = -\sum_i \frac{N_A \cdot e \cdot z_i \cdot c_i(r_j)}{\varepsilon_o \varepsilon_r} \{e^{-q_i \cdot \hat{\Psi}(x)/kT} - 1\} \qquad (41)$$

where $x = |r - r_j|$ and $\hat{\Psi}(x) = < \hat{\Psi}(x) >$.

If the exponentials are linearized the differential equation, eq. (41), will have the same form as the Debye-Hückel equation and $< \hat{\Psi}_j(r_j,r_j) >$ may then be written

$$< \hat{\Psi}_j(r_j,r_j) > = - \frac{q_j \cdot \kappa}{4\pi \cdot \varepsilon_o \varepsilon_r} \qquad (42)$$

where

$$\kappa^2 = \frac{\sum_i N_A \cdot e^2 \cdot z_i^2 \cdot c_i(r_j)}{\varepsilon_o \varepsilon_r \cdot kT} \qquad (43)$$

The last expression in the right in eq. (33) becomes

$$\int \rho(r_j) \int_0^1 < \hat{\Psi}_j(\lambda) > d\lambda \, dV = - \frac{kT}{12\pi} \int \kappa^3 \, dV = N_A \int f \, dV \qquad (44)$$

Concerning the calculations leading to equations (42) and (44) see appendix I.

E_{el}-TS, the electrostatic free energy plus the entropy from the ideal mixing of the components in the uncharged system, may now be calculated from equations (33) and (44).

$$E_{el} - TS = \frac{A}{2} \sigma \Phi_A + N_A \int \sum_i \{\frac{z_i e}{2} \cdot c_i \cdot \Phi + kT \cdot c_i \cdot (\ln \frac{c_i}{c_o} - 1)\} + f \, dV \qquad (45)$$

where f can be obtained from eq. (44) if the ion concentration is low. σ is the surface charge density of the aggregate and Φ_A is the potential at the surface. It is also possible to get a simple approximative expression for f if the ions in the aqueous part all have the same charge (see appendix I). If the concentration is in the range $0 \leq c \cdot z^6 \leq 20$ and the temperature is 298 K the approximative formula becomes

$$f = - 0.44 \cdot kT \cdot c^{1.42} \cdot z^{2.52} \qquad (46)$$

Approximative formulae can also be made for other temperatures and other concentration ranges, see appendix I.

3.7 DISPERSION FORCES

The dispersion interactions between macroscopic bodies may be treated in a rather exact way by the Lifshitz theory (ref. (38)). These calculations are often rather involved but if the retardation effects, coming from the finite velocity of light, can be omitted a much less cumbersome expression for the interaction energy can be obtained by summing allowed mode frequencies on the surfaces of the bodies. In ref. (39) such calculations are found for different geometries and distances between the bodies. Here only some comments about the simple case of two infinite plates of material 1. separated by a medium 2.

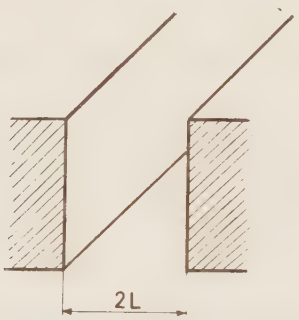

Figure 15. Schematic representation of two hydrocarbon plates separated by a water layer.

As an approximation, the free energy from the dispersion forces for such a system may be written

$$F = - A \cdot K/L^2 \qquad (47)$$

where A is the area of the two surfaces and K a constant depending on the composition in the different parts. K is in the hydrocarbon-water case $\simeq$ $\simeq 6.9 \cdot 10^{-23}$ J (ref. (39)) if L is less then 20 Å. If L = 10 Å, F calculated from (47) becomes

$$F = - 6.9 \cdot 10^{-5} \cdot A \quad (J) \tag{48}$$

This energy is at least one order of magnitude less than the electrostatic or surface energies per surface area in typical ionic amphiphile-water systems. It is therefore only in low-charged systems or systems with high salt concentrations that this type of energy will be important, which justifies the omission of the dispersion energy in the further calculations.

3.8 THE FREE ENERGY OF AN IONIC AMPHIPHILE - WATER SYSTEM

The different energy contributions have been obtained in the preceding chapters and they will here be put together to obtain an equation for the free energy of an ionic amphiphile-water system.

$$G = n_a \cdot \mu_a^o + n_{H_2O} \cdot \mu_{H_2O}^o + \sum_i n_i^w \cdot \mu_i^{ow} + \gamma \cdot A + A_{el} + kT \cdot \sum_i n_i^w (\ln \bar{c}_i - 1) +$$

$$+ N \cdot kT \cdot (\ln X_m - 1) \tag{49}$$

where N and n_i is the number of aggregates resp. component i and X_m is the mole fraction of aggregates. The summation is over all species in the aqueous part except water. Using the value of E_{el}-TS from eq. (45) equation (49) becomes

$$G = n_a \cdot \mu_a^o + n_{H_2O} \cdot \mu_{H_2O}^o + \sum_i n_i \cdot \mu_i^o + \gamma \cdot A + \frac{1}{2} \cdot \sigma \cdot \Phi_A \cdot A +$$

$$+ N_A \int \sum_i \{\frac{z_i e}{2} c_i \cdot \Phi + kT \cdot c_i \cdot (\ln c_i - 1)\} + f \, dV \tag{50 a}$$

where

$$\mu_i^o = \mu_i^{ow} - kT \cdot \ln c_o \tag{50 b}$$

Equation (50) will in the following chapters be used to characterize ionic amphiphile-water systems and it is therefore important to emphasize that the assumption that the free energy of the amphiphile molecules in an aggregate is described by $n_a \cdot \mu_a^o + \gamma A$ independently of the form and dimension of the aggregates is a very crude model. On the other hand if an improved

model of the aggregate energy can be obtained it can easily be incorporated into the model, but at present the experimental knowledge about aggregate energies is too small to base an improved model on. If there are more than one component in the aggregates, energy terms from mixing of the components in the hydrophobic part must be added to eq. (50) but such systems will be omitted until chapter 10.

4. THE POISSON - BOLTZMANN EQUATION

To be able to calculate A_{el} from eq. (45) both the concentrations c_i and the mean-potential Φ must be known in the aqueous part and on the charged surface.

The potential Φ may be calculated if the ion concentrations are known because the Poisson equation gives

$$\nabla^2 \cdot \Phi = - \frac{N_A \cdot e}{\varepsilon_o \varepsilon_r} \cdot \Sigma \, c_i \cdot z_i \qquad (37)$$

The problem is to determine the ion concentrations. The property of the system that will be used to determine the ion concentrations, is the fact that the free energy of the system is in a minimum when the system is in thermodynamic equilibrium. This means that the ions in the aqueous part will distribute in such a way that the free energy of the system will be in a minimum. But the only contribution to the free energy that depends on the ion distribution is E_{el}-TS (eq. (45)) which means that the ion concentrations will be given by the functions that minimize E_{el}-TS under the constraints $\int c_i \cdot dV$ constant for all i. Minimizing E_{el}-TS may be done by calculus of variation and especially by use of the Lagrangian multipliers (appendix II). From the equation of E_{el}-TS

$$E_{el} - TS = N_A \cdot \int \sum_i \{kT \cdot c_i \cdot (\ln \frac{c_i}{c_o} - 1) + \frac{1}{2} \cdot c_i \cdot z_i \cdot e \cdot (\Phi - \Phi_A)\} + f \, dV \qquad (51)$$

and the theory of Lagrangian multipliers (see appendix II) the condition that must be fullfilled for an extremum becomes

$$kT \cdot \ln c_i + e \cdot z_i \cdot \Phi + \frac{\partial f}{\partial c_i} + \lambda_i = 0 \qquad (52)$$

where λ_i is a constant (the Lagrangian multiplier).

Equation (52) may be rewritten into the following equation

$$c_i = c_{io} \cdot \exp\{- e \cdot z_i \cdot \Phi / kT - (\frac{\partial f}{\partial c_i} - \frac{\partial f}{\partial c_i}(R))/kT\} \qquad (53)$$

where c_{io} is the concentration of component i in a point where $\Phi = 0$.

If then the expressions for the c_i values (eq. (53)) are used in eq. (37) the modified Poisson-Boltzmann (MPB) equation is obtained.

$$\nabla^2\Phi = - \frac{N_A \cdot e}{\varepsilon_o \varepsilon_r} \Sigma z_i \cdot c_{io} \cdot \exp(- e \cdot z_i \cdot \Phi/kT) \cdot \exp\{ (- \frac{\partial f}{\partial c_i} + \frac{\partial f}{\partial c_i}(R))/kT\} \qquad (54)$$

The Poisson-Boltzmann equation may be obtained from eq. (54) if $(\partial f/\partial c_i - \partial f/\partial c_i(R))/kT$ is approximately zero.

$$\nabla^2\Phi = - \frac{N_A \cdot e}{\varepsilon_o \varepsilon_r} \Sigma z_i \cdot c_{io} \cdot \exp(- e \cdot z_i \cdot \Phi/kT) \qquad (55)$$

See also ref. (40) concerning the validity of the Poisson-Boltzmann equation.

For systems where the approximation leading to the PB-equation does not apply and eq. (54) is considered to be too difficult to use, another type of approximation also leading to a simple equation may be used.

If f may be written

$$f = K_1 \cdot (\Sigma c_i)^{K_2} \qquad (56)$$

where K_1 and K_2 are constants, and if the exponential $\exp\{\frac{\partial f}{\partial c_i}/\frac{\partial f}{\partial c_i}(R)-1\}$ may be linearized

$$\exp\{ \frac{\partial f}{\partial c_i} / \frac{\partial f}{\partial c_i}(R) - 1 \} \simeq \frac{\partial f}{\partial c_i} / \frac{\partial f}{\partial c_i}(R) \qquad (57)$$

the equation for the second exponential in eq. (54) becomes

$$\exp\{(- \frac{\partial f}{\partial c_i} + \frac{\partial f}{\partial c_i}(R))/kT\} \simeq \{\Sigma_i \frac{c_i(R)}{\Sigma_j c_j(R)} \exp(- z_i \cdot e \cdot \Phi/kT)\}^{K_3} \qquad (58\ a)$$

where

$$K_3 = (- \frac{\partial f}{\partial c_i}(R))/(kT + \frac{\partial f}{\partial c_i}(R)) \qquad (58\ b)$$

(eq. (53) has also been used in obtaining eq. (58 a)).

For systems where all ions in the water part have the same charge, f may according to appendix I be written as $- 0.44 \cdot kT \cdot c^{1.42} \cdot |z|^{2.52}$ which means that eq. (56) is fullfilled for these systems. Eq. (53) may then be written using the approximation eq. (58)

$$c = c_{10} \cdot \exp\{ \frac{- z \cdot e \cdot \Phi}{kT(1 - 0.262 \cdot |z|^{2.52} \cdot c_{10}^{0.42})} \} \qquad (59)$$

The approximation eq. (57) underestimates the second exponential in eq. (53) when $c/c_{10} >> 1$, but on the other hand eq. (53) has been obtained under the assumption of no effects from the volume of the ions, which may be questionable at high concentrations.

The effect from the volume of the ions on the free energy is certainly less than in salt solutions, because the probability of two ions with the same charge to be in contact is very little, but may nevertheless be considerable. An advantage in using eq. (59) is that the PB-equation can be used if the temperature is replaced by T^*

$$T^* = T \cdot (1 - 0.262 \cdot |z|^{2.52} \cdot c_{10}^{0.42}) \qquad (60)$$

The temperature used in calculating the dielectric constant ε_r shall however be T. Differences between the PB- and the MPB-equations are further discussed in chapter 6, where ion distributions in lamellar liquid crystalls are calculated.

5.CHEMICAL POTENTIALS

To use the expression for G, eq. (50) is cumbersome and the chemical potentials of the different components in a system will therefore be evaluated in this chapter.

$$\mu_i = \left(\frac{\partial G}{\partial n_i}\right)_{n_j} \tag{61}$$

On first sight it seems an impossible task to determine μ_i in a closed form especially as quantities as Φ_A, $\int c_i \cdot \ln c_i \, dV$ and $\int c_i \cdot \Phi \, dV$ depend on n_i in a way that can't be described by an analytic connection. However, by using the condition for optimum ion distribution (52) several simplifications arise and the equations for the chemical potentials can be calculated in a rather simple way. To simplify the calculations the expression for G is split up into two parts and the parts are differentiated individually.

$$G = G_1 + (E_{el} - TS) \tag{62}$$

where E_{el}-TS is

$$E_{el} - TS = \sum_i \int_V N_A \cdot kT \cdot c_i \cdot (\ln c_i - 1) \, dV + \sum_i \frac{1}{2} \cdot N_A \cdot z_i \cdot e \int_V c_i \cdot \bar{\Phi} \, dV +$$

$$+ \sum_i \frac{1}{2} \cdot N_A \cdot z_i \cdot e \cdot \int_V c_i \cdot \frac{1}{4\pi \cdot \varepsilon_o \varepsilon_r} \cdot \int_A \frac{\sigma}{|\vec{r} - \vec{x}|} \, dS_x \, dV +$$

$$+ \sum_i \frac{1}{2} \cdot \int_A \sigma \int_V \frac{N_A \cdot z_i \cdot e}{4\pi \cdot \varepsilon_o \varepsilon_r} \cdot \frac{c_i}{|\vec{r} - \vec{x}|} \, dV \, dS_x + \frac{1}{2} \int_A \int_A \frac{\sigma \cdot \sigma}{4\pi \cdot \varepsilon_o \varepsilon_r \cdot |\vec{r} - \vec{x}|} \, dS_r \, dS_x +$$

$$+ \sum_i N_A \int_V f(c_i) \, dV \tag{63}$$

The summation is here over all charged species in the aqueous part and $\bar{\Phi}$ is

$$\Phi' = \Phi - \int_A \frac{1}{4\pi \cdot \varepsilon_o \varepsilon_r} \cdot \frac{\sigma}{|\vec{r} - \vec{x}|} \, dS_x \tag{64}$$

where σ is the surface charge density of the amphiphilic aggregate. The potential Φ' can also be written

$$\Phi' = \frac{N_A \cdot e}{4\pi \cdot \varepsilon_o \varepsilon_r} \cdot \sum_i \int_V \frac{z_i \cdot c_i}{|\vec{r} - \vec{x}|} \, dV_x \tag{65}$$

The subscript x in dV_x means that the integration shall be done referring to the coordinates $\vec{x}$.

The derivative $\frac{\partial}{\partial n_p}\{E_{el}-TS\}$ may be divided into to parts

$$\frac{\partial}{\partial n_p}\{E_{el} - TS\} = \frac{\partial}{\partial H}\{E_{el} - TS\} \frac{dH}{dn_p} + \frac{\partial}{\partial n_p}\{E_{el} - TS\}_H \tag{66}$$

where H is a geometry dependent factor. For a micellar system H is the number of subsystems, in the lamellar case H is the area of the hydrophobic part and for a cylindrical system H is the length of the cylinders. $\frac{\partial}{\partial H}\{E_{el}-TS\}$ may for these systems be written

$$\frac{\partial}{\partial H}\{E_{el} - TS\} = \frac{1}{H}\{E_{el} - TS\} \tag{67}$$

The derivative of eq. (63) becomes

$$\frac{\partial}{\partial n_p}\{E_{el} - TS\} = \frac{1}{H}\frac{\partial H}{\partial n_p} \cdot \{E_{el} - TS\} + \sum_i N_A \cdot \Big[A(r) \frac{\partial r}{\partial n_p} \cdot kT \cdot c_i \cdot (\ln c_i - 1) +$$

$$+ z_i \cdot e \cdot \Phi \cdot c_i + f(c_i)\Big\}\Big]_{S_T} + \sum_i \frac{N_A \cdot z_i \cdot e}{4\pi \cdot \varepsilon_o \varepsilon_r} \int_V c_i \frac{\partial}{\partial n_p} \Big\{ \int_A \frac{\sigma}{|\vec{r} - \vec{x}|} \, dS_x \Big\} \, dV +$$

$$+ \frac{1}{2} \frac{1}{4\pi \cdot \varepsilon_o \varepsilon_r} \frac{\partial}{\partial n_p} \{ \int_A \int_A \frac{\sigma^2}{|\vec{r} - \vec{x}|} dS_r \, dS_x \} + \sum_i \int_V N_A \cdot kT \cdot \frac{\partial c_i}{\partial n_p} \ln c_i +$$

$$+ N_A \cdot z_i \cdot e \frac{\partial c_i}{\partial n_p} \Phi + N_A \frac{\partial f}{\partial c_i} \cdot \frac{\partial c_i}{\partial n_p} dV \qquad (68)$$

where the symbol $[...]_{S_T}$ denotes that the expression shall be calculated at the surface of the aqueous part.

$[...]_{S_T}$ becomes

$$\left[A(r) \frac{\partial r}{\partial n_p} \{...\}\right]_{S_T} = A(R) \frac{\partial R}{\partial n_p} \{...\}_R - A(b) \frac{\partial b}{\partial n_p} \{...\}_b \qquad (69)$$

Concerning the symbols, see fig. 16.

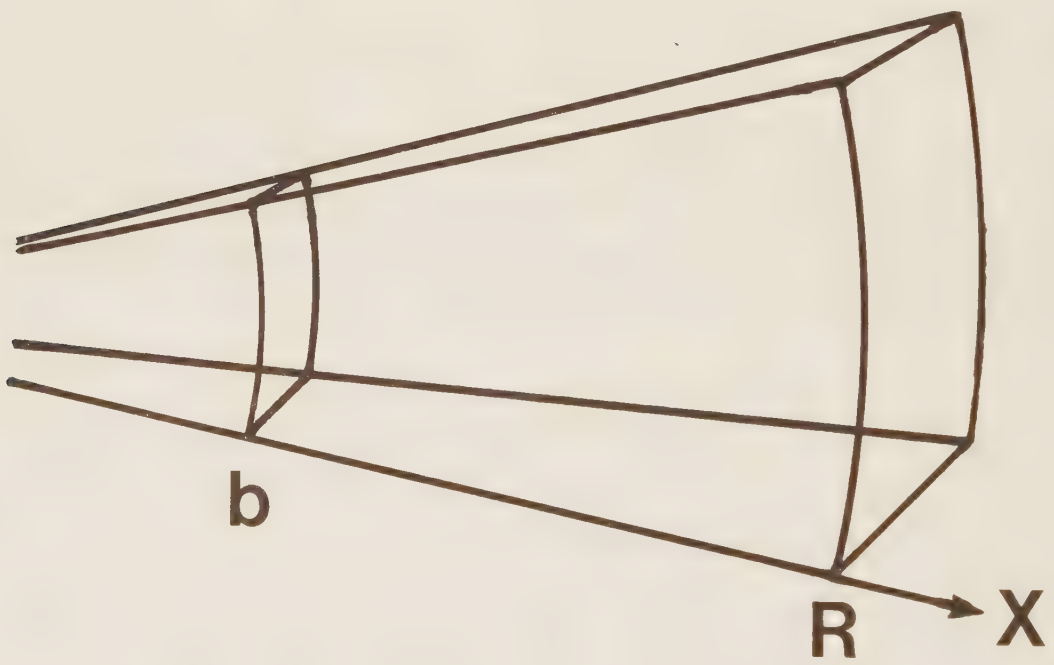

Figure 16. Schematic representation of the aqueous part in a subsystem.

X is for all systems the coordinates on a vector perpendicular to the surfaces of the aggregate and the subsystem.

Equation (68) can be simplified with use of the following equations.

$$\frac{1}{H}\frac{\partial H}{\partial n_p}\{A\cdot\sigma\}\,\Phi_A + \sum_i \frac{N_A\cdot z_i\cdot e}{4\pi\cdot\varepsilon_o\varepsilon_r}\int_V c_i \frac{\partial}{\partial n_p}\left\{\int_A \frac{\sigma}{|\vec{r}-\vec{x}|}\,dS_x\right\}_{H\ \text{constant}} dV +$$

$$+\frac{1}{2}\,\frac{1}{4\pi\cdot\varepsilon_o\varepsilon_r}\,\frac{\partial}{\partial n_p}\left\{\int_A\int_A \frac{\sigma^2}{|\vec{r}-\vec{x}|}\,dS_r\,dS_x\right\}_{H\ \text{constant}} =$$

$$= \frac{\partial}{\partial n_p}(A\cdot\sigma)\,\Phi_A - \frac{\partial b}{\partial n_p}\cdot A\cdot\frac{\sigma^2}{2\varepsilon_o\varepsilon_r} \qquad (70)$$

where b is the coordinates of the charged surface. The easiest way to understand equation (70) is that the left part times dn_p is just the electrostatic energy change when only the charges at the surface are allowed to change there number or location.

Since the free energy G in eq. (5?) has to be at a minimum the expression $\sum_i N_A \int \frac{\partial c_i}{\partial n_p}\{kT\cdot\ln c_i + z_i\cdot e\cdot\Phi + \frac{\partial f}{\partial c_i}\}\,dV$ in eq. (68) simplifies to

$$\sum_i N_A \int \frac{\partial c_i}{\partial n_p}\{kT\cdot\ln c_i + z_i\cdot e\cdot\Phi + \frac{\partial f}{\partial c_i}\}\,dV = -\sum_i N_A \int \lambda_i \frac{\partial c_i}{\partial n_p}\,dV \qquad (71)$$

The equation

$$\int N_A\cdot c_i\,dV = n_i \qquad (72)$$

makes a further simplification possible.

$$\lambda_i \frac{\partial n_i}{\partial n_p} = \frac{1}{H}\frac{\partial H}{\partial n_p}\lambda_i\cdot n_i + \lambda_i\cdot N_A\cdot\left[A(r)\,\frac{\partial r}{\partial n_p}\,c_i\right]_{S_T} + N_A\int\lambda_i\frac{\partial c_i}{\partial n_p}\,dV \qquad (73)$$

and equation (68) becomes

$$\frac{\partial}{\partial n_p}\{E_{el} - TS\} = \sum_i N_A \cdot \Big[A(r)\frac{\partial r}{\partial n_p}\{kT \cdot c_i \cdot (\ln c_i - 1) + z_i \cdot e \cdot \Phi \cdot c_i +$$

$$+ f(c_i) + \lambda_i \cdot c_i\}\Big]_{S_T} + \frac{1}{H}\frac{\partial H}{\partial n_p}\{E_{el} - TS + \sum_i \lambda_i \cdot n_i - A \cdot \sigma \cdot \Phi_A\} -$$

$$- \sum_i \lambda_i \frac{\partial n_i}{\partial n_p} + \frac{\partial}{\partial n_p}(A \cdot \sigma) \cdot \Phi_A - \frac{\partial b}{\partial n_p} \cdot A \cdot \frac{\sigma^2}{2\varepsilon_o \varepsilon_r} \qquad (74)$$

$A(r)\frac{\partial r}{\partial n_p}$ and $\frac{1}{H}\frac{\partial H}{\partial n_p}$ are easy to calculate for the lamellar, cylindrical and spherical geometries and the following calculations are therefore restricted to those systems.

The geometry depending factor H may be written

$$H = A/b^{d-1} \qquad (75)$$

where A is the area of the aggregates and d is a constant

geometry	lamellar	cylindrical	spherical
d	1	2	3

Equation (74) is transformed after a lot of algebra (see appendix III) to eq. (76).

$$\frac{\partial}{\partial n_p}\{E_{el} - TS\} = \sum_i \frac{\partial n_i}{\partial n_p}\{kT \cdot \ln c_{i0} + \frac{\partial f}{\partial c_i}(c_{i0}) - V_i \cdot U(R)\} + \frac{\partial n_a}{\partial n_p}\{z_a \cdot e \cdot \Phi_A -$$

$$- \frac{1}{n_a}(E^o_{el} + \int U(r)\, dV) + \frac{1}{n^o_a}\{V_T - n_a \cdot V_a\} \cdot U(R)\} + \frac{\partial b}{\partial n_p}\frac{A}{b} \cdot \{2E^o_{el}/A +$$

$$+ \frac{d \cdot b_1}{b - b_1}(E^o_{el}/A + \frac{1}{A}\int U(r)\, dV - b \cdot (\frac{R}{b})^d \cdot \frac{1}{d} U(R))\} \qquad (76)$$

where

$$U(r) = N_A \cdot \{\sum_i (kT \cdot c_i + c_i \frac{\partial f}{\partial c_i}) - f\} \qquad (77)$$

V_T is the total volume, V_i the volume of a molecule i, V_a the volume of the amphipilic molecule, (see appendix III) and b_1 the distance between the hydrophobic and the charged surface (see fig. 17).

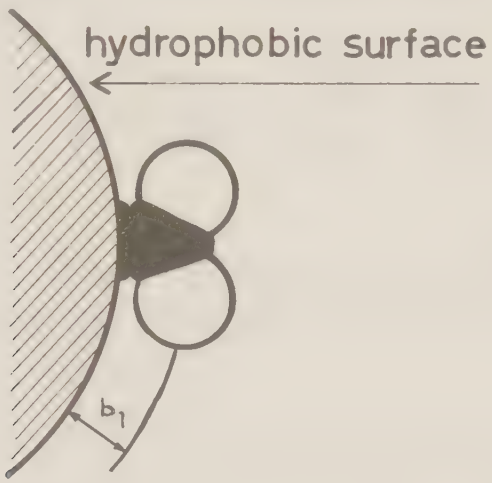

Figure 17. Schematic representation of the location of the hydrophobic surface.

If, as mentioned in chapter 3.5, the hydrophobic and the charged surfaces coincide, which means that $b_1 = 0$.

This will simplify $\frac{\partial}{\partial b}\{E_{el}-TS\}$

$$\frac{\partial}{\partial b}\{E_{el} - TS\} = \frac{1}{b} \cdot 2 \cdot E^o_{el} \qquad (78)$$

where E^o_{el} is $\frac{1}{2} \int \sigma \cdot \Phi \, dV$ and $\frac{\partial}{\partial b}\{E_{el}-TS\}$ has been calculated from eq. (76) according to the chain rule

$$\frac{\partial}{\partial n_p} = \sum_j \frac{\partial n_j}{\partial n_p} \cdot \frac{\partial}{\partial n_j} + \frac{\partial b}{\partial n_p} \cdot \frac{\partial}{\partial b} \qquad (79)$$

The only calculation that remains before the formulae for the chemical potentials are ready is to calculate $\partial(\gamma \cdot A_a)/\partial n_p$. From the connection A3 in appendix III, this can easily be done because

$$A_a = d \cdot n_a \cdot \bar{V}_a \cdot \frac{1}{b - b_1} \tag{80}$$

where A_a is the "hydrophobic" area and $\bar{V}_a$ is the hydrophobic volume of an amphiphilic molecule (see appendix III). The differentiation becomes

$$\frac{\partial}{\partial n_p}(\gamma \cdot A_a) = \gamma \cdot \frac{\bar{V}_a \cdot d}{b - b_1} \cdot \frac{\partial n_a}{\partial n_p} - \gamma \cdot \frac{A}{b} \cdot (1 - \frac{b_1}{b})^{d-2} \cdot \frac{\partial b}{\partial n_p} \tag{81}$$

The chemical potentials for the components in systems with lamellar or cylindrical symmetry may now be calculated from equations (50), (77), (79) and (81).

$$\mu_i = \mu_i^o + kT \cdot \ln c_{i0} + \frac{\partial f}{\partial c_i}(R) - V_i \cdot U(R) \tag{82}$$

$$\mu_{H_2O} = \mu_{H_2O}^o - V_{H_2O} \cdot U(R) \tag{83}$$

$$\mu_a = \mu_a^o + z_a \cdot e \cdot \Phi_A - \frac{1}{n_a}\{E_{el}^o + \int U(r)\, dV - (V_T - n_a \cdot V_a) \cdot U(R) - \gamma \cdot A_a\} \tag{84}$$

and

$$(\frac{\partial G}{\partial b})_{\text{all } n_j \text{ constant}} = \frac{A}{b}\{2E_{el}^o/A - \gamma\} \tag{85}$$

It must be noted that it is only in eq. (85) that the constraint $b_1 = 0$ is used, the other equations will be the same also when $b_1 \neq 0$.

In the micellar system there is an additional contribution to the chemical potentials due to the mixing of the subsystems and from eq. (2)

$$G_{mix} = kT \cdot N \cdot (\ln X_m - 1) \tag{2}$$

the following derivatives may be calculated

$$\frac{\partial G_{mix}}{\partial n_a} = N \cdot \frac{kT}{n_a} \cdot \ln X_m \tag{86}$$

and

$$\frac{\partial G_{mix}}{\partial n_i} = - N_A \cdot kT \cdot c_m \cdot V_i \tag{87}$$

where c_m is the micelle concentration.

The formulae (82 - 85) may also be calculated in a different way using Green functions in the equations for the potentials, concerning those calculations, see ref. (51).

6. ION DISTRIBUTIONS

Before thermodynamic quantities such as chemical potentials, enthalpies and so on can be calculated the ion distribution must be known. This can be obtained from the Poisson-Boltzmann (PB) equation (55) or from the MPB equation (54). The main problem with these equations is that they are non-linear, which means that they often are very difficult to solve. This chapter will therefore begin with one of the few systems where an analytic solution to the PB-equation can be obtained, a lamellar system with only one kind of ions in the aqueous part. Later other systems where analytical solutions exist will be presented and in the next chapter systems where only numerical solutions are available will be treated.

The parameters that occur in the PB-equation are besides the temperature T, the geometry parameters b and R and some universal constants as N_A, e, ε_0 also the dielectric constant ε_r. The dielectric constant is temperature dependent and may for water be written (see ref. (30))

$$\varepsilon_r = 306.7 \cdot \exp(-T/218.6) \tag{88}$$

To solve the PB-equation is not enough to get an unique solution, the solution must besides also coincide with some boundary conditions, for example

$$\Phi(R) = \frac{\partial \Phi}{\partial r}(R) = 0 \tag{89}$$

But there are also restrictions at the surface of the aggregates. From Gauss´law follows

$$\frac{\partial \Phi}{\partial r}(b) = -\frac{\sigma}{\varepsilon_0 \varepsilon_r} \tag{90}$$

The electrostatic potential inside the aggregates is here assumed constant. Let´s then begin to solve the PB-equation.

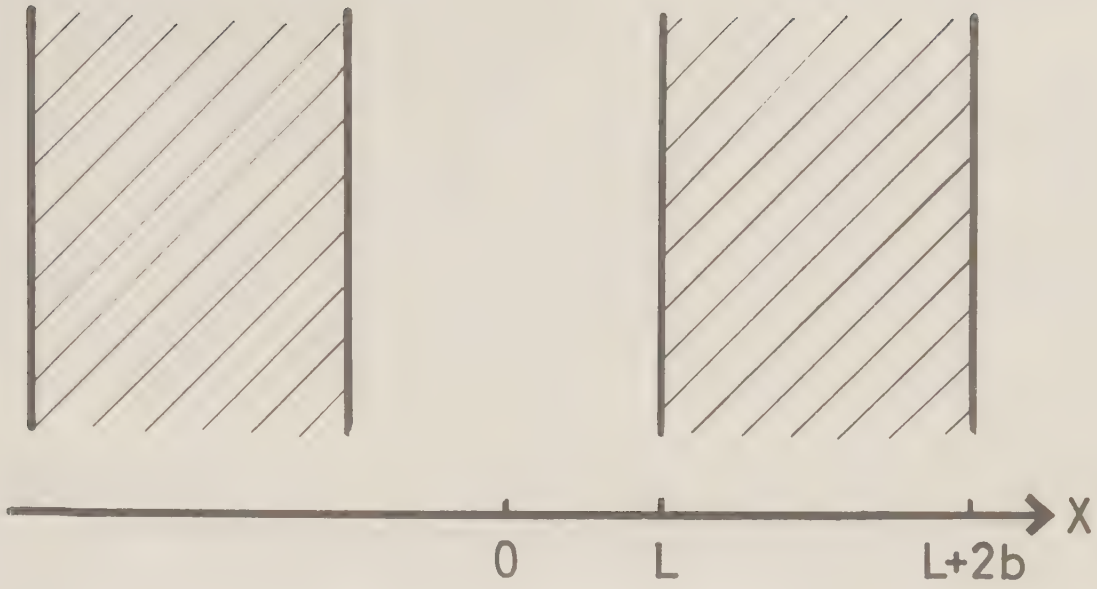

Figure 18. Schematic representation of a lamellar system. The thickness of the amphiphilic layer is 2•b and the thickness of the water layer is 2•L.

If the ions in the aqueous part have the same charge, the PB-equation becomes

$$\frac{d^2\Phi}{dx^2} = - \frac{N_A \cdot e \cdot z \cdot c}{\varepsilon_o \varepsilon_r} \exp\{- z \cdot e \cdot \Phi / kT\} \qquad (91)$$

This equation can easily be solved (see ref. (41)) and the result becomes

$$\exp\{z \cdot e \cdot \Phi / kT\} = \cos^2 (s \cdot \frac{X}{L}) \qquad (92)$$

where 2•L is the thickness of the water layer and s a constant that must satisfy

$$s \cdot \tan s = - \frac{\sigma \cdot z \cdot e \cdot L}{2 \cdot \varepsilon_o \varepsilon_r \cdot kT} \qquad (93)$$

s may also be written

$$s = \left(\frac{N_A \cdot e^2 \cdot z^2}{2 \cdot \varepsilon_o \varepsilon_r \cdot kT} \right)^{1/2} \cdot L \cdot \sqrt{c_{i0}} \qquad (94)$$

from which c_{i0} can be calculated if s is known. The ion distribution becomes

$$c_i = c_{i0} / \{\cos^2 (s \cdot \frac{X}{L})\} \qquad (95)$$

The line of action in using these equations is first to solve eq. (93) and then to use the obtained s-value in the other equations.

Concentration profiles calculated from the PB- and MPB-equations are in fig. 19 plotted for a system with z = 1, σ = -0.2 C/m^2 and L = 10 Å.

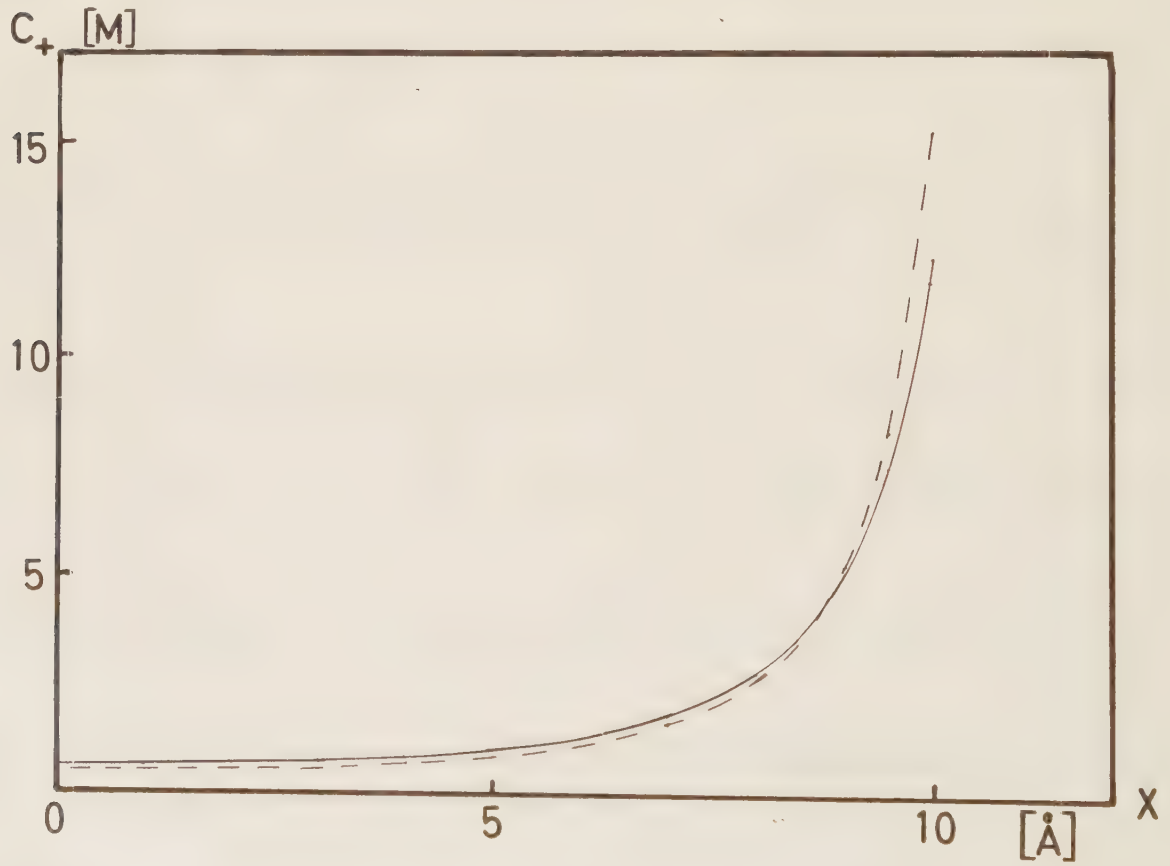

Figure 19. Concentration profile between two charged plates at 298 K for monovalent ions. The plate distance is 20 Å and the surface charge density is -0.2 C/m^2. The full line represents values from the PB equation and the dotted line values from the MPB equation.

The main difference between the two concentration profiles, is that the ion concentration in the vicinity of the charged surface is slightly higher when calculated with the modified Poisson-Boltzmann equation than with the usual PB-equation. This effect is more pronounced in fig. 20 where the fraction of ions p_b within 3 Å from the charged surface is plotted as a function of L. The formula used to calculate p_b is (ref. (41))

$$p_b = -\frac{2 \cdot \varepsilon_o \varepsilon_r \cdot kT}{L \cdot e \cdot z \cdot \sigma} \{\tan s - \tan (s(1 - \frac{3}{L}))\} \qquad (96)$$

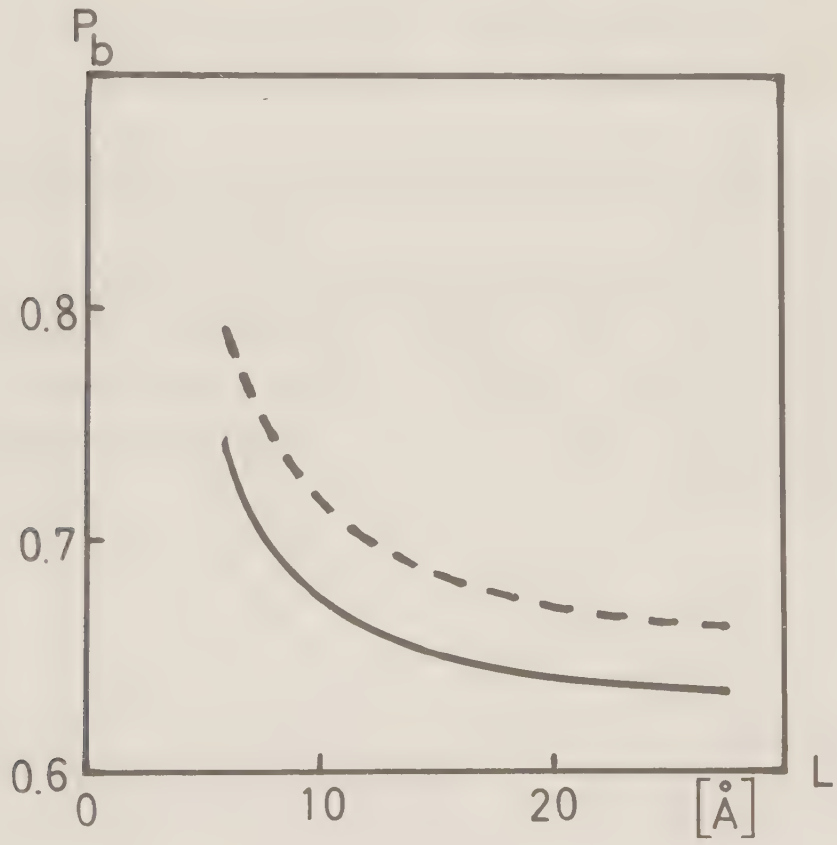

Figure 20. Fraction of bound ions within 3 Å from a charged surface as a function of the thickness of the water layer. The surface charge density is - 0.2 C/m^2 and the temperature is 298 K. The full line represents values from the PB equation and the dotted line values from the MPB equation.

One from a thermodynamic point of view very important parameter c_{i0}, the concentration in the midplane between two charged surfaces, is calculated and plotted as a function of L in fig. 21. As can be seen the difference between the c_{i0} values calculated by the two methods is considerable.

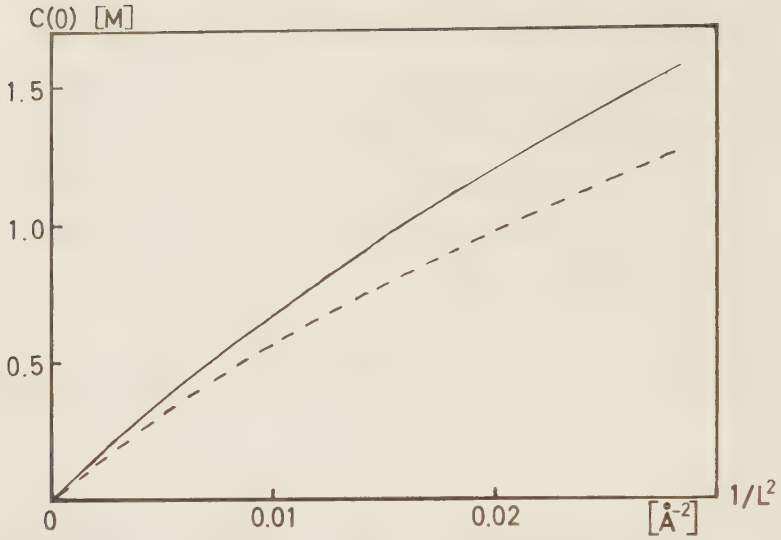

Figure 21. The counterion concentration in the midplane between two plates as a function of $1/L^2$. The parameters are the same as in fig. 20.

The solution of the PB equation becomes rather involved for systems where salt is also present. In this chapter will therefore only some approximative connections be mentioned, the complete solutions can be found in ref. (50). One striking feature of salt solutions is that the counterions are distributed rather evenly over the whole volume (see fig. 22).

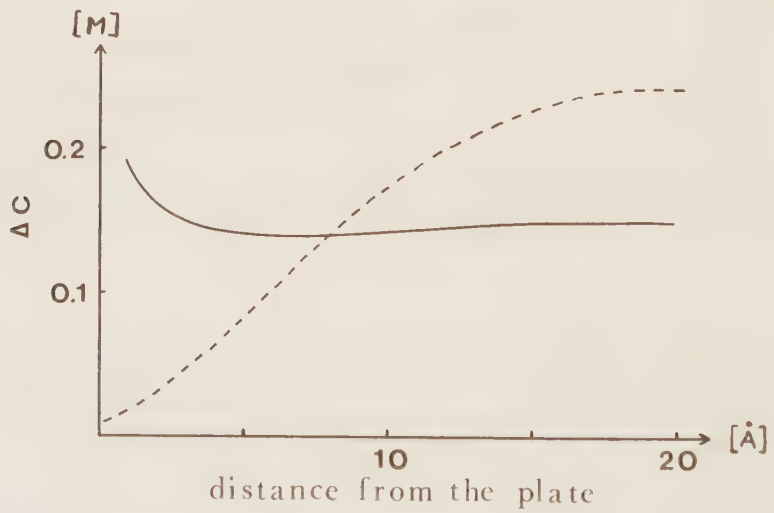

Figure 22. The distribution of the added salt. Full line counterions, dotted line coions. Distance between the plates 40 Å, surface charge density - 0.2 C/m^2 and salt concentration 0.15 M.

This property suggests that an approximative equation for the counterion concentration may be written

$$c(x) \simeq c^{o}(x) + c_{salt} \tag{97}$$

where $c^{o}(x)$ is the counterion concentration with no added salt. This expression (97) is only valid when all the counterions have the same charge. No simple expressions can be found for other cases. From eq. (97) it is also possible to calculate the fraction of counterions within Δ Å from the charged surface. The approximate formula becomes

$$\frac{n_b}{n_T} \simeq \frac{n_b^{o} + \Delta \cdot N_A \cdot c_{salt}}{n_T} \tag{98}$$

where n_T is the total number of counterions per unit area and n_b^{o} is the number of counterions per unit area within Δ Å from the surface at zero salt concentration. The accuracy of eq. (98) is illustrated in fig. 23.

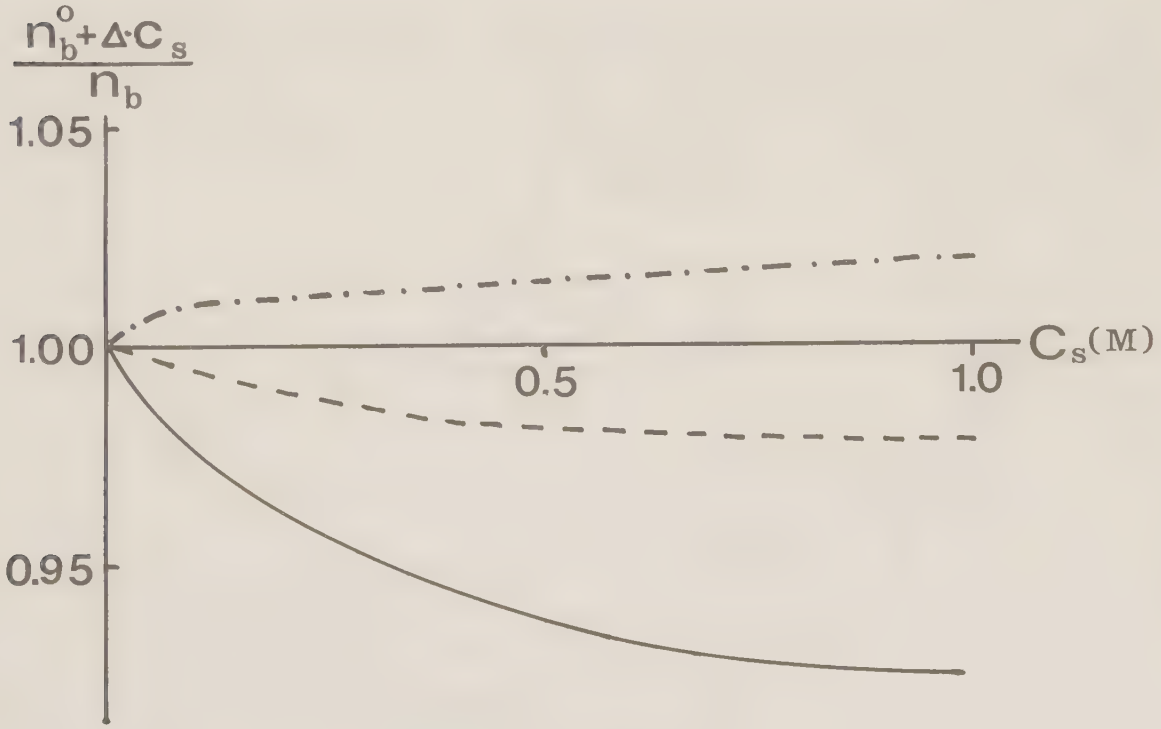

Figure 23. An illustration of the accuracy of eq. (98). The ratio between the approximate and "exact" values of bound ions as a function of salt concentration. (-•-•-) L=∞, σ = - 0.4 C/m^2, (- - -) L = 20 Å, σ = - 0.2 C/m^2, (———) L = ∞, σ = - 0.08 C/m^2.

The thermodynamically very important concentration at the midpoint between the two surfaces can also be calculated according to eq. (97). The accuracy of using eq. (97) to determine c_{+0} values is illustrated in fig. 24.

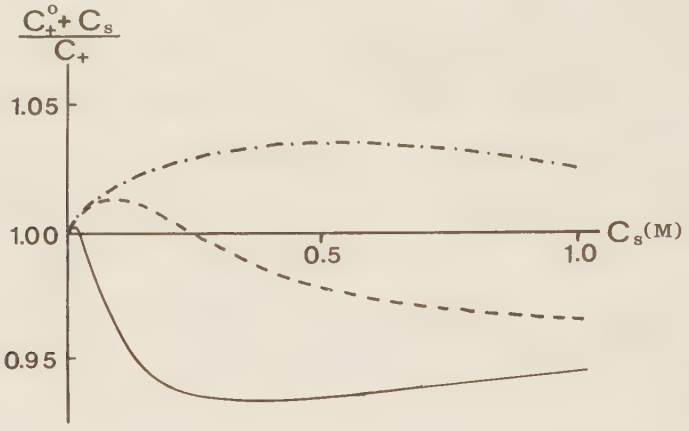

Figure 24. An illustration of the accuracy of eq. (97) for calculating c_{+0}. The ratio of the approximate value obtained from eq. (97) and the "exact" value, from a solution of the PB eq., is plotted as a function of salt concentration. $\sigma = -0.2$ C/m^2, (-•-•-) L=10 Å, (- - -) L=20 Å and (———) L=40 Å.

For coions there is always a substantial difference between the "true" concentration and the mean salt concentration. This can be seen in fig. 22 and in fig. 25 where the ratio between c_{-0} and c_{salt} is plotted as a function of the salt concentration c_s.

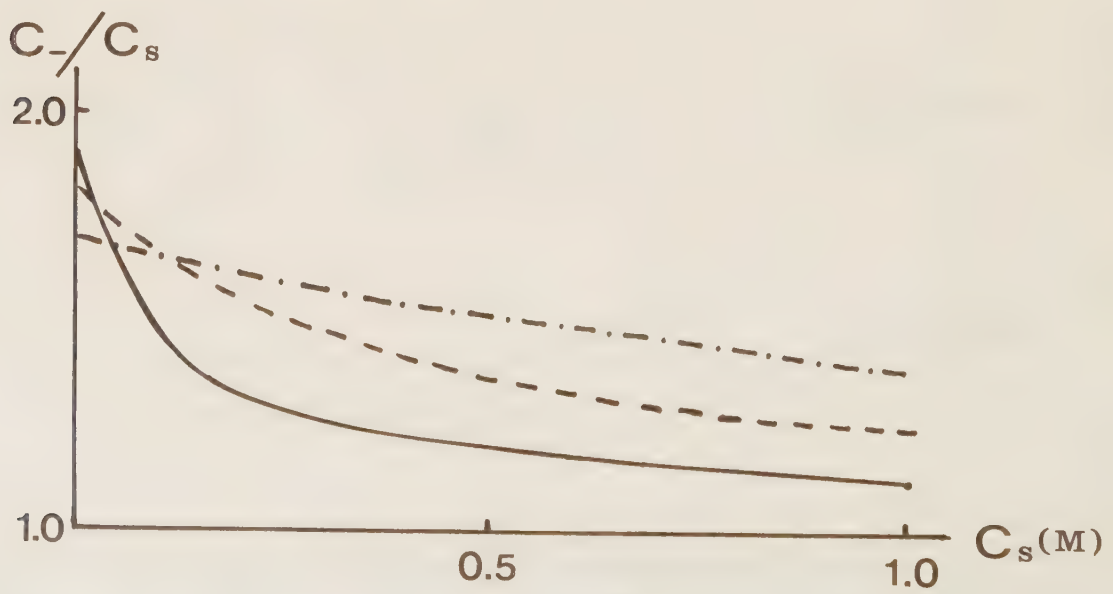

Figure 25. The ratio between c_{-0} and c_{salt} as a function of salt concentration c_{salt}. Parameters as in fig. 24.

The ion distributions for systems with other geometries than lamellar will be treated rather briefly mainly because the main characteristics are the same as in the lamellar case.

First the cylindrical case where also an analytic solution to the PB-equation exists.

$$\exp(z \cdot e \cdot \Phi / kT) = \frac{r^2}{R^2} \{\cos(s \cdot \ln \frac{r}{R}) - \frac{r}{s} \sin(s \cdot \ln \frac{r}{R})\}^2 \qquad (99)$$

where R is the radius of the subsystem (see fig. 26) and s a constant that must satisfy

$$\{s + \frac{1}{s} (\frac{\sigma \cdot z \cdot e \cdot b}{2 \cdot kT \cdot \varepsilon_o \varepsilon_r} + 1)\} \cdot \tan(s \cdot \ln \frac{R}{b}) = - \frac{\sigma \cdot z \cdot e \cdot b}{2 \cdot kT \cdot \varepsilon_o \varepsilon_r} \qquad (100)$$

b is the radius of the aggregate (see fig. 26).

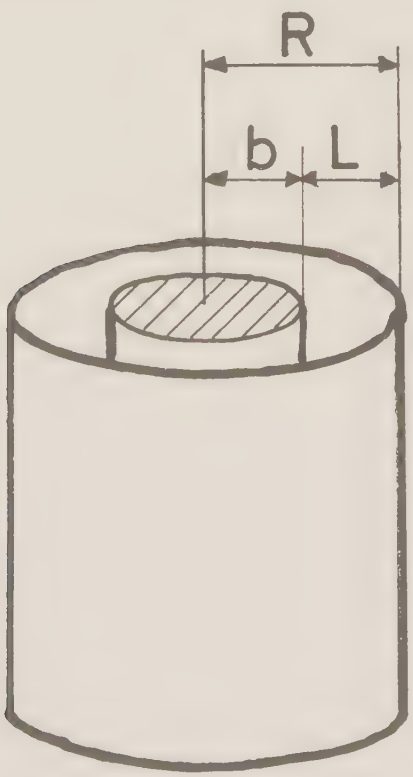

Figure. 26 Schematic representation of a cylindrical subsystem. The radius of the amphiphilic aggregate is b and the radius of the subsystem is R.

If $-\sigma \cdot e \cdot z \cdot b/(2 \cdot kT \cdot \varepsilon_o \varepsilon_r) < \{\ln(R/b)\}/\{1 + \ln(R/b)\}$ the constant s in eq. (100) becomes complex and the trigonometric functions will then change to the corresponding hyperbolic functions. The concentration at R is

$$c_{i0} = \frac{2 \cdot kT \cdot \varepsilon_o \varepsilon_r}{N_A \cdot z_i^2 \cdot e^2 \cdot R^2} \cdot (1 + s^2) \qquad (101)$$

Concerning the calculations that give equations (99 - 101), see appendix IV, (see also ref. (42) and (43)).

When also salt is present there exists no analytic solution to the PB-equation in the case of cylindrical symmetry. For spherical symmetry there exists no analytic solution to the PB equation if not the electrostatic potential is small enough to allow a linearization of the exponential functions. Since the potential seldom is so small it will for this symmetry as in the case of a salt solution in cylindrical symmetry be necessary to use numerical solutions of the PB equation. The next chapter will therefore treat this subject.

7. NUMERICAL SOLUTIONS OF THE POISSON-BOLTZMANN EQUATION

To solve the PB-equation is often a difficult numerical problem because the c_{i0}-values are usually not known and must be determined in an iterativ process, where each iteration involves a numerical solution of the differential equation. A method will be presented here that has turned out to be favourable in solving the PB-equation under these conditions. The problem is to solve

$$\frac{1}{r^{d-1}} \frac{d}{dr}\left(r^{d-1} \cdot \frac{d\Phi}{dr}\right) = - \frac{e \cdot N_A}{\varepsilon_o \varepsilon_r} \cdot \sum_i c_{i0} \cdot z_i \cdot \exp(- e \cdot z_i \cdot \Phi / kT) \qquad (102)$$

with the following boundary conditions

$$\Phi(R) = \frac{d\Phi}{dr}(R) = 0 \qquad (103)$$

and

$$\frac{d\Phi}{dr}(b) = - \frac{\sigma}{\varepsilon_o \varepsilon_r} \qquad (104)$$

To simplify the calculations set

$$r = x \cdot R \qquad (105)$$

and

$$\Phi_1 = e \cdot \Phi / kT \qquad (106)$$

Equation (102) then becomes

$$\frac{1}{x^{d-1}} \frac{d}{dx}\left(x^{d-1} \cdot \frac{d\Phi_1}{dx}\right) = - \frac{e^2 \cdot N_A}{\varepsilon_o \varepsilon_r \cdot kT} \cdot \sum_i R^2 \cdot c_{i0} \cdot z_i \cdot \exp(- z_i \cdot \Phi_1) \qquad (107)$$

and the boundary condition (104) may then be written

$$\frac{b}{R} \cdot \frac{d\Phi_1(b/R)}{dx} = - \frac{\sigma \cdot b \cdot e}{\varepsilon_o \varepsilon_r \cdot kT} \tag{108}$$

The strategy in the method is to first calculate Φ, $d\Phi/dx$, $d^2\Phi/dx^2$, $d^3\Phi/dx^3$ and $d^4\Phi/dx^4$ at x and then calculate Φ and $d\Phi/dx$ at $x + \Delta x$ where Δx can be calculated from

$$\Delta x = \frac{1}{N} \cdot \frac{d^3\Phi/dx^3}{d^4\Phi/dx^4} \tag{109}$$

where N is a calculation parameter, more about it later. $\Phi(x + \Delta x)$ becomes according to the MacLaurin formula

$$\Phi(x + \Delta x) = \Phi(x) + \frac{d\Phi}{dx} \cdot \Delta x + \frac{1}{2} \cdot \frac{d^2\Phi}{dx^2} \cdot \Delta x^2 + \frac{1}{6} \cdot \frac{d^3\Phi}{dx^3} \cdot \Delta x^3 +$$

$$+ \frac{1}{24} \cdot \frac{d^4\Phi}{dx^4} \cdot \Delta x^4 \tag{110}$$

and $d\Phi(x + \Delta x)/dx$ may be calculated in the same way.

$$\frac{d\Phi(x + \Delta x)}{dx} = \frac{d\Phi(x)}{dx} + \frac{d^2\Phi}{dx^2} \cdot \Delta x + \frac{1}{2} \cdot \frac{d^3\Phi}{dx^3} \cdot \Delta x^2 + \frac{1}{6} \cdot \frac{d^4\Phi}{dx^4} \cdot \Delta x^3 \tag{111}$$

When $\Phi(x + \Delta x)$ and $d\Phi(x + \Delta x)/dx$ are known $d^2\Phi/dx^2$, $d^3\Phi/dx^3$ and $d^4\Phi/dx^4$ can be calculated from the PB-equation according to

$$\frac{d^2\Phi_1}{dx^2} = - \frac{d-1}{x} \cdot \frac{d\Phi_1}{dx} - \frac{e^2 \cdot N_A}{\varepsilon_o \varepsilon_r \cdot kT} \sum_i R^2 \cdot c_{i0} \cdot z_i \cdot \exp(- z_i \cdot \Phi_1) \tag{112 a}$$

$$\frac{d^3\Phi_1}{dx^3} = \frac{(d-1)}{x^2} \cdot \{\frac{d\Phi_1}{dx} - x \cdot \frac{d^2\Phi_1}{dx^2}\} + \frac{e^2 \cdot N_A}{\varepsilon_o \varepsilon_r \cdot kT} \cdot \frac{d\Phi_1}{dx} \cdot$$

$$\cdot \sum_i R^2 \cdot c_{i0} \cdot z_i^2 \cdot \exp(- z_i \cdot \Phi_1) \qquad (112\ b)$$

$$\frac{d^4\Phi_1}{dx^4} = - \frac{(d-1)}{x^3} \{2 \frac{d\Phi_1}{dx} - 2x \frac{d^2\Phi_1}{dx^2} + x^2 \frac{d^3\Phi_1}{dx^3}\} + \frac{e^2 \cdot N_A}{\varepsilon_o \varepsilon_r \cdot kT} \cdot$$

$$\cdot \sum_i R^2 \cdot c_{i0} \cdot z_i^2 \cdot (\frac{d^2\Phi_1}{dx^2} - z_i (\frac{d\Phi_1}{dx})^2) \cdot \exp(- z_i \cdot \Phi_1) \qquad (112\ c)$$

This process is then repeated with the new x value and the process is going on until $x \cdot d\Phi_1/dx \geq - \sigma \cdot b \cdot e/(\varepsilon_o \varepsilon_r \cdot kT)$. The last Δx is then recalculated to match

$$(x + \Delta x) \frac{d\Phi_1}{dx} = - \frac{\sigma \cdot b \cdot e}{\varepsilon_o \varepsilon_r \cdot kT} \qquad (113)$$

Both b/R and $\Phi_1(b/R)$ are now known, but the whole process must be repeated from the beginning with another step length Δx until the numerical errors in the process can be neglected. It is here the N-parameter in eq. (109) is convenient to use. The N value can be given for example by the equation

$$N_i = 2 \cdot N_{i-1} \qquad (114)$$

where i and i-1 are two successive calculation rounds. Often only a few iterations are needed especially if the values are Richardsson extrapolated (see ref. (53)). If the c_{i0} values satisfy the problem in question the calculated b/R and/or such values as the number of ions i shall also satisfy the problem. If not, a new set of c_{i0} values must be tested. There are many different ways of choosing the new c_{i0} values but the best course of action is to use a minimizing program where the quantity that shall be

minimized is $\sum_j |Y_j - Z_j|$. Y_j is the calculated b/R or the number of ion i and Z_j is the corresponding "real" value. The calculations become for systems containing only one type of ions very simple, especially if the b/R value is free to adjust in the calculation. In that case every calculation gives a R-value and a c_{i0} value. The calculations become of course much more complicated in systems where the b-value are free to adjust.

8. AGGREGATE SIZE

The optimal sizes of the aggregates are determined by the condition $(\partial G/\partial b)_n = 0$. For micellar systems where the aggregates have a finite size there will be a distribution of sizes but this effect will be neglected, for simplicity.

The partial derivative $(\partial G/\partial b)_n$ has been evaluated explicitly in connection with the calculation of the chemical potentials and the following equation was obtained.

$$(\frac{\partial G}{\partial b})_n = \frac{A}{b} \cdot \{2E^o_{el}/A - \gamma\} \tag{85}$$

For micellar systems there is an additional term due to the mixing of the subsystems.

$$(\frac{\partial G_{mix}}{\partial b})_n = - \frac{A}{b} \cdot \frac{3}{4\pi \cdot b^2} \cdot kT \ln X_m \tag{115}$$

Eq. (85) will also be slightly different if γ depends on b.

$$(\frac{\partial G}{\partial b})_n = \frac{A}{b} \cdot \{2E^o_{el}/A - \gamma - b \frac{d\gamma}{db}\} \tag{116}$$

It is from eq. (116) clear that by calculating $2E^o_{el}/A$ for different systems with known geometry and size, there will be an opportunity to test if it is possible to assume γ independent of b. It is of course very important that the dimension b is free to adjust in the test systems. In systems where the parameter b is equal to b_{max} (see eq. (12)) b is not free to adjust and eq. (116) can't then be used to calculate γ.

Is it then possible to find systems where the both requirements, aggregate size known and $b \neq b_{max}$ are fulfilled? The answer is yes. Most simple carboxylate soaps form liquid crystalline phases at high concentrations. For these systems, low angle X-ray diffraction experiments have shown how the dimensions of the aggregates vary with water content. The only disadvantage of these systems is that they only exist in concentrated solutions at "high" temperatures and it may therefore be difficult to estimate if the γ-values

calculated at these high ion concentrations will be the same as in systems where the amphiphile concentration is low. E^o_{el}/A will therefore be calculated for systems with different ion concentrations (although all are high) to be able to verify if γ is depending on b or some other parameter. The calculation of E^o_{el}/A is especially simple for lamellar liquid crystalline systems since a lot of experimental data are available and the equation for E^o_{el}/A may be expressed in a simple form (see ref. (50)):

$$E^o_{el}/A = kT\{-\frac{\sigma}{z\cdot e} - N_A\cdot L\cdot \Sigma c_{io}\} \simeq kT\{-\frac{\sigma}{z\cdot e} - N_A\cdot L\cdot c_{io}\} \qquad (117)$$

where the second equality follows from the assumption that the amount of monomeric amphiphile or salt in the aqueous region is negligible. For given values of σ and L obtained from X-ray data, the concentration c_{io} can be obtained from relations (93) and (94). Figure 27 shows the calculated value of $2E^o_{el}/A$ from the PB equation for a series of potassium soaps at 86 °C. The experimental values are from Gallot and Skoulios (36).

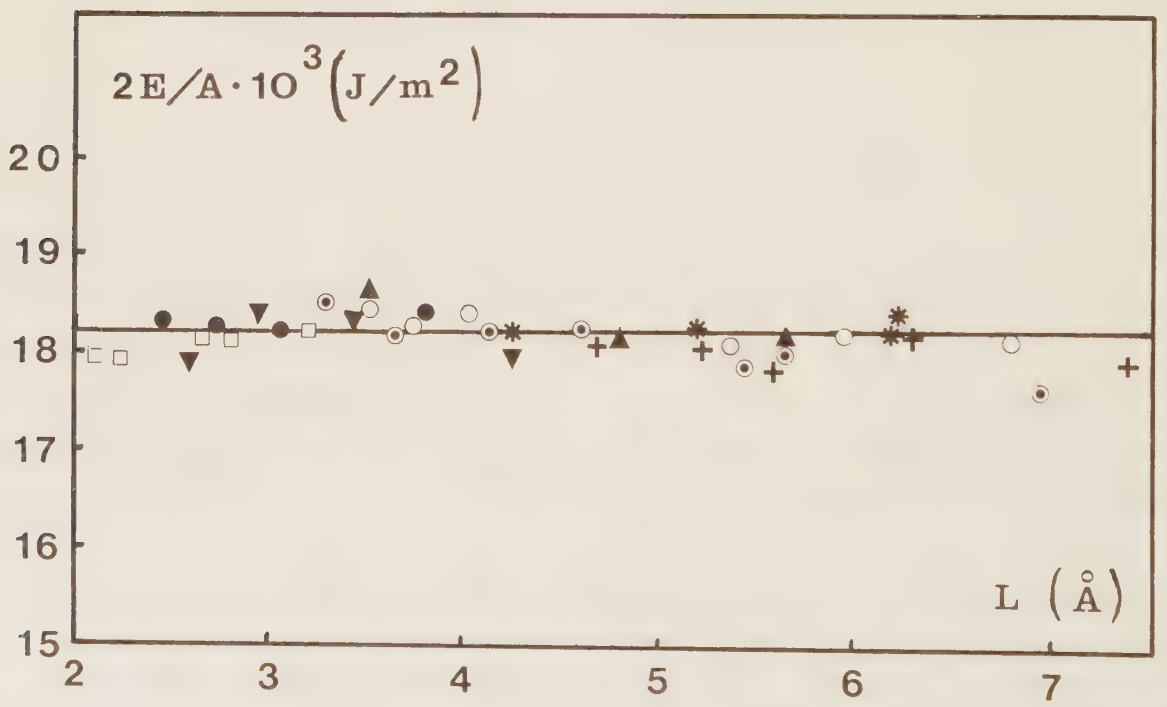

Figure 27. Two times the electrostatic energy per unit area, $2E_{el}/A$, as a function of the thickness of the water layer L for the lamellar mesophase of some potassium soaps at 86 °C. □ = C_8K, ● = $C_{10}K$, ▼ = $C_{12}K$, ▲ = $C_{14}K$, ⊙ = $C_{16}K$, ○ = $C_{18}K$, ✱ = $C_{20}K$ and ✚ = $C_{22}K$. The X-ray data is from ref. (36).

In spite of the fact that there are substantial variations in σ and L the quantity $2E^{o}_{el}/A$ remains constant around $18.2 \cdot 10^{-3}$ N/m. It is quite remarkable that the $2E^{o}_{el}/A$ value is constant over such an extensive concentration range, especially for the highest concentrations where the assumption leading to the PB equation must break down.

Although the most extensive studies have been performed for potassium soaps at 86 ^{o}C there exist some experimental data for other temperatures and counterions (36). In table 3 it is shown that the calculated value of γ is rather insensitive to temperature.

Table 3. Two times the electrostatic energy per unit area for the lamellar mesophase of potassium soaps at different temperatures.

T (K)	$2E_{el}/A$ (mJ/m^2)
377	18.4 ± 0.1
359	18.2 ± 0.2
338	18.2 ± 0.1
318	17.8 ± 0.1

The variation with counterion in the alkali metal series is also insignificant as shown by the data of table 4.

Table 4. Two times the electrostatic energy per unit area for the lamellar mesophase of soaps with different counterions at 359 K.

counterion	$2E_{el}/A$ (mJ/m^2)
Na^+	17.9 ± 0.3
K^+	18.2 ± 0.2
Rb^+	18.8 ± 0.3
Cs^+	18.6 ± 0.2

A large counterion dependence would directly indicate that essential contributions had been left out in the free energy expression (eq. (50)). The value of γ is considerably smaller than $\gamma = 51$ mJ/m^2 found for interfaces between water and pure aliphatic hydrocarbons, but the difference may probably be refered to differences in the possibility of the amphiphile molecules to move perpendicular to the surface. This statement is based on the fact that a charged amphiphile molecule is not anchored at the surface with the same strength as a corresponding uncharged molecule.

Another explanation to the discrepancy between the γ values, that the difference is due to different water "structures" in the vicinity of charged respectively uncharged surfaces, is not so probable because a partial replacement of the water by other uncharged molecules affect the γ value in a rather modest way (see fig. 28)).

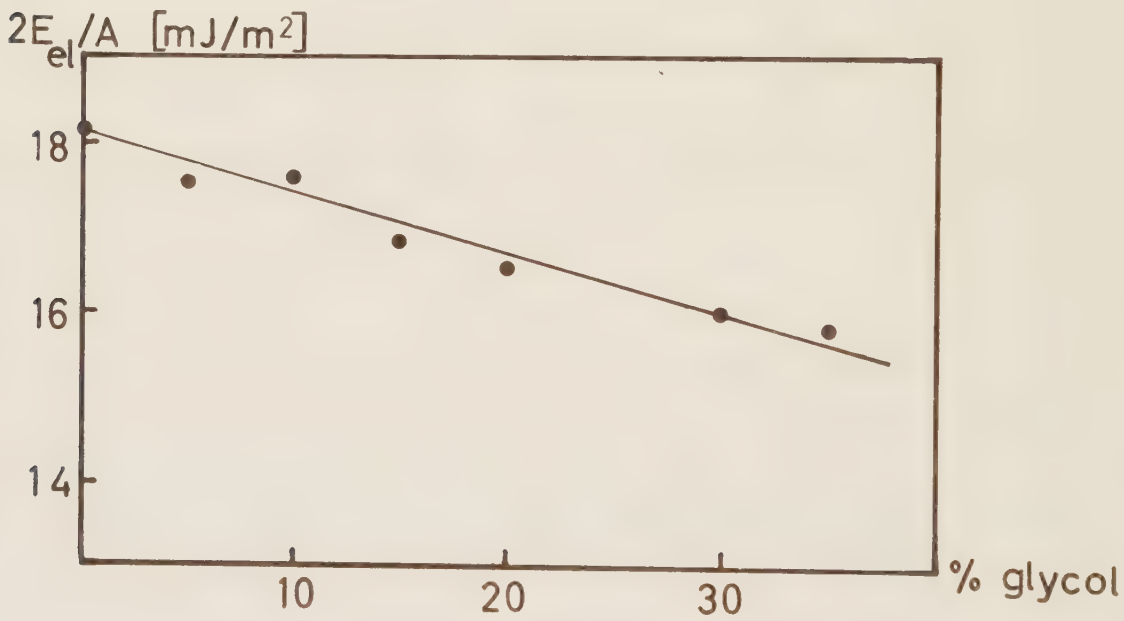

Figure 28. The effect on E_{el} by partially replacing the water by glycol in a lamellar mesophase of potassium dodecanoate and water at 70 °C. The X-ray data is from ref. (44).

The γ values in fig. 28 have been calculated from the experimental values in ref. (44) and the dielectric constant to be used is that of a glycol-water mixture (see ref. (44)).

At higher water contents the potassium soaps form hexagonal phases, for which the γ-values also may be calculated. The PB-equation is however very difficult to solve in a hexagonal system, but if the system is approximated to a system with cylindrical symmetry there is no problem in solving the PB-equation.

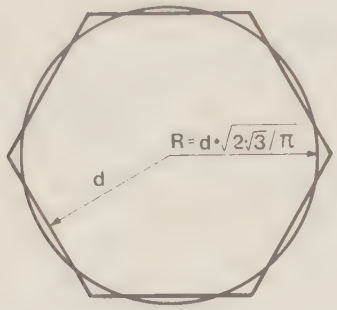

Figure 29. Schematic representation of a hexagonal and a cylindrical subsystem. The volume of the two systems is the same.

Errors will of course be introduced in going from hexagonal to cylindrical symmetry especially in concentrated systems where the distance between the aggregates is very short. The equation for E^o_{el}/A will in a salt-free cylindrical system be (see appendix IV).

$$\frac{E^o_{el}}{A} = kT\{-\frac{\sigma}{z\cdot e} - N_A\cdot\frac{R^2}{b}\cdot c_{10}\ \ln\left(\frac{R}{b}\right) + \frac{2\varepsilon_o\varepsilon_r\cdot kT}{e^2z^2b}\ \cdot$$

$$\cdot\ \ln\{\left(\frac{R}{b}\right)^2 + \frac{\sigma\cdot(4RT\cdot\varepsilon_o\varepsilon_r + \sigma\cdot F\cdot b)}{b\cdot 2\varepsilon_o\varepsilon_r\cdot kT\cdot e^2z^2\cdot N_A\cdot c_{10}}\}\} \qquad (118)$$

where c_{10} may be calculated from equations (100) and (101). $2E^o_{el}/A$ has been calculated for a serie of potassium soaps, n = 8 to n = 22, from equation (118). The experimental values of b and R are from ref. (36).

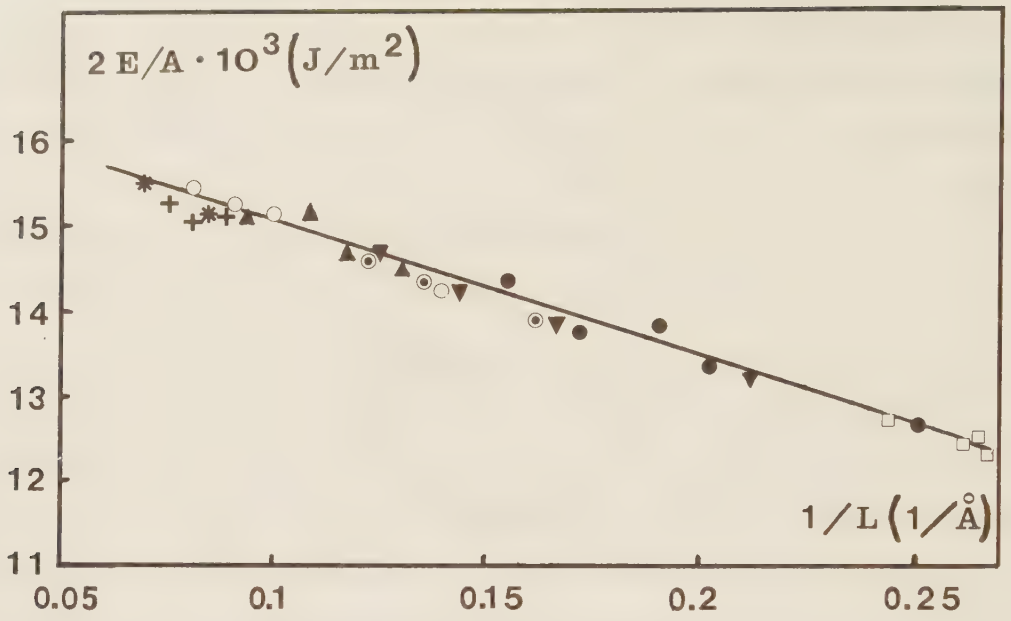

Figure 30. $2E_{el}/A$ as a function of the inverse thickness of the water layer 1/L for the hexagonal mesophase of some potassium soaps at 86 °C. The designations are the same as in fig. 27.

The $2E^{o}_{el}/A$ values are as distinguished from the lamellar case, depending on the amphiphile concentration (see fig. 30). A part of the discrepancy can perhaps be explained from the difference between hexagonal and cylindrical symmetry. Another possibility is that the surface energy γA shall be replaced by

$$G_s = \gamma \cdot A_s \qquad (119)$$

where A_s is a "surface of tension" calculated with a characteristic length $(b-\Delta)$ instead of b. The change in the expression of $(\partial G/\partial b)_n$ is easy to execute and may be found in ref. (51). If a Δ value of 1.8 Å is assumed, indeed a mean value of $18 \cdot 10^{-3}$ N/m for γ is obtained, but the deviations from the mean value are of such an order that one can question the validity of the procedure (see fig. 31).

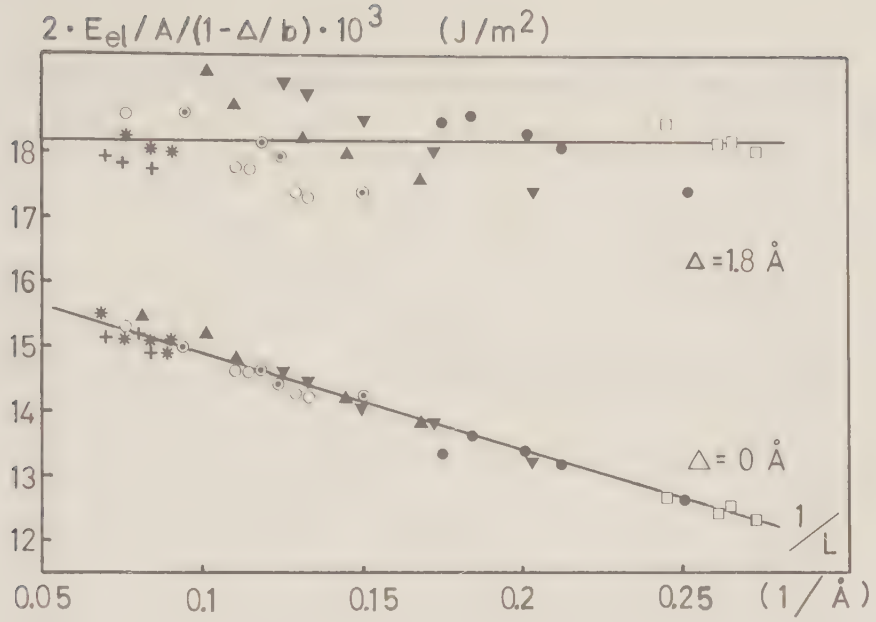

Figure 31. $2E_{el}/A$ as a function of the inverse thickness of the water layer $1/L$ for the hexagonal mesophase of some potassium soaps at 86 °C. The characteristic length defining the surface of tension is assumed to be $(b - \Delta)$ Å. The designations are the same as in fig. 27.

The variation with counterion in the alkali metal series is for these systems also insignificant as can be seen in fig. 32.

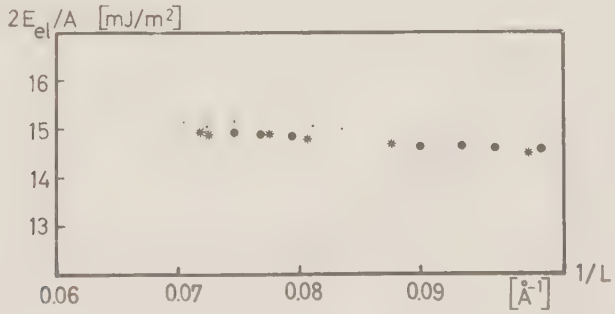

Figure 32. $2E_{el}/A$ as a function of the inverse thickness of the water layer $1/L$ for the hexagonal mesophase of C_{22} with different counterions at 86°C. ⊙= K, ✱ = Rb and ● = Cs. The X-ray data is from ref. (36).

To replace γA by γA_s is not the only possibility to explain the deviation of γ from a constant value. Another explanation is that the lateral mobility of the amphiphilic molecules in an aggregate must strongly be restricted by the electrostatic repulsion between the charged groups. This means that the entropy from this mobility depends on the surface area per monomer and this dependence may perhaps explain the γ values.

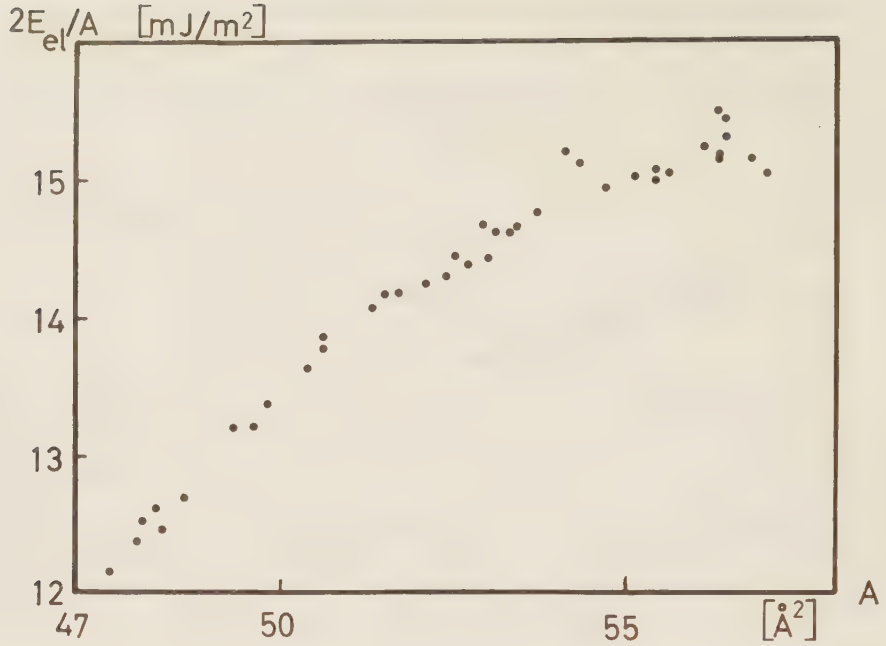

Figure 33. $2E_{el}/A$ as a function of the surface area per monomer in cylindrical aggregates. The X-ray data is from ref. (36).

A disadvantage with this explanation is that the same type of arguments also may be used for the lamellar systems, but the γ value is in the lamellar case,as can be seen in fig. 34, independent of the surface area per monomer. It is therefore only possible to rationalize the γ values in the cylindrical case from this assumption.

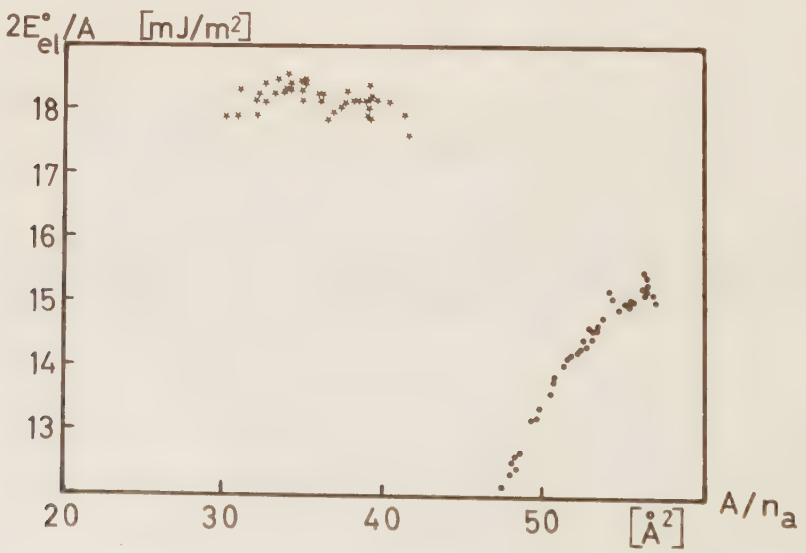

Figure 34. $2E_{el}/A$ as a function of the surface area per monomer. ★ in lamellar aggregates, ● in cylindrical aggregates. The X-ray data is from ref. (36).

Another important effect is that the radii of the cylinders are close to the length of an extended soap molecule, which is the maximal extent of an aggregate. If the values in fig. 30 are plotted against b over b_{max} where b_{max} is the length of an extended soap molecule the following figure appears.

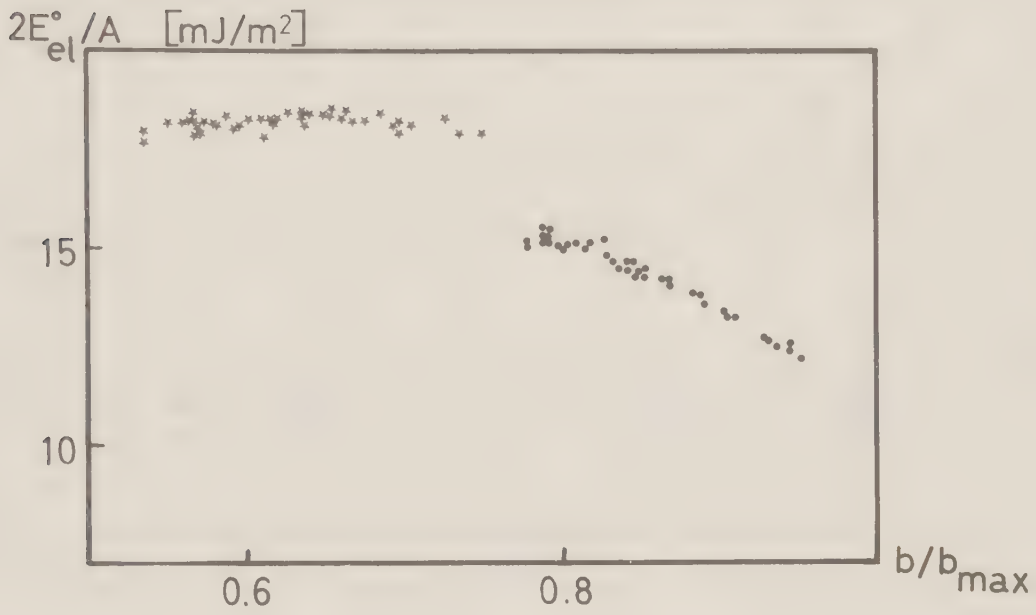

Figure 35. $2E_{el}/A$ as a function of b/b_{max} for a serie of lamellar aggregates (★) and a serie of cylindrical aggregates (●). The $2E_{el}/A$ values are calculated from the PB eq. and the X-ray data is from ref. (36).

It is tempting to draw the conclusion from fig. 35 that G_c expressed as a step function is a too broad simplification of the system and instead to replace the step function with a function depending on b/b_{max}. This is perhaps the best way in attacking the problem, but it is also with this assumption peculiar that the γ values in the lamellar case are independent of b/b_{max}. But the most probable explanation is that the different errors in the model cancel each other in a way that makes γ constant. That it probably is so can be seen from the corresponding calculations with the modified PB equation, see fig. 36. (The only difference when calculating E^{o}_{el}/A from the MPB equation instead of calculating if from the PB equation is to exchange T by T^{*}, see eq. (60)).

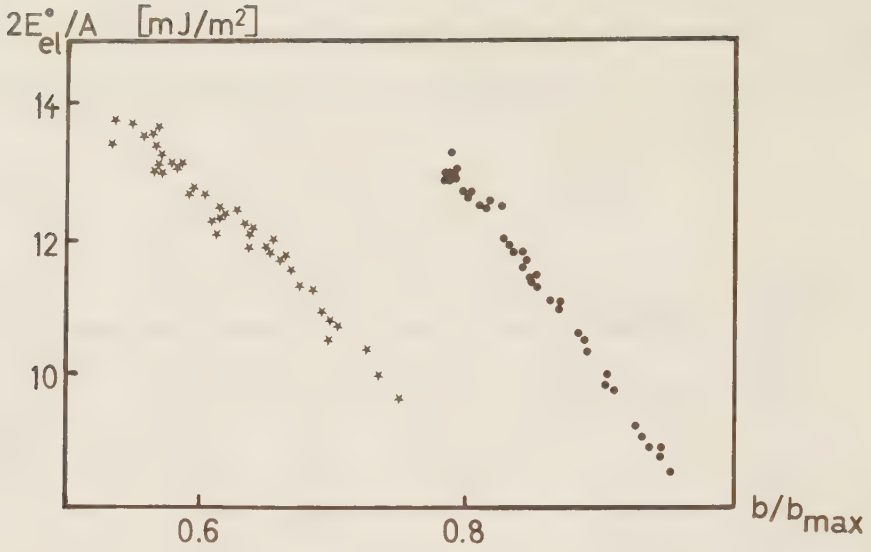

Figure 36. $2E_{el}/A$ as function of b/b_{max} for a serie of lamellar aggregates (★) and a serie of cylindrical aggregates (●). The $2E_{el}/A$ values are calculated from the MPB eq. and the X-ray data is from ref.(36).

The $2E^{o}_{el}/A$ value is here no longer constant in the lamellar case and this is especially pronounced in the limit $b/b_{max} \to 1$. That the $2E^{o}_{el}/A$ curve for the lamellar case is shifted to lower b/b_{max} values is easy to understand because the fraction of amphiphilic molecules with the length b is much less in cylindrical than in lamellar systems. That the reduction of the E^{o}_{el}/A values is much higher in the lamellar than in the cylindrical case when calculated with the MPB instead of the PB equation depends on the fact that the ion concentrations are higher in the lamellar systems.

It is at this stage not possible to obtain a function of the b/b_{max} dependence in γ, because of the uncertainty in the $2E^{o}_{el}/A$ values. The equation for the minimum energy $(\partial G/\partial b) = 0$, may be very sensitive to perturbations, an additional contribution to the free energy although quite small compared with G, may therefore affect the equation for $(\partial G/\partial b)$ considerably. My opinion is therefore that a constant γ value shall be used although the deviation is considerable, especially for the short-chained soaps, but since the origin of this effect is not yet thoroughly analyzed it would be hazardous to use an assumed b/b_{max} function. It is suggested to use

$$\gamma_{PB} = 18 \cdot 10^{-3} \text{ N/m} \qquad \text{and} \qquad \gamma_{MPB} \simeq 15 \cdot 10^{-3} \text{ N/m} \tag{120}$$

where PB stands for Poisson-Boltzmann and MPB for modified Poisson-Boltzmann.

It may look strange that γ is allowed to have different values depending on the way in which E^o_{el}/A is calculated, but if the difference between the true G_{el} and the G_{el} calculated from the PB or the MPB equations approximately may be written as a constant multiplied by the area of the aggregate, then the difference can be incorporated in the γ value.

A clear demonstration of the effect of the constraint $b \leq b_{max}$ can be found for the surfactant Aerosol OT (di-2-ethyl hexyl sodium sulphosuccinate) which forms a lamellar phase in the composition range 8 - 71 % w/w (45,46). In this range $2E^o_{el}/A$ calculated from the PB equation varies between $12 \cdot 10^{-3}$ and $8 \cdot 10^{-3}$ N/m but the lamellar thickness is constant at b = 9.8 Å corresponding to an extended chain. If the γ value had been calculated for this system there had of course been a considerable difference between different amphiphile concentrations which clearly demonstrates that one must be careful in using equation (81), especially when $b \simeq b_{max}$.

9. PHASE EQUILIBRIA

The condition for equilibrium between two phases α and β is that the chemical potentials of all electrically neutral combinations of species are equal in the two phases i.e.

$$(\mu_i)_\alpha = (\mu_i)_\beta \tag{121}$$

for all i. This equation together with the explicit expressions for the chemical potentials (equations 78 - 80) gives an opportunity to calculate phase diagrams from the thermodynamic model.

The equations that must be satisfied if two phases are in equilibrium will be discussed in this chapter and the validity of the theory will as often as possible be tested against experiment. The first property of amphiphile-water systems that shall be discussed is the pronounced ability of the amphiphilic molecules to form aggregates.

The question is, can the thermodynamic model explain why amphiphilic molecules at low concentrations exist as monomers in a water solution but if the concentration is raised to a certain level (CMC) begin to form aggregates? To be able to answer this question, the equations that give the number of molecules in the aggregates and in the water part must be developed. This can be done in the following way. First from eq. (121) the following equation is obtained.

$$\mu_a^{agg} = \mu_a^{H_2O} \tag{122}$$

μ_a^{agg} stands for the chemical potential of an amphiphilic molecule in an aggregate and $\mu_a^{H_2O}$ is the chemical potential of an amphiphilic molecule in the aqueous solution. If the equations for $\mu_a^{H_2O}$ and μ_a^{agg}, eq. (82) and eq. (84) are used the following equation is obtained.

$$\mu_a^{o\,H_2O} + kT \cdot \ln c_{a0} + \frac{\partial f}{\partial c_a}(c_{a0}) - V_a \cdot \{U(R) + N_A \cdot kT \cdot c_m\} =$$

$$= \mu_a^{o\ agg} + z_a \cdot e \cdot \Phi_A - \frac{1}{n_a} \{E_{el}^o + \int U(r)\, dV - (V_T - n_a \cdot V_a) \cdot U(R) -$$

$$- \gamma \cdot A_a - N \cdot kT \cdot \ln X_m\} \qquad (123)$$

The aggregates are in this case assumed to be micelles. Equation (123) may also be written

$$c_{a0} \cdot \exp\{\frac{1}{kT} \frac{\partial f}{\partial c_a}(c_{a0})\} = \exp\{\frac{\mu_a^{o\ agg} - \mu_a^{o\ H_2O}}{kT}\} \cdot \exp\{-\frac{z_a \cdot e \cdot \Phi_A}{kT}\} \cdot$$

$$\cdot \exp\{-\frac{1}{kT} (E_{el}^o + \int U(r)\, dV - V_T \cdot U(R) - \gamma \cdot A_a - N \cdot kT \cdot \ln X_m -$$

$$- n_a \cdot N_A \cdot kT \cdot c_m \cdot V_a)/n_a\} \qquad (124)$$

From eq. (124) it is now possible to calculate c_{a0} in an iterativ process. If R and b are known the process becomes

1. Make an intelligent guess of the c_{a0}-value.

2. c_{i0} for $i \neq a$ is then calculated from the PB- or MPB-equation. If more than two components are present in the water part a relation between the c_{i0}-values must be known. For example the ratio between the concentrations of the components.

3. When all the c_{i0}-values are known the expressions on the right in eq. (124) can be calculated.

4. c_{a0} is then calculated from eq. (124).

5. The calculated c_{a0}-value is then used in a new calculation cycle and the process is going on until the c_{a0}-values are consistent. At a first sight this seems to be a very laborious process but except for the most dilute systems, or systems where the hydrophobicity of the amphiphilic

molecule is very low, the value of c_{a0} is small enough to have no influence on the solution of the PB or MPB equation and a new iteration is only rarely needed.

If on the other hand b is free to adjust the calculations are more involved. Then it is also necessary to make an initial guess of b and when the PB or MPB equation is solved use eq. (85) to test if the b value used is the optimal one. If not, a new b value is assumed and the process is repeated until the used b is the optimal one. When now b and the c_{a0} value are known the amount of amphiphile in the water part can be calculated and for a SDS (sodium dodecyl sulphate) solution, Gunnarsson (29) obtained the following results for the micelle concentration using the PB-equation.

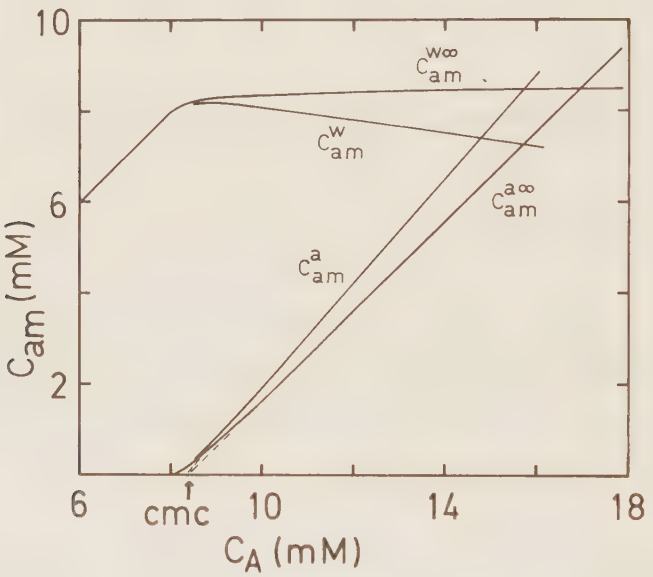

Figure 37. The concentration of monomeric amphiphile c_{am}^{w}, $c_{am}^{w\infty}$ and of micellized amphiphile c_{am}^{a}, $c_{am}^{a\infty}$ as a function of the total amphiphile concentration for dodecyl sulphate. The values are calculated from the cell model and from the infinite dilution approximation (superscript ∞). Temperature 25 ^{o}C.

Other termodynamic quantities that can be calculated and tested against experimental values are ion activities and Gunnarsson has also calculated these parameters for SDS solutions at different concentrations.

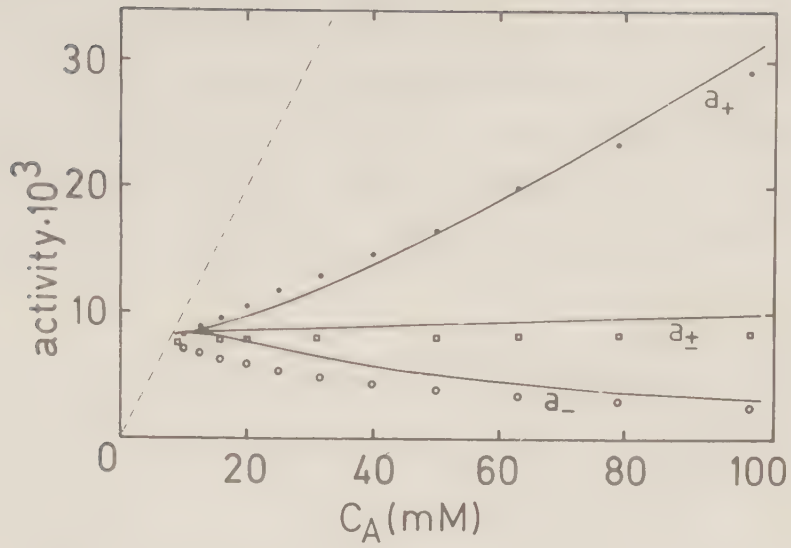

Figure 38. Single ion and mean ion activities in sodium dodecyl sulfate solutions as a funtion of the total amphiphile concentration. The calculated values are from ref. (29) and the experimental values are from ref. (54).

The amount of amphiphile in the water part can also be calculated for other systems than micellar. The amount of AOT in the water part of the lamellar phase is in fig. 39 plotted as a function of the total amphiphile concentration. The experimental values of the dimensions in the system used in the calculations are from ref. (46).

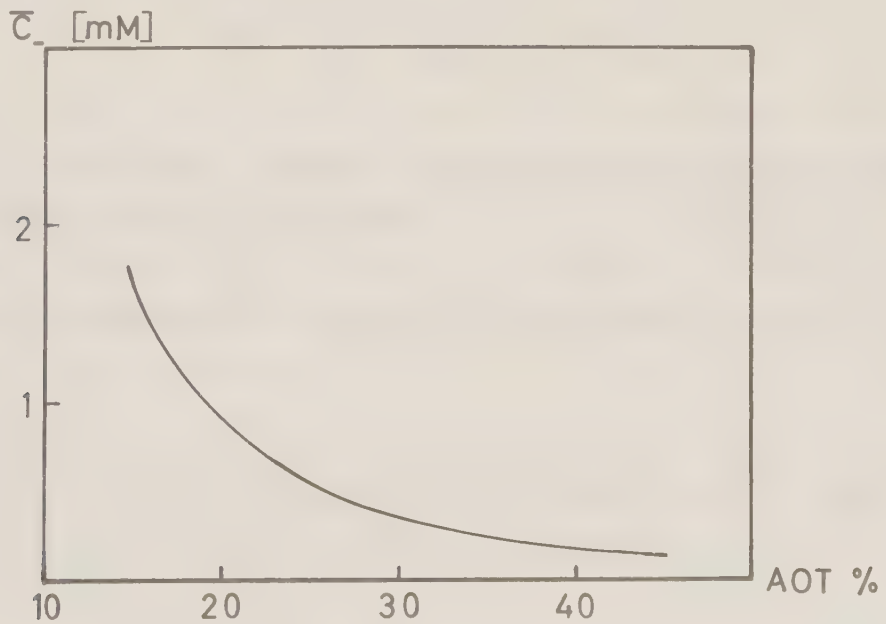

Figure 39. The amount of dissolved AOT in the aqueous region at 298 K.

Based on the fact that the chemical potentials of all the components in an amphiphile-water system can be calculated, a "characteristic" curve of the system can be made. A "characteristic" curve is a plot of the chemical potential $\mu_+ + \mu_-$ of the electroneutral surfactant versus μ_{H_2O}, where all other chemical potentials are constant. This shall show up to be a most convenient way of representing phase equilibria calculations. For each type of phase micellar, hexagonal or lamellar, one obtains a curve as shown in fig. 40.

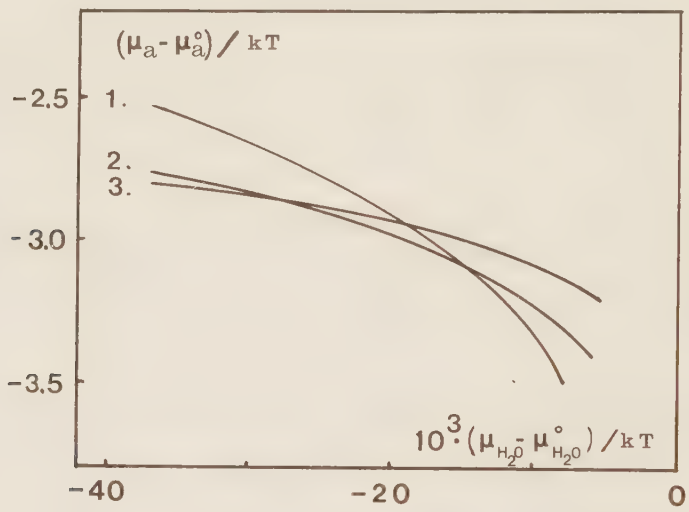

Figure 40. The chemical potential of the amphiphile molecule μ_{am} as a function of the chemical potential of the water μ_{H_2O}. 1. is for a spherical, 2. is for a cylindrical and 3. is for a lamellar system. At the intersections the different phases are in equilibrium with each other.

Eq. (117) is satisfied at the intersection of two curves and at this point the two phases are at equilibrium. From the intersections of the calculated lines in fig. 40 which are obtained for the system $C_7H_{15}COOK$ - -water the stability regions for the different phases are directly obtained by calculating the compositions of the phases at the intersection points.

Explicit calculations of phase equilibria have been performed for a series of potassium carboxylate soaps. The phase boundaries have been determined at 86 ^oC from the PB equation. The calculations have been performed in two

different ways. In the first series, experimental values of b are used while in the second series b is calculated from eq. (81). The results summarized in table 5 show that irrespective of the details of the calculations there is a remarkably good agreement with experimentally determined phase boundaries (36, 47). Particulary the extension of the two-phase regions are accurately predicted.

Table 5. Calculated and experimental phase boundaries.

soap	Phase boundaries in % w/w			
	spherical	cylindrical	lamellar	
$C_{12}K$	- 29	40 - 62	68 -	a.
	- 35	43 - 58	66 -	b.
	- 36	44 - 59	66 -	exp.
$C_{14}K$	- 28	39 - 64	70 -	a.
	- 34	41 - 58	66 -	b.
	- 32	40 - 56	64 -	exp.
$C_{16}K$	- 27	38 - 66	71 -	a.
	- 31	39 - 58	66 -	b.
	- 27	34 - 55	63 -	exp.
$C_{18}K$	- 25	36 - 66	72 -	a.
	- 29	36 - 58	65 -	b.
	- 22	29 - 54	62 -	exp.

a: Phase boundaries calculated using a priori determined values for the aggregate dimension b.

b: Phase boundaries calculated using experimental values for the aggregate dimensions.

A test of the generality of the method is obtained by calculations on the system AOT-water. AOT has two hydrocarbon chains and is thus more apt to form lamellar and reversed hexagonal phases. Using the value $\gamma = 18 \cdot 10^{-3}$ N/m obtained from the carboxylate soap systems the phase diagram has been calculated. In this case, the reversed hexagonal phase is also allowed. Concerning the chemical potentials for the components in the reversed hexagonal phase, see chapter 11. Using the estimated value $\mu_a^{o\ H_2O} - \mu_a^{o\ amph} = 13.5$ kT the model gives a good description of the association behaviour over the entire concentration range (except for the existence of a cubic phase which is not treated in the model). At the maximum size, spherical AOT micelles contain six monomers and the cooperativity of the micelle formation is rather weak. According to the calculations, micelles start to form in the concentration region 0.15 - - 0.25 % w/w of AOT (experimental estimate, 0.20 % w/w). At 0.8 % a two phase region appears which extends to 8 % AOT (experimental values, 1.2 - 10 %) where it is in equilibrium with a lamellar phase which extends up to 58 % (experimentally 71 %). At 78 % (experimentally 81 %) a reversed hexagonal phase appears. Also for this case the model rather accurately describes the rather delicate balance between the different phase structures.

It is also straightforward to extend the model to three-component systems. The only difference is that the equations for the chemical potentials of the components in the aggregates will depend on the mole ratios of the components. This will be treated more in detail in the following chapter.

10. MULTICOMPONENT SYSTEMS

In this chapter multicomponent systems - systems with more than one component present in the aggregates - will be treated.

Systems with many components in the water part may be treated by the theory developed in the preceding chapters. The two most important differences between bi- and multicomponent systems are.

1. There will be an additional contribution G^{-} to G due to the entropy of mixing of the components in the aggregates. This contribution can for simplicity be written as an ideal mixing and

$$G^{-} = kT \cdot \sum_{ia} n_{ia} \cdot \ln X_{ia} \qquad (125)$$

where the summation is over all components in the aggregate and X_{ia} is the mole fraction of component ia in the aggregate.

2. The γ-value depends on all X_{ia} and there will be a term $(\partial\gamma/\partial n_i) \cdot A_a$ when taking the derivative of $\gamma \cdot A_a$.

The only change in the equations of the chemical potentials (82 - 84) is in μ_{ia}, the chemical potential of the components in the aggregate where two additional terms are added.

$$\mu_{ia} = \mu^{o}_{ia} + z_{ia} \cdot e \cdot \Phi_A + kT \cdot \ln X_{ia} - \frac{V^{-}_{ia}}{\sum_{ja} n_{ja} \cdot V^{-}_{ja}} \{E^{o}_{el} + \int U(r)\, dV -$$

$$- (V_T - \sum n_{ja} \cdot V^{-}_{ja} \cdot \frac{V_i}{V^{-}_{ia}}) \cdot U(R) - A_a \left(\gamma + \frac{d\gamma}{dn_{ia}} \cdot \frac{\sum n_{ja} \cdot V^{-}_{ja}}{V^{-}_{ia}}\right)\} \qquad (126)$$

and the contribution from mixing of the micelles becomes

$$\frac{\partial G_{mix}}{\partial n_{ia}} = N \cdot \frac{V^{-}_{ia}}{\sum n_{ja} \cdot V^{-}_{ja}} \cdot kT \cdot \ln X_m \qquad (127)$$

The expression for $\partial G/\partial b$ (eq. (85)) is however unaffected of the changes and that gives an oppotunity to test the X_{ia} dependence in γ. In fig. 41 is $2E_{el}/A$ for different carboxylate soap - alcohol - water mixtures plotted as a function of the molar ratio of alcohol in the aggregates. All values are for lamellar systems and $2E_{el}/A$ has been calculated from the PB equation.

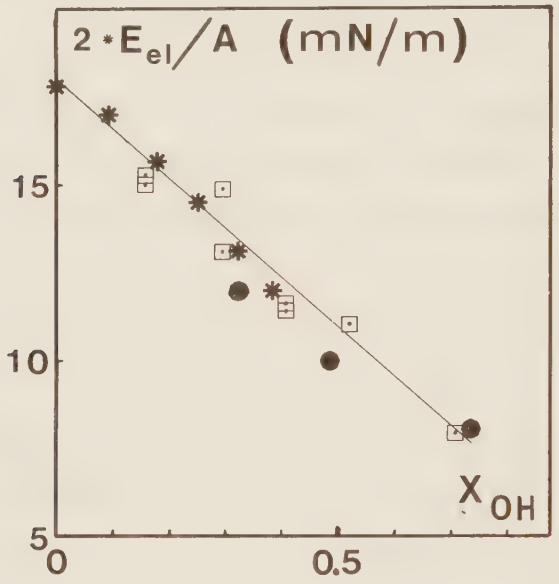

Figure 41. $2E_{el}/A$ as a function of the mole fraction of alcohol for the lamellar systems, ✱ caprate, decanol at 55 °C, ⊡ caprate, octanol at 20 °C and ● caprylate, decanol at 20 °C. The X-ray data is from ref. (49) and (55).

The straight line in the figure is the equation

$$\gamma = \sum_{ja} \gamma_{ja} \cdot X_{ja} \qquad (128)$$

where $\gamma_{COO^-} = 18 \cdot 10^{-3}$ N/m and $\gamma_{OH} = 4 \cdot 10^{-3}$ N/m.

When the γ_{COO^-} and γ_{OH} values are fixed the equations (85) and (128) may be used to estimate aggregate dimensions in three-component systems.

The thickness of the amphiphilic layer is in fig. 42 plotted against the amount of alcohol for a soap-water mixture.

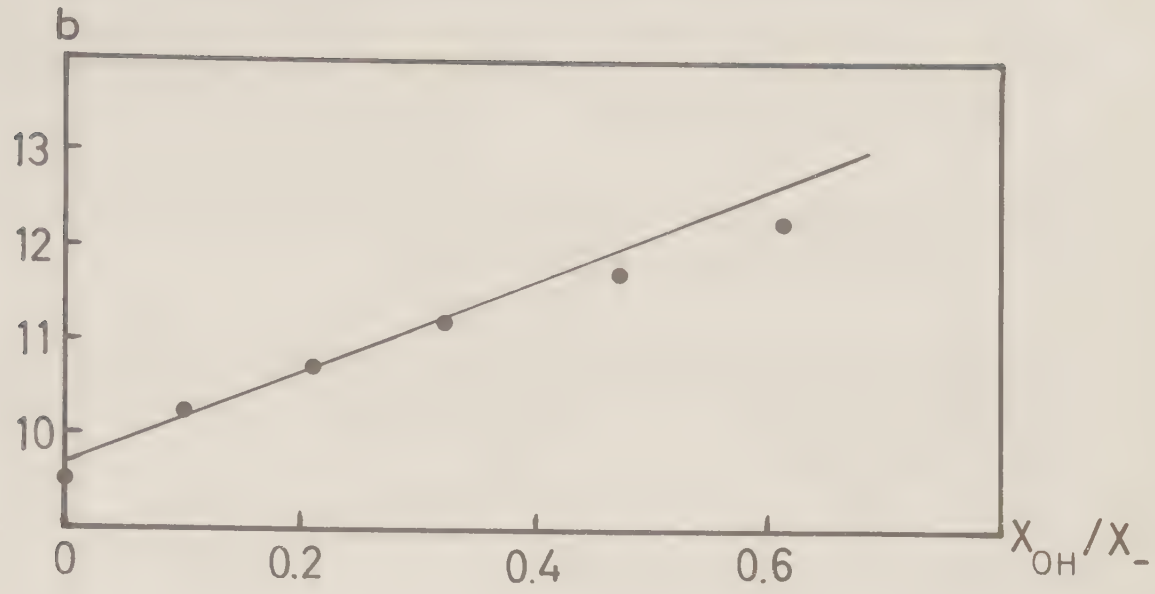

Figure 42. Calculated thickness of the lamellar amphiphile aggregate as a function of the mole fraction of alcohol for the three component system potassium caprate-decanol-water at 55°C. The X-ray data ● is from ref. (55).

The curves of constant thickness of the amphiphilic layer are in fig. 43 drawn for the system potassium caprate - octanol - water at 20 °C. The dotted curve is where the amphiphilic molecules are at there maximal length $b = b_{max}$. Here must be noted that $b = b_{max}$ is equivalent to say that the area per amphiphilic molecule is as small as possible.

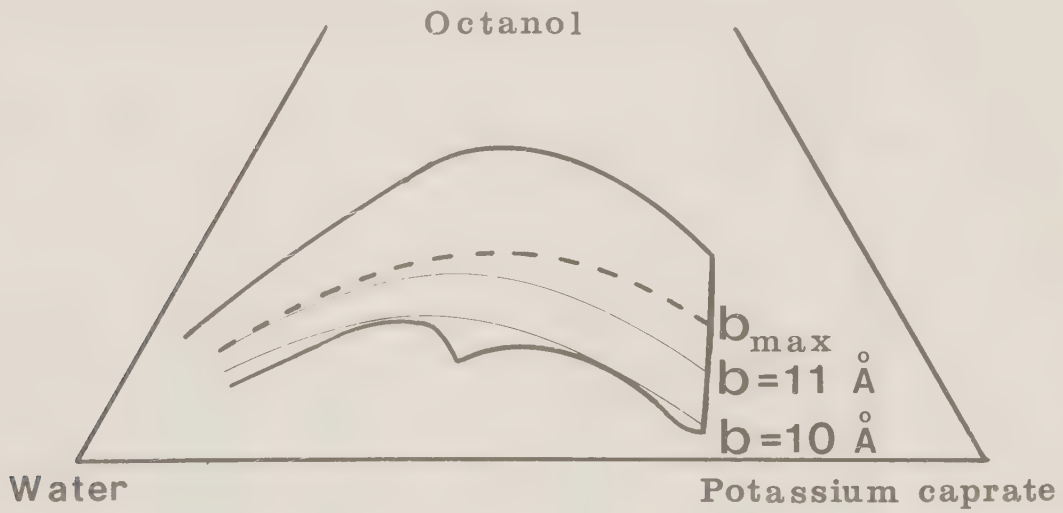

Figure 43. Calculated lines of constant and maximal aggregate thickness plotted for the lamellar mesophase of the three component system potassium caprate-octanol-water at 20 °C.

There are two interesting properties that can be seen in fig. 43.

1. The area per amphiphilic molecule is in a large part of the lamellar phase at its minimum value.

2. The phase boundaries nearly coincide with constant thickness curves calculated from the thermodynamic model.

The formula for the thickness of the amphiphilic layer when $b = b_{max}$ is, if the minimum area of the amphiphilic molecules A_{min} is about the same for the components,

$$2 \cdot b_{max} = \frac{2}{A_{min}} \cdot \Sigma X_{ja} \cdot V_{ja} \qquad (129)$$

At 20 ^{o}C the values of V_{COO}/A_{min} for potassium caprate and V_{OH}/A_{min} for octanol is approximately

$$V_{COO}/A_{min} \simeq 12.7 \text{ Å} \quad \text{and} \quad V_{OH}/A_{min} \simeq 10.5 \text{ Å}$$

Experimental X-ray values of b for the system can be found in table 6 (the experimental values are from ref. (49)).

Table 6. Aggregate dimensions for the lamellar mesophase in the system caprate-octanol-water from X-ray measurements (ref.(49)).

Composition (%)			The thickness of the amphiphilic layer
KC_{10}	Oct.	H_2O	2 • b
64.0	3.9	32.1	19.7
64.3	7.1	28.6	20.8
59.3	11.1	29.6	20.8
59.1	14.8	26.1	21.9
52.3	13.1	34.6	20.1
53.8	23.1	23.1	23.4
41.4	17.7	40.9	20.1
42.8	28.6	28.6	22.5
29.1	19.5	51.4	21.3
25.0	37.5	37.5	21.6
19.4	29.1	51.4	21.3
15.6	23.3	61.1	21.5
8.6	12.9	78.5	21.4

The same type of curves is in fig. 44 drawn for the system octanoate - decanol - water at 20 °C, and in table 7 are the corresponding experimental values (ref. (49)).

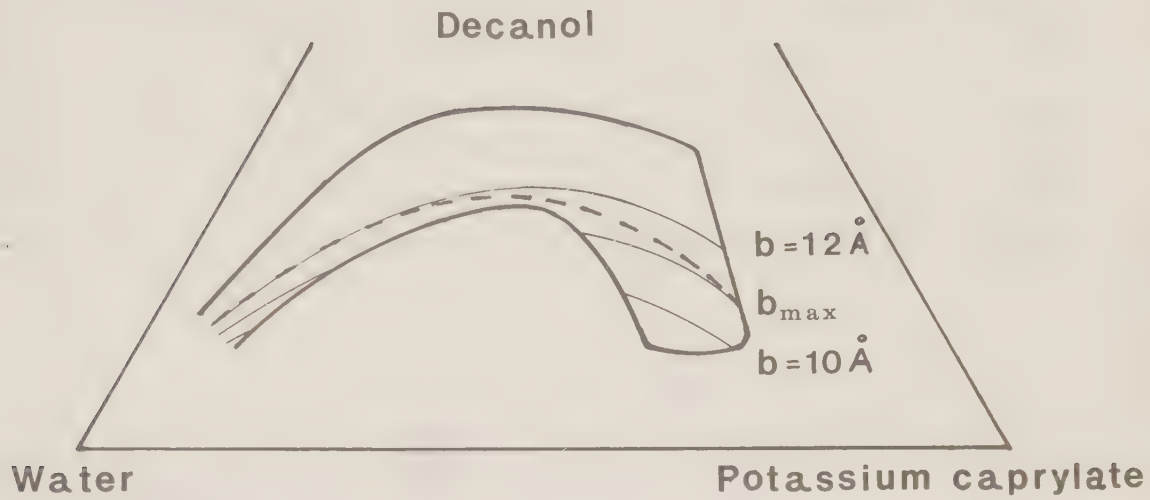

Figure 44. Calculated lines of constant and maximal aggregate thickness plotted for the lamellar mesophase of the three component system potassium caprylate-decanol-water at 20 °C.

Table 7. Aggregate dimensions for the lamellar mesophase in the system caprylate-decanol-water from X-ray measurements (ref. (49)).

Composition (%)			The thickness of the amphiphilic layer
KC_8	Dec.	H_2O	2 • b
62.5	12.4	25.1	19.4
60.0	12.0	28.0	19.0
55.8	23.9	20.3	21.8
51.3	21.9	26.8	20.4
44.7	36.6	18.7	24.0
39.8	32.5	27.7	22.4
37.0	30.3	32.7	21.9
23.3	41.4	35.3	23.8
18.9	33.7	47.4	23.9
18.8	43.9	37.3	23.9
13.5	31.6	54.9	24.3
6.0	14.1	79.9	26.5

It is now also possible to predict phase boundaries for three-component systems. The calculation process that was used in chapter 9 to predict phase boundaries in two component systems can also be used in this case if the chemical potential of the alcoholic component can be assumed constant during a calculation process. The strategy is now to assume a value of the chemical potential of the alcohol. This is equivalent to say that the c_{OH} concentration (c_{OH} is the concentration of alcohol in the aqueous part) shall be at a fixed value. When the restriction c_{OH} = constant is fulfilled the calculations will be exactly the same as in chapter 9. From the intersections of the calculated characteristic lines the composition of the different phases in equilibrium are obtained and the tie-line can be drawn (see fig. 45).

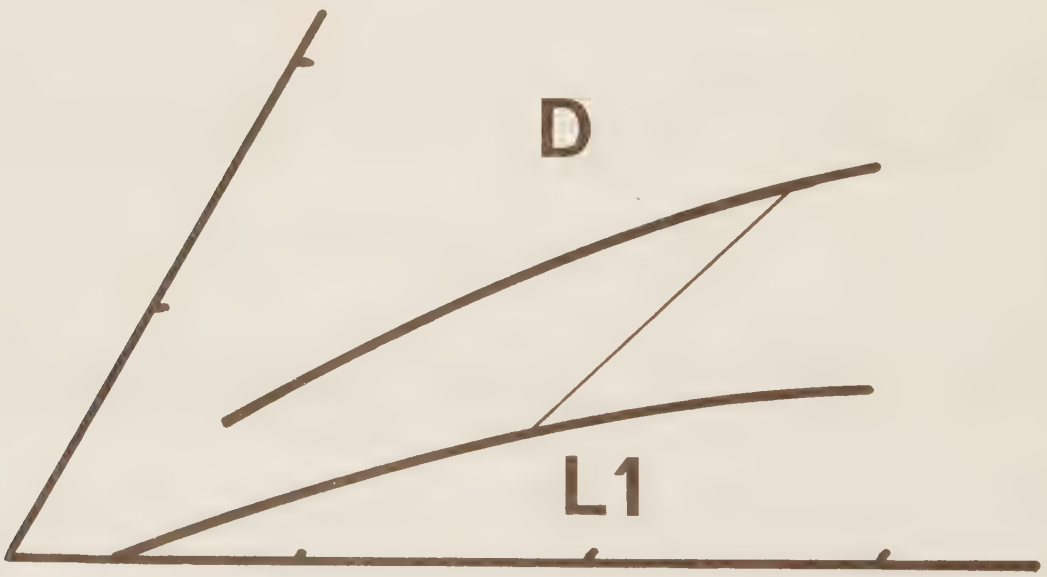

Figure 45. A convenient way to represent two different mesophases in equilibrium is to draw a tie-line between the two different compositions that are in equilibrium.

If the c_{OH} concentration then is changed to another value a new tie-line is calculated and by repeating this process a theoretical phase-diagram of a three-component system may be constructed. The three-phase triangles that exist in three-component systems will in this model be the concentrations where all three characteristic lines intersect at the same point and can consequently be predicted.

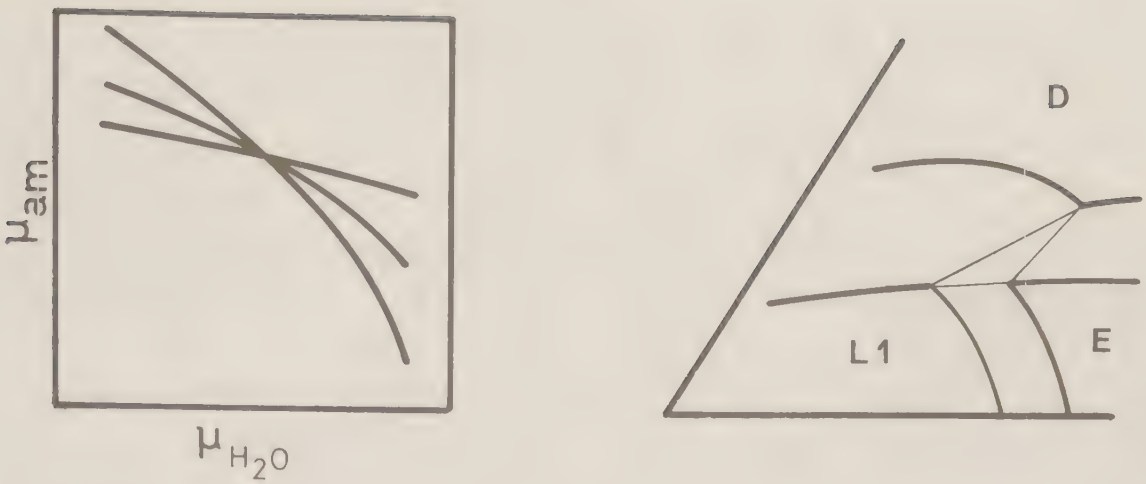

Figure 46. A three phase triangle is obtained when three characteristic lines intersect at the same point.

It must however be pointed out that not all characteristic line intersections will predict phase equilibria. When the characteristic line of another phase is below an intersection point this phase will of course be the most stable one (see fig. 47).

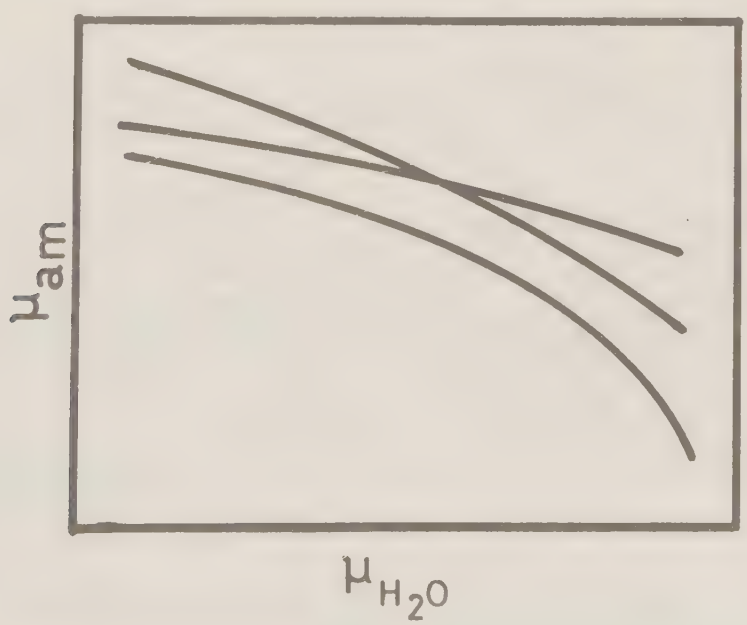

Figure 47. Characteristic lines.

The constraint that c_{OH} shall be constant in a calculation serie is a difficult problem to solve and there are perhaps better ways to do it than the method presented here.

1. Make an intelligent guess on the value of X_{OH}.

2. Calculate all c_{iO} values.

3. If the c_{OH} value is not the predicted one, repeat the calculations with a new X_{OH}.

The phase boundaries of the three-component system decanoate - octanol - water have been calculated with the proposed method and the result can be seen in fig. 48. The experimental phase diagram is found in fig. 49. Although the difference between the theoretical and the experimental phase diagrams is significant, the main characteristics are the same. The underestimate of the extension of the L_1 phase in the theoretical model probably depends on the ability of the micelles to grow to rods or discs at high amphiphile concentrations, an effect not included in the present model.

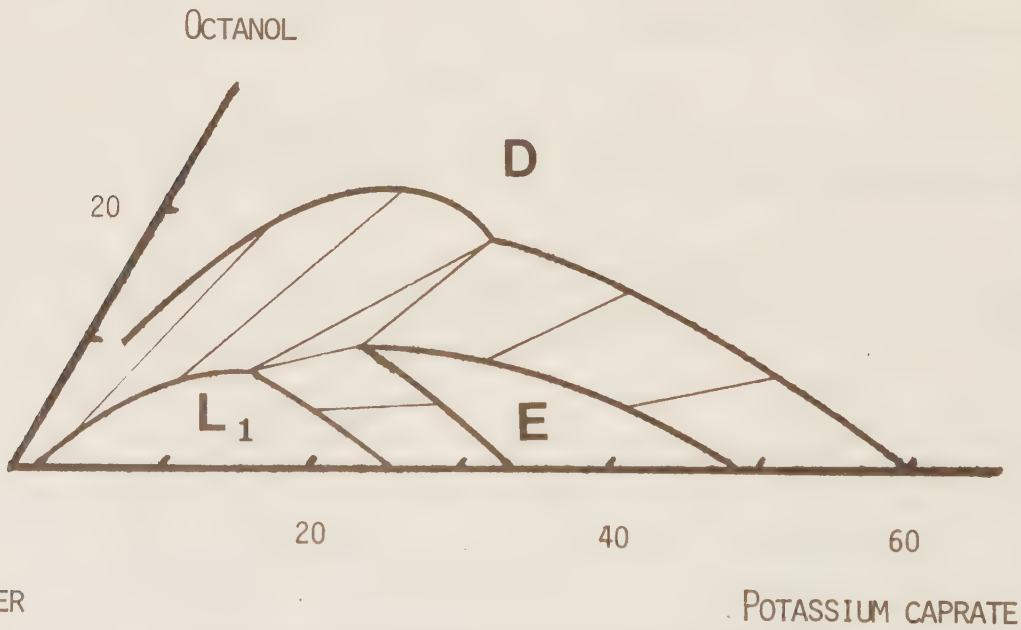

Figure 48. Calculated phase diagram for the three component system potassium caprate-octanol-water at 20°C.

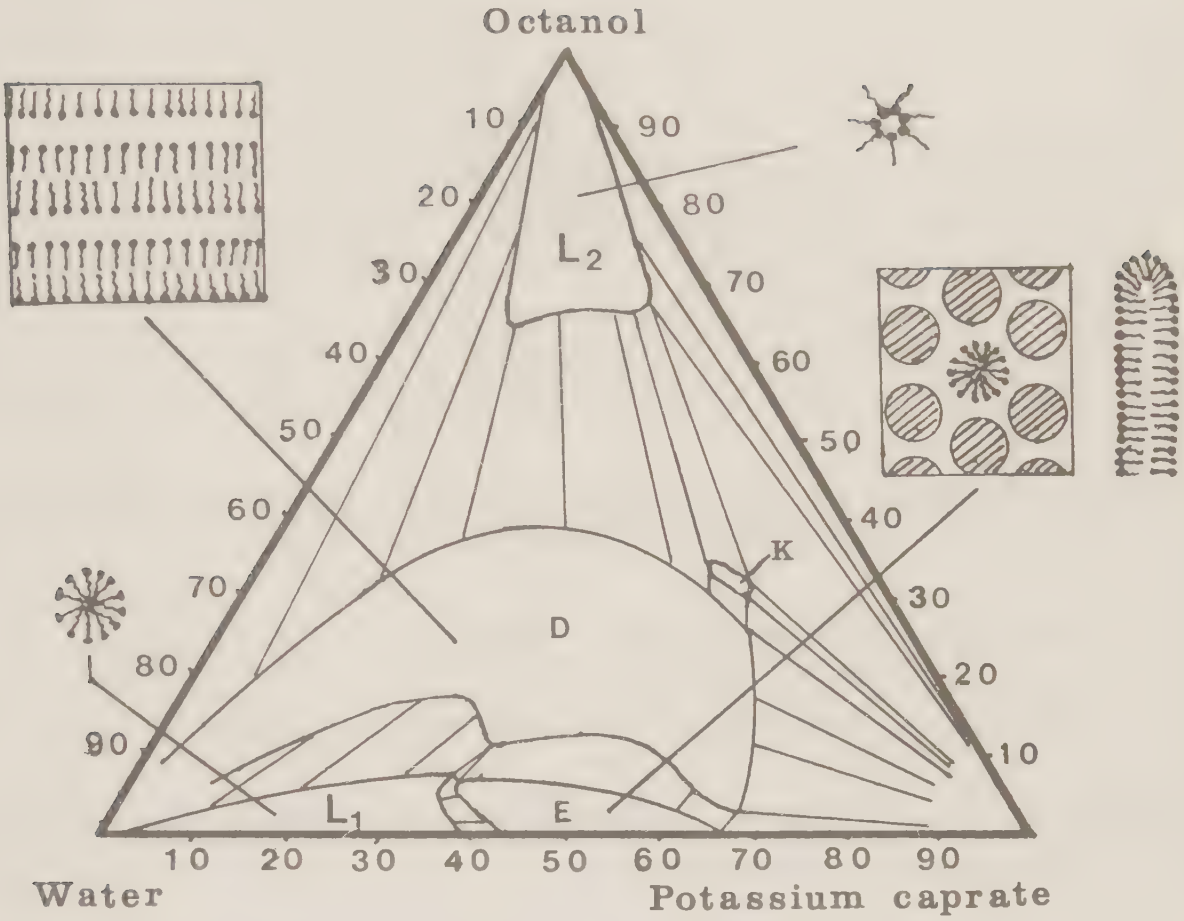

Figure 49. Phase diagram of the ternary system potassium caprate-octanol-water at 20 °C. From ref. (49).

The assumption that the amphiphilic molecules in the aggregates are anchored with there polar part at the interface that has been used in the preceding calculations may be questionable in some cases. Especially if the third component is an hydrocarbon there must be an opportunity for the molecules to be in the interior of the aggregates. This new assumption must of course change the theory but if the following assumptions are made the changes can easily be handled.

1. The aggregates are split into two parts, an interior part I and a "palisade" part II (see fig. 50).

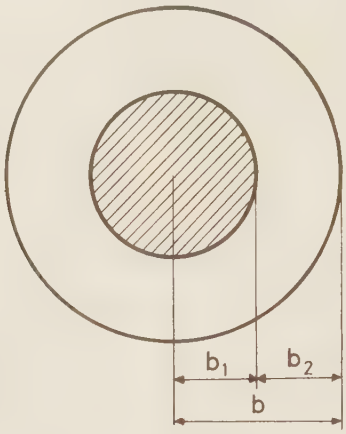

Figure 50. Schematic representation of the palisade part and the interior of an amphiphilic aggregate.

2. There will be no charged groups in part I.

3. The molecules in part II will be anchored at the surface.

The chemical potentials of the components in the aggregate (see eq. (122)) will be altered in the following ways.

a. μ^o_{ia} is now the "standard" chemical potential of a component in I or II depending on the location of ia.

b. X_{ia} is in the same way the mole fraction of component ia in I or II depending on the location of ia.

There will however be a problem with the derivative db/dn which now depends on both b_I and b_{II} (see fig. 50). But on the other hand the ratio b_I/b_{II} is dependent on the number of molecules in part I and II. It will therefore be possible to replace db/dn by the derivatives of db_{II}/dn, dn_I/dn and dn_{II}/dn and this will now be done.

From the volume ratio of parts I and II the following equation may be obtained

$$\left(\frac{b}{b_I}\right)^d = 1 + \frac{\sum n_{ja,II} \cdot \bar{V}_{ja}}{\sum n_{ja,I} \cdot \bar{V}_{ja}} \tag{130}$$

where $n_{ja,I}$ stands for the number of molecules ja in part I and in the same way $n_{ja,II}$ is the number of molecules ja in part II. The derivative $(A/b)\cdot(db/dn_i)$ may now be calculated.

$$\frac{A}{b} \cdot \frac{db}{dn_i} = \frac{A}{b_I} \cdot \frac{db_I}{dn_i} + \frac{\bar{V}_{ia}}{b} \cdot \left\{ \sum_{ja} \frac{dn_{ja,II}}{dn_i} - \left(\left(\frac{b}{b_I}\right)^d - 1\right) \cdot \sum_{ja} \frac{dn_{ja,I}}{dn_i} \right\} \tag{131}$$

But $b = b_I + b_{II}$ and equation (131) becomes

$$\frac{A}{b} \cdot \frac{db}{dn_i} = \frac{A}{b_{II}} \cdot \frac{db_{II}}{dn_i} - \bar{V}_{ia} \cdot \frac{b_I}{b_{II}\, b} \left\{ \sum_{ja} \frac{dn_{ja,II}}{dn_i} - \left(\left(\frac{b}{b_I}\right)^d - 1\right) \cdot \right.$$

$$\left. \cdot \sum_{ja} \frac{dn_{ja,I}}{dn_i} \right\} \tag{132}$$

The chemical potentials of the components in parts I and II become

$$\mu_{ia,I} = \mu^o_{ia,I} + kT \cdot \ln X_{ia,I} + H_1 + \left(\frac{b}{b_I}\right)^{d-1} \cdot \frac{\bar{V}_{ia}}{b_{II}} \cdot H_2 \tag{133}$$

$$\mu_{ia,II} = \mu^o_{ia,II} + z_{ia} \cdot e \cdot \Phi_A + kT \cdot \ln X_{ia,II} + H_1 \tag{134}$$

where

$$H_2 = 2 \cdot E^o_{el}/A - \gamma \tag{135}$$

and

$$H_1 = -\frac{\bar{V}_{ia}}{\sum_{ja} n_{ja}\cdot\bar{V}_{ja}} \cdot \{E^o_{el} + \int U(r)\, dV - (V_T - n_{ja}\cdot\bar{V}_{ja}\cdot\frac{V_i}{\bar{V}_{ia}})\cdot U(R) -$$

$$- A_a\cdot(\gamma + \frac{\partial\gamma}{\partial n_{ia,II}} \cdot \frac{\sum n_{ja}\cdot\bar{V}_{ja}}{\bar{V}_{ia}}) + \frac{\sum n_{ja}\cdot\bar{V}_{ja}\cdot b_I}{b\cdot b_{II}} \cdot H_2\} \qquad (136)$$

The summation is over all components in the whole aggregate.

It can easily be shown for the lamellar case (d=1) (see eq. A20 in appendix III) that $H_1 + \bar{V}_{ia}\cdot H_2/b_{II} = 0$ which means that the chemical potential of ia will be constant if $X_{ia,I} = 1$ (only one component in part I). This means that the hydrocarbons are allowed to be in part I of a lamellar system only if the phase is in equilibrium with pure hydrocarbon (if the $\mu^o_{ia,I}$ value is the same as in pure hydrocarbons).

From the condition of chemical equilibrium $\mu_{ia,I} = \mu_{ia,II}$ the following equation may be obtained.

$$(b_I/b)^{d-1} = \bar{V}_{ia}\cdot H_2/(b_{II}\cdot\{\mu^o_{ia,II} - \mu^o_{ia,I} + kT\cdot\ln(X_{ia,II}/X_{ia,I})\}) \qquad (137)$$

It is interesting to see that if b_{II} is free to adjust (H_2 is then zero), then $b_I = 0$ or

$$\mu^o_{ia,II} - \mu^o_{ia,I} + kT\cdot\ln(X_{ia,II}/X_{ia,I}) = 0 \qquad (138)$$

The earlier obtained calculation process in calculating phase diagrams can together with equations (137) and (138) also be used for this type of systems and especially if only one component is allowed to be in part I then this type of systems will render no calculation difficulties.

11. SYSTEMS OF THE REVERSED TYPE

All systems in the previous chapters were of a type where the aggregates are surronded by water. In this chapter systems of the reversed type, where the water and amphiphile regions have changed place (see fig. 51), shall be treated.

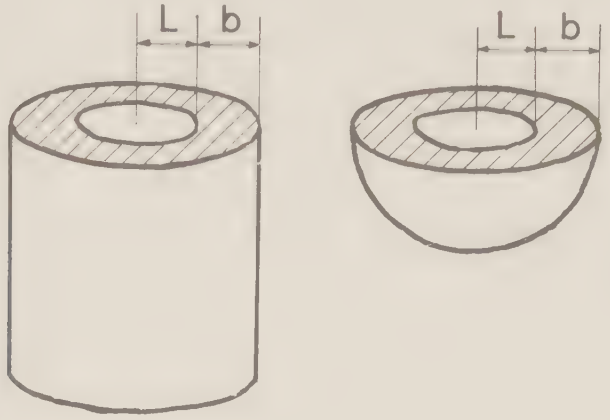

Figure 51. Designations used for the reversed systems.

Note that the lamellar system may be treated both as a normal and a reversed system. Eq. (50) for the free energy G may also be used for reversed systems. When calculating the chemical potentials the equations of chapter 5 may be used up to eq. (73) except that $-\partial b/\partial n_p$ is replaced by $\partial L/\partial n_p$ (concerning the definition of L, see fig. 51). The definition of $(\partial L/\partial n_p)\cdot\{E_{el}-TS\}$ may be transformed to the following equation in the same manner as the calculations in appendix III (concerning the calculations, see appendix V).

$$\frac{\partial}{\partial n_p}\{E_{el} - TS\} = \frac{\partial n_i}{\partial n_p}\, kT\cdot\ln c_{iL} + \frac{\partial f}{\partial c_i}(L) + \frac{V_i}{\Sigma\, n_j\cdot V_j}\cdot(E^o_{el} - \int U(r)\, dV)\} -$$

$$- A_{a,min}\cdot 2\cdot E^o_{el}/A\cdot\frac{\partial n_a}{\partial n_p} - \frac{dA^{\prime}}{dn_p}\cdot 2\cdot E^o_{el}/A \qquad (139)$$

where

$$A^{\prime} = A - n_a\cdot A_{a,min} \qquad (140)$$

It is also assumed that $b_1 = 0$.

Adding the derivative of $\gamma \cdot A$ gives the chemical potentials.

$$\mu_i = \mu_i^o + kT \cdot \ln c_{iL} + \frac{\partial f}{\partial c_i}(L) + \frac{V_i}{\Sigma n_j \cdot V_j} (E_{el}^o - \int U(r)\, dV) \qquad (141)$$

$$\mu_{H_2O} = \mu_{H_2O}^o + \frac{V_{H_2O}}{\Sigma n_j \cdot V_j} (E_{el}^o - \int U(r)\, dV) \qquad (142)$$

$$\mu_a = \mu_a^o - A_{a,min} \cdot (2 \cdot E_{el}^o / A - \gamma) \qquad (143)$$

and

$$\frac{\partial G}{\partial A} = - (2 \cdot E_{el}^o / A - \gamma) \qquad (144)$$

The summation $\Sigma n_j \cdot V_j$ is over all components in the water part.

These equations are much easier to handle than the corresponding equations for the normal systems and as shall be seen the extendence of the theory to multicomponent systems does not complicate the equations.

If the amphiphilic region is divided into two parts, one outer part I and a "palisade" part II (see fig. 52) the following changes in the theory must be made.

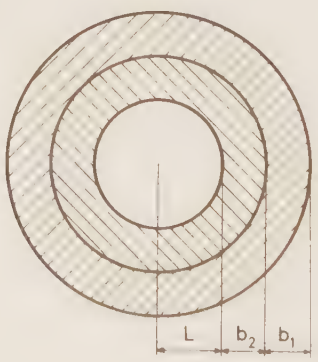

Figure 52. Schematic representation of the palisade part of a reversed system.

1. The contributions to the free energy from the mixing of the components in part I and II must be added.

2. The γ value will depend on the mole ratios in part II.

3. If the system is reversed micelles there will be a free energy contribution from the mixing of the micelles. The water part and part II will in the calculation of this energy contribution be regarded as one unit. The derivative of G_{mix}^{mic} then becomes

$$\frac{dG_{mix}^{mic}}{dn_p} = kT \cdot \frac{dN}{dn_p} \cdot \ln\left(\frac{N}{N + n_I}\right) + kT \cdot \frac{dn_I}{dn_p} \cdot \ln\left(\frac{n_I}{N + n_I}\right) \qquad (145)$$

where N is the number of reversed micelles and n_I is the number of molecules in part I.

dN/dn_p may be calculated from the following equation

$$N \cdot (V_{aq})^2 = A^3 \qquad (146)$$

$$\frac{dN}{dn_p} = \frac{3 \cdot N}{A} \cdot \frac{dA'}{dn_p} + \frac{3 \cdot N}{A} \cdot \frac{d}{dn_p}(\Sigma\, n_{ja,II} \cdot A_{ja,II,min}) -$$

$$- \frac{2 \cdot N}{\Sigma\, n_i \cdot V_i} \cdot \frac{d}{dn_p}(\Sigma\, n_i \cdot V_i) \qquad (147)$$

The chemical potentials for this kind of system may be written

$$\mu_i = \mu_i^o + kT \cdot \ln c_{iL} + \frac{\partial f}{\partial c_i}(L) + \frac{V_i}{\Sigma\, n_j \cdot V_j} \{E_{el}^o - \int U(r)\, dV -$$

$$- 2 \cdot N \cdot kT \cdot \ln\left(\frac{N}{N + n_I}\right)\} \qquad (148)$$

$$\mu_{H_2O} = \mu_{H_2O}^o + \frac{V_{H_2O}}{\Sigma\, n_j \cdot V_j} \{E_{el}^o - \int U(r)\, dV - 2 \cdot N \cdot kT \cdot \ln\left(\frac{N}{N + n_I}\right)\} \qquad (149)$$

$$\mu_{ia,II} = \mu^{o}_{ia,II} - A_{ia,II,min}\cdot\{2\cdot E^{o}_{el}/A - \gamma - \frac{3\cdot N}{A}\cdot kT\cdot\ln(\frac{N}{N + n_I})\} +$$

$$+ \frac{d\gamma}{dn_{ia,II}}\cdot A + kT\cdot\ln X_{ia,II} \qquad (150)$$

$$\mu_{ia,I} = \mu^{o}_{ia,I} + kT\cdot\ln X_{ia,I} + kT\cdot\ln(\frac{n_I}{N + n_I}) \qquad (151)$$

and

$$\frac{dG}{dA} = -\{2\cdot E^{o}_{el}/A - \gamma - \frac{3\cdot N}{A}\cdot kT\cdot\ln(\frac{N}{N + n_I})\} \qquad (152)$$

It is from eq. (151) clear that the chemical potentials in part I are not affected by the water or palisade part for the lamellar and reversed hexagonal systems. For the lamellar case this has already been shown in chapter 10.

From these equations it is possible to calculate phase equilibria if the PB equation may be solved and it shows up to be no problem. Especially if the water part only contains counterions because then there exists an analytic solution to the PB equation in the reversed cylindrical case and in the reversed micellar case a polynom approximation can be made.

The solution of the PB equation in the reversed cylindrical case is (see appendix VI)

$$\Phi(r) = \frac{2\cdot kT}{z\cdot e}\cdot\ln\{1 - \frac{\sigma\cdot e\cdot z\cdot L}{4\cdot\varepsilon_o\varepsilon_r\cdot kT}\cdot(1 - r^2/L^2)\} \qquad (153)$$

$$c(L) = -\frac{2\cdot\sigma}{N_A\cdot e\cdot z\cdot L}\cdot(1 - \frac{\sigma\cdot e\cdot z\cdot L}{4\cdot\varepsilon_o\varepsilon_r\cdot kT}) \qquad (154)$$

and E_{el}/A becomes

$$E_{el}/A = kT \cdot \{- \frac{\sigma}{e \cdot z} - \frac{4 \cdot \varepsilon_o \varepsilon_r \cdot kT}{L \cdot e^2 \cdot z^2 \cdot N_A} \cdot \ln(1 - \frac{\sigma \cdot e \cdot z \cdot L}{4 \cdot \varepsilon_o \varepsilon_r \cdot kT})\} \quad (155)$$

The PB equation in the reversed micellar case may be transformed to

$$\frac{1}{x^2} \cdot \frac{d}{dx}(x^2 \cdot \frac{d\Phi_1}{dx}) = - K_1 \cdot \exp(- \Phi_1) \quad (156)$$

where

$$x = r/L \quad (157)$$

$$\Phi_1 = e \cdot z \cdot \Phi / kT \quad (158)$$

$$K_1 = e^2 \cdot z^2 \cdot N_A \cdot c(L) \cdot L^2 / (\varepsilon_o \varepsilon_r \cdot kT) \quad (159)$$

and the boundary condition $(d\Phi(L)/dr) = \sigma/(\varepsilon_o \varepsilon_r)$ becomes

$$\frac{d\Phi_1}{dx}(1) = \frac{\sigma \cdot e \cdot z \cdot L}{\varepsilon_o \varepsilon_r \cdot kT} = K_2 \quad (160)$$

It is now possible to solve eq. (156) numerically with the boundary condition (160) and a connection between K_1 and K_2 may then be obtained. $\sqrt{K_1}$ is in fig. 53 plotted as a function of K_2.

The connection between E_{el}/A and K_2 may be obtained in the same way (see fig. 54).

These connections may also be written as polynom approximations if they shall be used in numerical calculations.

When there also is salt present in the aqueous part the PB equation must be solved in a numerical way, but this is often easy to do and the methods used in chapter 7 apply also to this case.

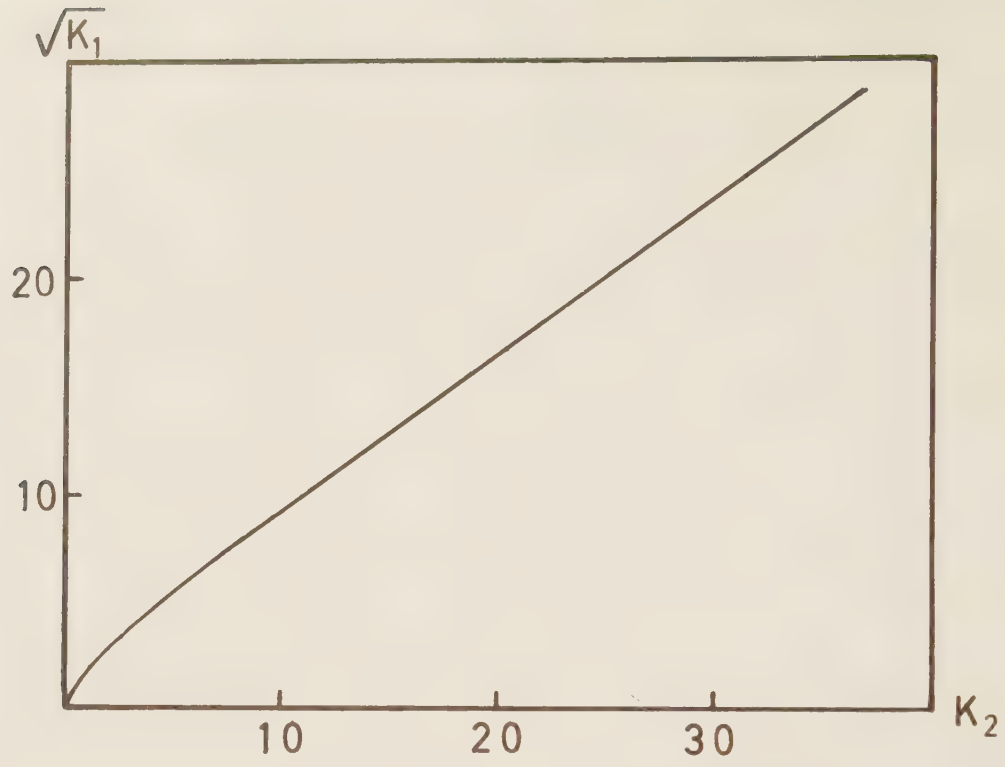

Figure 53. $\sqrt{K_1}$ as a function of K_2.

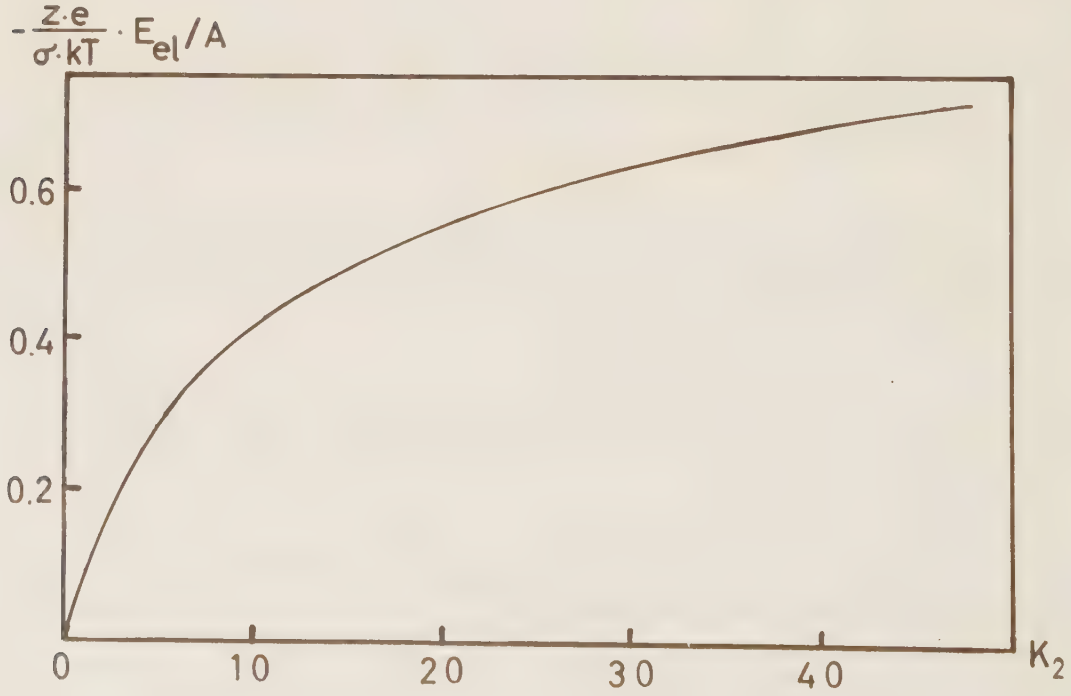

Figure 54. $-\frac{e \cdot z}{\sigma \cdot kT} \cdot E_{el}/A$ as a function of K_2.

CONCLUDING REFLECTIONS

Is it from the model presented in this work possible to describe more complicated amphiphile-water systems, or must a completely new model be made? The best way to get an answer to this question is to test different theoretical predictions against experimental values and from the agreement between theory and experiment decide if the model can be used. Some deficiencies in the model have however already appeared, especially the idealization of all interactions except the electrostatic in and at the surface of the amphiphilic aggregates by two parameters μ_a^o and $\gamma \cdot A$. These assumptions must probably be modified when more knowledge of the systems is achieved.

The ability of the model to predict phase equilibria in the systems studied up to now is probably dependent on the high charge densities in these systems. The electrostatic interactions are then the dominating contribution to the free energy and the PB or MPB equations probably describe the electrostatic interactions in a rather good way.

In low charge systems the situation is quite different and it will not be surprising if the predictions from the model deviate from the experimental determinations for such systems.

An advantage with the presented calculation model is that the number of energy contributions from different interactions can be extended without considerable complications in the calculation process. It is first when the effect of different possible interactions are tested as a deeper understanding of the thermodynamics of amphiphile-water systems can be achieved.

It is probable that many of the questions here described will be answered in a near future, and it is my hope that this work in a modest way can contribute to the understanding of amphiphile-water systems.

References

1. Winsor, P., Chem. Rev. 68, 1 (1968)

2. Ekwall, P., in "Advances in Liqiud Crystals" (G. Brown, Ed.) Vol. 1, p. 1, Academic Press, New York, 1975.

3. Tiddy, G.J.T., Phys. Reports 57, 1 (1980).

4. Fontell, K., Mol. Cryst. Liq. Cryst., in press.

5. Charvolin, J. and Rigny, P., J. Chem. Phys. 58, 3999 (1973).

6. Rosenholm, J.B. and Lindman, B., J. Colloid Interface Sci. 57, 362 (1976).

7. Ulmius, J. and Wennerström, H., J. Magn. Reson. 28, 309 (1977).

8. Rosenholm, J.B., Hakala, M.-R. and Stenius, P., Mol. Cryst. Liq. Cryst. 45, 285 (1978).

9. Lindblom, G. and Wennerström, H., Biophys. Chem. 6, 167 (1977).

10. Wennerström, H. and Lindman, B., Phys. Rep. 52, 1 (1979).

11. Ekwall, P., Danielsson, I. and Stenius, P., in "Surface Chemistry and Colloids", (M. Kerker, Ed.), MTP Intern. Rev. Sci., Phys. Chem. Ser. 1, vol 7, p. 97, Butterworths, London 1972.

12. Gunnarsson, G., to be published.

13. Hill, T.L., "Statistical Mechanics", Addison and Wesley, Reading Mass. 1960.

14. Wennerström, H., Lindman, B., Söderman, O., Drakenberg, T. and Rosenholm, J.B., J. Amer. Chem. Soc. 101, 6860 (1979).

15. Henriksson, U., Klason, T., Ödberg, L. and Eriksson, J.-C., Chem. Phys. Letters 52, 554 (1979).

16. Lindblom, G., Lindman, B. and Mandell, L., J. Colloid Interface Sci. 42, 400(1973).

17. Wennerström, H., Persson, N.-O. and Lindman, B., in "Colloidal Dispersion and Micellar Behaviour", (K.L. Mittal, Ed.), ACS Symposia Series 9, p. 253, American Chemical Society, Washington D.C. 1975.

18. Danielsson, I., Rosenholm, J.B., Stenius, P. and Backlund, S., Progr. Colloid and Polymer Sci. 61, 1 (1976).

19. Hamnerius, Y., Lundström, I., Paulsson, L.E., Fontell, K. and Wennerström, H., Chem. Phys. Lipids 22, 135 (1978).

20. Lindman, B. and Wennerström, H., in "Topics in Current Chemistry", Vol. 87, p. 1, Springer Berlin 1980.

21. Wennerström, H. and Lindman, B., J. Phys. Chem. 83, 2931 (1979).

22. Tanford, C., "The hydrophobic effect", Wiley, New York 1973.

23. Franks, F., "Water a comprehensive treatise", (F. Franks, Ed.), Vol. 4, chap. 2, Plenum Press, New York 1974.

24. Goodman, D.S., J. Amer. Chem. Soc. 80, 3887 (1958).

25. McAuliffe, C., J. Phys. Chem. 70, 1267 (1966).

26. Kinoshita, K., Ishikawa, H. and Shinoda, K., Bull. Chem. Soc. Japan 30, 1081 (1958).

27. Gill, S.J., Nichols, N.F. and Wadsö, I., J. Chem. Thermodyn. 8, 445 (1976).

28. Nichols, N.F. et al., J. Chem. Thermodyn. 8, 1081 (1976).

29. Gunnarsson, G., Jönsson, B. and Wennerström, H., J. Phys. Chem. 84, 3114 (1980).

30. Weast, R.C., "Handbook of Chemistry and Physics", CRC Press.

31. Brun, T.S., Høiland, H. and Vikingstad, E., J. Colloid Interface Sci. 63, 89 (1978).

32. Vikingstad, E. and Høiland, H., J. Colloid Interface Sci. 64, 510 (1978).

33. Aniansson, E.A.G., J. Phys. Chem. 82, 2805 (1978).

34. Mandell, L., Fontell, K., Lehtinen, H. and Ekwall, P., Acta Polytechn. Scand. Chem. Met. Series, no. 74, (1968).

35. Vikingstad, E., Thesis, Kjemisk Institutt, Universitetet i Bergen (1980).

36. Gallot, P.B. and Skoulios, A., Kolloid Z. Z. Polym. 208, 37 (1966).

37. Bjerrum, N., Z. Physik Chem. 119, 145 (1926).

38. Dzyaloshinskii, I.E., Lifshitz, E.M. and Pitaevskii, L.P., Advan. Phys. 10, 165 (1961).

39. Mahanty, J. and Ninham, B.W., "Dispersion Forces", Academic Press, London (1976).

40. Jönsson, B., Wennerström, H. and Halle, B., J. Phys. Chem. 84 2179 (1980).

41. Engström, S. and Wennerström, H., J. Phys. Chem. 82, 2711 (1978).

42. Fuoss, R., Katchalsky, A. and Lifson, S., Proc. Natl. Acad. Sci. 37, 579 (1951).

43. Alfrey, T., Berg, P.W. and Morawetz, H., J. Polym. Sci. 7, 543 (1951).

44. Gilg, P.B., Francois, J. and Skoulios, A., Kolloid Z. Z. Polym. 205, 139 (1965).

45. Ekwall, P., Mandell, L. and Fontell, K., J. Colloid Interface Sci. 33, 215 (1970).

46. Fontell, K., J. Colloid Interface Sci. 44, 318 (1973).

47. McBain, J.W. and Sierichs, W.C., J, Amer. Oil Chem. Soc. 25, 221 (1948).

48. Staples, E.J. and Tiddy, G.J.T., J. Chem. Soc. Faraday I, 74, 2530 (1978).

49. Ekwall, P., Mandell, L. and Fontell, K., J. Colloid Interface Sci. 31, 508 (1969).

50. Jönsson, B. and Wennerström, H., Chem. Scr. 15, 40 (1980).

51. Jönsson, B. and Wennerström, H., J. Colloid Interface Sci., in press.

52. Arfken, G., "Mathematical methods for physicists", Academic Press.

53. Björck, A. and Dahlquist, G., "Numeriska metoder", Gleerups, Lund 1969.

54. Cutler, S.G., Mears, P. and Hall, D.G., J. Chem. Soc. Faraday I, 74, 1758 (1978).

55. Fontell, K., unpublished results.

56. Ekwall, P., Mandell, L. and Fontell, K., Mol. Cryst. Liq. Cryst. 8, 157 (1969).

Appendix I

The contribution to the free energy from the pair correlation between the ions.

The value of the "fluctuation potential" $\hat{\Psi}(x)$ will in this appendix be calculated from eq. (41).

$$\frac{1}{x^2} \cdot \frac{d}{dx}(x^2 \cdot \hat{\Psi}(x)) = - \sum_i \frac{N_A \cdot e \cdot z_i \cdot c_i}{\varepsilon_o \varepsilon_r} \cdot \{\exp(- z_i \cdot e \cdot \hat{\Psi}/kT) - 1\} \qquad (41)$$

where $x = |r - r_j|$, c_i the mean concentration of i at r_j and $\hat{\Psi}(x) = \langle \hat{\Psi} | r - r_j | \rangle$.

It is only possible to solve eq. (41) in an analytic way if the exponential is linearized.

$$\exp(- z_i \cdot e \cdot \hat{\Psi}/kT) = 1 - z_i \cdot e \cdot \hat{\Psi}/kT \qquad A1$$

and eq. (41) becomes

$$\frac{1}{x^2} \cdot \frac{d}{dx}(x^2 \cdot \frac{d\hat{\Psi}}{dx}) = \kappa^2 \cdot \hat{\Psi} \qquad A2$$

where

$$\kappa^2 = \sum_i \frac{N_A \cdot e^2 \cdot z_i^2 \cdot c_i}{\varepsilon_o \varepsilon_r \cdot kT} \qquad A3$$

The solution to eq. A2 is

$$\hat{\Psi} = A \cdot \frac{e^{-\kappa \cdot x}}{x} \qquad A4$$

where A is a constant of integration, that may be determined from the boundary condition

$$(\frac{\partial \hat{\Psi}}{\partial x})_{x \to 0} = - \frac{1}{4\pi \cdot \varepsilon_o \varepsilon_r} \cdot \frac{z_j \cdot e}{x^2} \qquad A5$$

The radius of the ion has in eq. A5 been assumed to be zero, but the calculations may also be performed without this limitation. The calculation will however be more involved in this case.

Combining A4 and A5 gives

$$\hat{\Psi} = \frac{z_j \cdot e}{4\pi \cdot \varepsilon_o \varepsilon_r} \cdot \frac{e^{-\kappa \cdot x}}{x} \qquad \text{A6}$$

and the equation for $\hat{\Psi}_j$ will then be

$$\hat{\Psi}_j = - \frac{z_j \cdot e}{4\pi \cdot \varepsilon_o \varepsilon_r} \cdot \kappa \qquad \text{A7}$$

It must here be remembered that $\exp(- z_i \cdot e \cdot \hat{\Psi}/kT)$ in eq. (41) stands for the pair correlation function $g_{ij}(r,r_j)$ (eq. (40)) and that $g_{ij}(r,r_j)$ can't be less then zero and it is zero only if $r \leq a$.

$$g_{ij}(r,r_j) = 0 \qquad r \leq a \qquad \text{A8}$$

where a is the distance of closest approach for two ions. It is therefore only possible to do the linearization A1 if

$$|z_i \cdot e \cdot \hat{\Psi}/kT| \leq 1 \qquad \text{A9}$$

This condition may be fulfilled if the concentration is small or if there are only ions with the same charge in the solution. If there only are ions of the same charge the distance of closest approach can be assigned a x-value that satisfies

$$|z_i \cdot e \cdot \hat{\Psi}(a)/kT| = 1 \qquad \text{A10}$$

If $x \leq a$ the solution to eq. (41) becomes

$$\hat{\Psi} = B + \Sigma \frac{N_A \cdot e \cdot c_i \cdot z_i}{6 \cdot \varepsilon_o \varepsilon_r} \cdot x^2 + \frac{z_j \cdot e}{4\pi \cdot \varepsilon_o \varepsilon_r} \cdot \frac{1}{x} \qquad \text{A11}$$

where B is a constant.

The values of B and also of A (eq. A4) may be calculated form the following boundary conditions.

$$\hat{\Psi}(x\to a, x<a) = \hat{\Psi}(x\to a, x>a) \qquad \text{A12}$$

and

$$\frac{d\hat{\Psi}}{dx}(x\to a, x<a) = \frac{d\hat{\Psi}}{dx}(x\to a, x>a) \qquad \text{A13}$$

If the concentration of ions is small equations A9 and A10 give

$$A = (z_j \cdot e)/(4\pi \cdot \varepsilon_o \varepsilon_r) \qquad \text{A14}$$

$$B = -(z_j \cdot e \cdot \kappa)/(4\pi \cdot \varepsilon_o \varepsilon_r) \qquad \text{A15}$$

But B is $\hat{\Psi}_j$ and will in this case be the same as eq. A7.

$$\hat{\Psi}_j = -\frac{z_j \cdot e \cdot \kappa}{4\pi \cdot \varepsilon_o \varepsilon_r} \qquad \text{A7}$$

The expression for B may at high ion concentrations differ remarkably from A15 because eq. A10 must here also be fulfilled. (Observe that this approximation is valid only if the ions have the same charge).

By combining equations A4, A10 - A13 the following expressions are obtained.

$$\frac{A}{a} \cdot e^{-\kappa \cdot a} = \frac{kT}{z_i \cdot e} \qquad \text{A16a}$$

$$\frac{N_A \cdot e \cdot z_i \cdot c_i}{6 \cdot \varepsilon_o \varepsilon_r} \cdot a^2 + \frac{e \cdot z_i}{4\pi \cdot \varepsilon_o \varepsilon_r} \cdot \frac{1}{a} + B = \frac{kT}{z_i \cdot e} \qquad \text{A16b}$$

$$A(1 + \kappa \cdot a) \cdot e^{-\kappa \cdot a} = \frac{z_i \cdot e}{4\pi \cdot \varepsilon_o \varepsilon_r} - \frac{N_A \cdot e \cdot c_i \cdot z_i}{3 \cdot \varepsilon_o \varepsilon_r} \cdot a^3 \qquad \text{A16c}$$

==>

$$A = a \cdot \frac{kT}{z_i \cdot e} \cdot \exp(\kappa \cdot a) \qquad \text{A17a}$$

$$B = - \frac{kT}{2 \cdot z_i \cdot e} \cdot \kappa \cdot a \cdot (2 + \kappa \cdot a) \qquad \text{A17b}$$

$$\kappa \cdot a = \left(\frac{3 \cdot z_i^2 \cdot e^2 \cdot \kappa}{4\pi \cdot \varepsilon_o \varepsilon_r \cdot kT} + 1 \right)^{1/3} - 1 \qquad \text{A17c}$$

$$\Rightarrow$$

$$B = - \frac{kT}{2 \cdot z_i \cdot e} \left\{ \left(\frac{3\kappa^3}{4\pi \cdot N_A \cdot c_i} + 1 \right)^{2/3} - 1 \right\} \qquad \text{A18}$$

But B is the same as $\hat{\Psi}_j$ and it is consequently also possible to calculate $\hat{\Psi}_j$ for this type of systems. The value of $\hat{\Psi}_j$ is in fig. A1 plotted as a function of the ionconcentration.

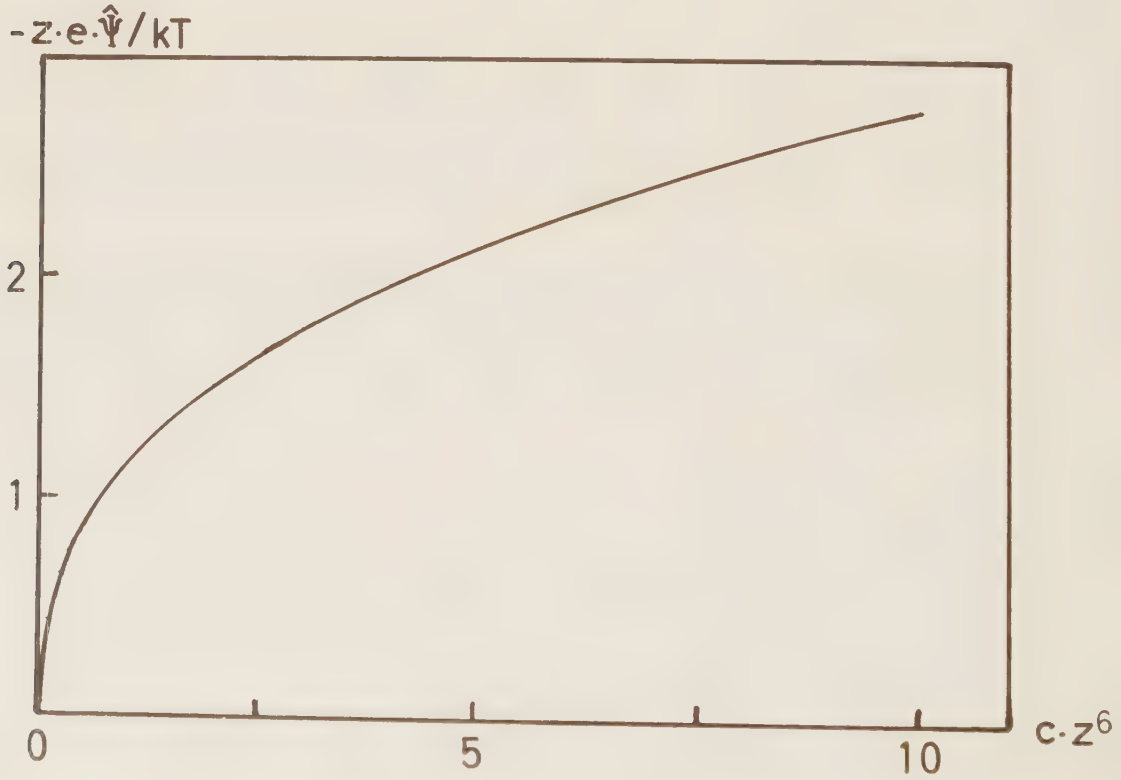

Figure A1. $- z \cdot e \cdot \hat{\Psi}_j / kT$ as a function of $c \cdot z^6$ at 298 K.

The free energy associated with the $\hat{\Psi}_j$-value may then be calculated from the integral

$$\Delta\hat{A} = \int_V \int_0^1 \hat{\Psi}_j(\lambda)\, d\lambda\, dV \qquad \text{A19}$$

The integration over the charging parameter λ gives

$$\int_0^1 \hat{\Psi}_j(\lambda)\, d\lambda = -\frac{kT}{4 \cdot z_i \cdot e} \{(1+Y)^{2/3} - 1 + \ln\left(\frac{(1+Y)^{1/3} - 1}{Y/3}\right) +$$

$$+ \frac{2}{\sqrt{3}} \cdot \arctan\left(\frac{1}{\sqrt{3}} \cdot \left(\frac{(1+Y)^{1/3} - 1}{(1+Y)^{1/3} + 1}\right)\right)\} \qquad \text{A20}$$

where

$$Y = \frac{3\kappa^3}{4\pi \cdot N_A \cdot c_i} = \frac{3}{4\pi} \cdot \left(\frac{e^2}{\varepsilon_0 \varepsilon_r \cdot kT}\right)^{3/2} \cdot \left(N_A \cdot c \cdot z_i^6\right)^{1/2} \qquad \text{A21}$$

The value of A20 is in fig. A2 plotted against the ionconcentration.

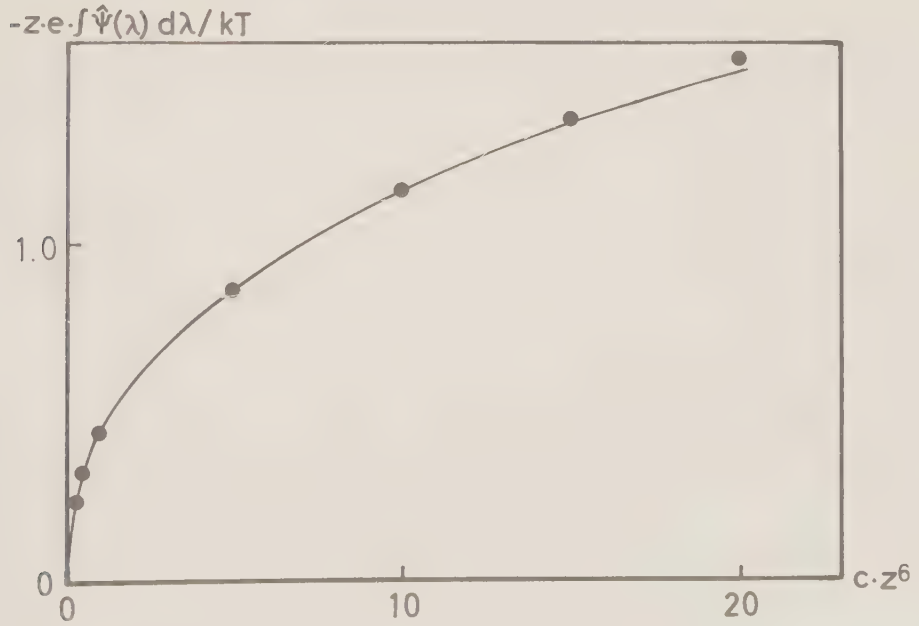

Figure A2. ● $= -z \cdot e \int_0^1 \hat{\Psi}_j(\lambda)\, d\lambda/kT$ as a function of $c \cdot z^6$.

From fig. A2 it is clear that the complicated equation A14 may, at T = 298 K, be approximated with the following equation

$$\frac{z_j \cdot e}{kT} \cdot \int_0^1 \hat{\Psi}_j(\lambda)\, d\lambda \simeq -0.44 \cdot (c_j \cdot z_j^6)^{0.42} \qquad \text{A22}$$

The free energy associated with the pair correlation has here only been calculated for the two cases low ion concentration and systems with only one kind of ions. For a concentrated salt-solution the approximation done in eq. (40) is no longer valid, but the potential from a charged surface is for these systems often very short-ranged and the electrostatic free energy can therefore as a crude approximation be written

$$A_{el} \simeq A_{el}^{o} + A_{el}^{salt} \qquad \text{A23}$$

where A_{el}^{o} is the electrostatic free energy calculated from the mean-potential $\langle \Psi(r) \rangle$ and A_{el}^{salt} is the electrostatic energy of an electrically neutral salt solution.

Appendix II

Calculus of variations.

The problem of minimizing an integral of the following form (A1) will in this appendix be discussed.

$$J = \int_V f(y(\vec{x}),\dot{x}) + K_1 \cdot y(\dot{x}) \int_V \frac{K_2 \cdot y(\vec{s})}{|\vec{x} - \vec{s}|} \, d\vec{s} \, d\dot{x} \qquad A1$$

where K_1 and K_2 are constants.

To be able to minimize J, a function $n(\vec{x})$ is introduced that is arbitrary except for the restriction that it must be differentiable and a scale factor α is also introduced. Then an arbitrary $y(\vec{x})$-function may be written

$$y(\vec{x},\alpha) = y(\vec{x},0) + \alpha \cdot n(\vec{x}) \qquad A2$$

where $y(\vec{x},0)$ is the unknown part that will minimize J.

$$J(\alpha) = \int_V f(y(\vec{x},\alpha),\vec{x}) \, d\vec{x} + K_1 \int_V \int_V \frac{K_2 \cdot y(\vec{x},\alpha) \cdot y(\vec{s},\alpha)}{|\vec{x} - \vec{s}|} \, d\vec{s} \, d\vec{x} \qquad A3$$

and the condition for an extreme value is

$$\left(\frac{\partial J(\alpha)}{\partial \alpha}\right)_{\alpha=0} = 0 \qquad A4$$

but

$$\frac{\partial J(\alpha)}{\partial \alpha} = \int_V \frac{\partial f}{\partial y} \cdot \frac{\partial y}{\partial \alpha} \, d\vec{x} + K_1 \int \int K_2 \frac{\frac{\partial y(\vec{x},\alpha)}{\partial \alpha} \cdot y(\vec{s},\alpha) + \frac{\partial y(\vec{s},\alpha)}{\partial \alpha} \cdot y(\vec{x},\alpha)}{|\vec{x} - \vec{s}|} \, d\vec{s} \, d\vec{x}$$

A5

From symmetry the second integral may be written

$$\int\int \frac{\frac{\partial y(\vec{x},\alpha)}{\partial\alpha} \cdot y(\vec{s},\alpha) + \frac{\partial y(\vec{s},\alpha)}{\partial\alpha} \cdot y(\vec{x},\alpha)}{|\vec{x} - \vec{s}|} \, d\vec{s} \, d\vec{x} =$$

$$= 2 \cdot \int \frac{\partial y(\vec{x},\alpha)}{\partial\alpha} \int \frac{y(\vec{s},\alpha)}{|\vec{x} - \vec{s}|} \, d\vec{s} \, d\vec{x} \qquad \text{A6}$$

and eq. A5 becomes

$$\frac{\partial J(\alpha)}{\partial\alpha} = \int_V \frac{\partial y}{\partial\alpha} \{\frac{\partial f}{\partial y} + 2 \cdot K_1 \int \frac{K_2 \cdot y(\vec{s},\alpha)}{|\vec{x} - \vec{s}|} \, d\vec{s}\} \, d\vec{x} \qquad \text{A7}$$

but from the definition of $n(\vec{x})$, (A2)

$$\partial y/\partial\alpha = n(\vec{x}) \qquad \text{A8}$$

equation A7 becomes

$$0 = (\frac{\partial J}{\partial\alpha})_{\alpha=0} = \int n(\vec{x}) \cdot \{\frac{\partial f}{\partial y} + 2 \cdot K_1 \int \frac{K_2 \cdot y(\vec{s},\alpha)}{|\vec{x} - \vec{s}|} \, d\vec{s}\} \, d\vec{x} \qquad \text{A9}$$

Since $n(\vec{x})$ is arbitrary the condition for the existence of an extreme, is satisfied only if the term in the bracket itself is zero. The condition for an extremum is thus

$$\frac{\partial f}{\partial y} + 2 \cdot K_1 \int \frac{K_2 \cdot y(\vec{s})}{|\vec{x} - \vec{s}|} \, d\vec{s} = 0 \qquad \text{A10}$$

The calculations may be generalized to a case where y is several dependent variables and where there are constraints appearing in the form of integrals (see ref. (52)).

$$\int_V y_i \, d\vec{x} = \text{constant} \qquad \text{A11}$$

Equation A10 then becomes

$$\frac{\partial f}{\partial y_i} + 2 \cdot K_i \sum_j \int \frac{K_j \cdot y_j(\vec{s})}{|\vec{x} - \vec{s}|} \, d\vec{s} + \lambda_i = 0 \qquad \text{A12}$$

where λ_i is a constant (Lagrangian multiplier, see ref. (52).

Appendix III

Energy calculations for normal systems.

The equations for A(R), $\partial R/\partial n_p$ and $\partial H/\partial n_p$ will be evaluated in this appendix and eq. (74) will also be converted to an equation only containing derivatives of the form $\partial n_i/\partial n_p$, $\partial n_a/\partial n_p$ or $\partial b/\partial n_p$, where b is defined by the location of the charged surface.

There are two possibilities to estimate A.

1. If the volume per monomer, defined by the volume inclosed by the charged surface divided by the number of molecules there, is independent of the aggregate geometry the area becomes

$$A = d \cdot n_a \cdot V_a / b \qquad A1$$

where V_a is the volume of the amphiphile molecule, see chapter 3.5.

2. To assume that the "hydrophobic" volume per monomer defined by the hydrocarbon volume V_a^- is independent of aggregate geometry. The area A is then a distance b_1, out from the hydrophobic surface. A then becomes

$$A = d \cdot n_a \cdot V_a^- \cdot (1 - b_1/b)^{-d}/b \qquad A2$$

$(1/H)\ (\partial H/\partial n_p)$ may now be calculated

$$\frac{1}{H} \cdot \frac{\partial H}{\partial n_p} = \frac{1}{n_a} \cdot \frac{\partial n_a}{\partial n_p} - \frac{d}{b - b_1} \cdot \frac{\partial b}{\partial n_p} \qquad A3$$

Equation (51) may together with eq. (52) be converted to

$$E_{el} - TS = \sum_i \int N_A \cdot \{kT \cdot c_i \cdot (\ln c_{i0} - 1) - \frac{1}{2} \cdot c_i \cdot z_i \cdot e(\Phi - \Phi_A)\} +$$

$$+ N_A \cdot f - N_A \cdot c_i \cdot \{ \frac{\partial f}{\partial c_i} - \frac{\partial f}{\partial c_i} (R) \} \, dV + A \cdot \sigma \cdot \Phi_A \qquad A4$$

and from this follows

$$E_{el} - TS + \sum_i \lambda_i \cdot n_i - A \cdot \sigma \cdot \Phi_A = - N_A \cdot \int (\sum_i \{kT \cdot c_i + \frac{1}{2} \cdot c_i \cdot z_i \cdot e(\Phi - \Phi_A) +$$

$$+ c_i \cdot \frac{\partial f}{\partial c_i} \} - f) \, dV \qquad \text{A5}$$

where eq. (52) has been used.

Combining equations (52), (73) and A5 gives

$$\frac{\partial}{\partial n_p}(E_{el} - TS) = A(R) \cdot \frac{\partial R}{\partial n_p} \cdot N_A \cdot \{ \sum_i (- kT \cdot c_{i0} - c_{i0} \cdot \frac{\partial f}{\partial c_i}(R)) + f(R)\} -$$

$$- A \cdot \frac{\partial b}{\partial n_p} \cdot N_A \cdot \{ \sum_i (- kT \cdot c_{ib} - c_{ib} \cdot \frac{\partial f}{\partial c_i}(b)) + f(b)\} -$$

$$- \frac{1}{H} \cdot \frac{\partial H}{\partial n_p} \cdot N_A \cdot \int \{ \sum_i (kT \cdot c_i + \frac{1}{2} \cdot c_i \cdot z_i \cdot e(\Phi - \Phi_A) + c_i \cdot \frac{\partial f}{\partial c_i}) - f\} \, dV +$$

$$+ \sum_i \frac{\partial n_i}{\partial n_p} \{kT \cdot \ln c_{i0} + \frac{\partial f}{\partial c_i}(c_{i0})\} + z_a \cdot e \cdot \Phi_A \cdot \frac{\partial n_a}{\partial n} - \frac{A \cdot \sigma^2}{2 \cdot \varepsilon_o \varepsilon_r} \cdot \frac{\partial b}{\partial n_p} \qquad \text{A6}$$

The equations for $A \cdot \partial R / \partial n_p$ may be obtained from the expression for the volume of the systems.

$$V_T = \sum_j n_j \cdot V_j = \frac{A(R) \cdot R}{d} \qquad \text{A7}$$

where the summation is over all species. Derivation of A7 gives

$$A(R) \cdot \frac{\partial R}{\partial n_p} = V_T \cdot d \cdot \frac{\partial \ln R}{\partial n_p} \qquad \text{A8}$$

but

$$\frac{n_a \cdot V_a^-}{V_T} = \left(\frac{b - b_1}{R} \right)^d \qquad \text{A9}$$

and the equation for $A(R) \cdot \partial R/\partial n_p$ becomes

$$A(R) \cdot \frac{\partial R}{\partial n_p} = \frac{A \cdot R^d}{(b - b_1) \cdot b^{d-1}} \cdot \frac{\partial b}{\partial n_p} + \sum_i \frac{\partial n_i}{\partial n_p} \cdot V_i - \frac{\partial n_a}{\partial n_p} \cdot V_-^- \cdot$$

$$\cdot \left\{ \left(\frac{R}{b - b_1} \right)^d - V_-/V_-^- \right\} \qquad \text{A10}$$

Equation A6 may now be written

$$\frac{\partial}{\partial n_p}(E_{el} - TS) = \sum_i \frac{\partial n_i}{\partial n_p} \cdot \{kT \cdot \ln c_{i0} - N_A \cdot V_i \cdot \sum_j (kT \cdot c_{j0} + c_{j0} \cdot \frac{\partial f}{\partial c_j}(R)) +$$

$$+ N_A \cdot V_i \cdot f(R) + \frac{\partial f}{\partial c_i}(R) \} + \frac{\partial n_a}{\partial n_p} \cdot \left[z_a \cdot e \cdot \Phi_A - \frac{1}{n_a} \cdot N_A \cdot \int \{ \sum_i (kT \cdot c_i + \right.$$

$$+ \frac{1}{2} \cdot c_i \cdot z_i \cdot e \cdot (\Phi - \Phi_A) + c_i \cdot \frac{\partial f}{\partial c_i}) - f \} \, dV + V_a^- \cdot \{ \left(\frac{R}{b - b_1} \right)^d - \frac{V_a}{V_a^-} \} \cdot N_A \cdot$$

$$\left. \cdot (kT \cdot \sum_j c_{j0} - f(R) + \sum_j c_{j0} \cdot \frac{\partial f}{\partial c_j}(c_{j0}) \right] + \frac{\partial b}{\partial n_p} \cdot \{ \frac{d}{b - b_1} \cdot (kT \sum_j n_j +$$

$$+ N_A \cdot \int \{ \sum_j (\frac{1}{2} \cdot c_j \cdot z_j \cdot e \cdot (\Phi - \Phi_A) + c_j \cdot \frac{\partial f}{\partial c_j}) - f \} \, dV) + \frac{A \cdot N_A \cdot R^d}{(b - b_1) \cdot b^{d-1}} \cdot$$

$$\cdot (- \sum_j kT \cdot c_{j0} + f(R) - \sum_j c_{j0} \cdot \frac{\partial f}{\partial c_j}(R)) - A \cdot N_A \cdot (- \sum_j kT \cdot c_{jb} + f(b) -$$

$$- \sum_j c_{jb} \cdot \frac{\partial f}{\partial c_j}(b)) - \frac{A \cdot \sigma^2}{2 \cdot \varepsilon_o \varepsilon_r} \} \qquad \text{A11}$$

This involved equation may be simplified by introducing

$$U(r) = N_A \cdot (\sum_j kT \cdot c_j - f + \sum_j c_j \cdot \frac{\partial f}{\partial c_j}) \qquad \text{A12}$$

$$\frac{\partial}{\partial n_p}(E_{el} - TS) = \sum_i \frac{\partial n_i}{\partial n_p} \cdot \{kT \cdot \ln c_{i0} + \frac{\partial f}{\partial c_i}(R) - V_i \cdot U(R)\} +$$

$$+ \frac{\partial n_a}{\partial n_p} \cdot \{z_a \cdot e \cdot \Phi_A - \frac{1}{n_a} \cdot \int (\frac{1}{2} \cdot N_A \cdot \sum_i c_i \cdot z_i \cdot e \cdot (\Phi - \Phi_A) + U(r)) \, dV +$$

$$+ V_a' \cdot \{(\frac{R}{b - b_1})^d - \frac{V_a}{V_a'}\} \cdot U(R) \} + \frac{\partial b}{\partial n_p} \cdot \{ \frac{d}{b - b_1} \cdot$$

$$\cdot \int (\frac{1}{2} \cdot N_A \cdot \sum_i c_i \cdot z_i \cdot e \cdot (\Phi - \Phi_A) + U(r)) \, dV - \frac{A \cdot b \cdot R^d}{(b - b_1) \cdot b^d} \cdot U(R) +$$

$$+ A \cdot U(b) - \frac{A \cdot \sigma^2}{2 \cdot \varepsilon_o \varepsilon_r} \} \qquad \text{A13}$$

The expression in the last bracket may be reduced because

$$N_A \cdot kT \cdot \int \{r^d \cdot \frac{\partial(\Sigma c_i)}{\partial r}\} \, dr = N_A \cdot kT \cdot \left[r^d \cdot \Sigma c_i \right]_b^R - d \cdot kT \cdot b^{d-1} \cdot \frac{1}{A} \cdot \Sigma n_i \qquad \text{A14}$$

but from eq. (53)

$$c_i = c_{i0} \cdot \exp(- z_i \cdot e \cdot \Phi / kT) \cdot \exp(- \{\frac{\partial f}{\partial c_i} - \frac{\partial f}{\partial c_i}(c_{i0})\}/kT) \qquad (53)$$

The left part of A14 becomes

$$N_A \cdot kT \cdot \int \{r^d \cdot \frac{\partial(\Sigma c_i)}{\partial r}\} \, dr = - N_A \cdot \sum_i z_i \cdot e \cdot \int \{r^d \cdot c_i \cdot \frac{\partial \Phi}{\partial r}\} \, dr -$$

$$- N_A \cdot \sum_i \int \{r^d \cdot c_i \cdot \frac{\partial}{\partial r}(\frac{\partial f}{\partial c_i})\} \, dr \qquad \text{A15}$$

but from the Poissons equation

$$N_A \cdot \Sigma\, c_i \cdot z_i \cdot e = - \varepsilon_o \varepsilon_r \cdot \nabla^2 \cdot \Phi = - \frac{\sigma \cdot r}{r^{d-1}} \cdot \frac{d}{dr}\left(r^{d-1} \cdot \frac{d\Phi}{dr}\right) \qquad A16$$

The first part on the right in eq. A16 becomes

$$- N_A \cdot \sum_i z_i \cdot e \int \{ r^d \cdot c_i \cdot \frac{\partial \Phi}{\partial r} \}\, dr = - \frac{(2-d) \cdot b^{d-1}}{A} \cdot \int \{ \frac{1}{2} \cdot N_A \cdot \sum_i c_i \cdot z_i \cdot e \cdot$$

$$\cdot (\Phi - \Phi_A) \}\, dV - \sigma^2 \cdot b^d / (2 \cdot \varepsilon_o \varepsilon_r) \qquad A17$$

and together with the connection

$$\sum_i \frac{\partial}{\partial r}\left(\frac{\partial f}{\partial c_i}\right) \cdot c_i = \sum_i \frac{\partial}{\partial r}\left(c_i \frac{\partial f}{\partial c_i}\right) - \frac{\partial f}{\partial r} \qquad A18$$

The following equation may be obtained

$$\frac{b^{d-1}}{A} \cdot \int \{(2-d) \cdot \frac{1}{2} \cdot N_A \cdot \sum_i c_i \cdot z_i \cdot e \cdot (\Phi - \Phi_A) - d \cdot U(r)\}\, dV + \frac{\sigma^2 \cdot b^d}{2 \cdot \varepsilon_o \varepsilon_r} =$$

$$= b^d \cdot U(b) - R^d \cdot U(R) \qquad A19$$

and eq. A14 becomes

$$\frac{\partial}{\partial n_p}(E_{el} - TS) = \sum_i \frac{\partial n_i}{\partial n_p}\{kT \cdot \ln c_{iO} + \frac{\partial f}{\partial c_i}(R) - V_i \cdot U(R)\} + \frac{\partial n_a}{\partial n_p}\{z_a \cdot e \cdot \Phi_A -$$

$$- \frac{1}{n_a} \cdot (E^o_{el} + \int U(r)\, dV) + V_a' \cdot \{\left(\frac{R}{b-b_1}\right)^d - \frac{V_a}{V_a'}\} \cdot U(R)\} + \frac{\partial b}{\partial n_p} \cdot \frac{A}{b} \cdot \{2 \cdot E^o_{el}/A +$$

$$+ \frac{d \cdot b_1}{b-b_1} \{E^o_{el}/A + \frac{1}{A} \int U(r)\, dV - \frac{b}{d} \cdot \frac{R^d}{b^d} \cdot U(R)\} \} \qquad A20$$

where

$$\int \frac{1}{2} \cdot N_A \cdot e \cdot \sum_i z_i \cdot c_i \cdot (\Phi - \Phi_A)\, dV = E_{el}^{o} \qquad \text{A21}$$

Appendix IV

The solution to the Poisson-Boltzmann equation for a system with cylindrical symmetry and no salt present.

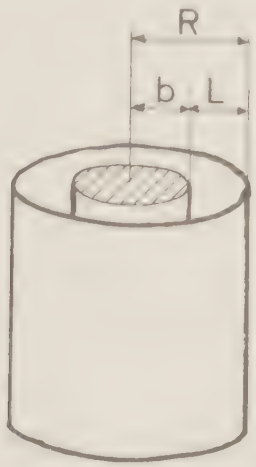

Figure A1. Schematic representation of a cylindrical subsystem. The radius of the amphiphilic aggregate is b and the radius of the subsystem is R.

The PB-equation becomes for this type of system

$$\frac{1}{r}\frac{d}{dr}\left(r\,\frac{d\Phi}{dr}\right) = -\,c_{io}\,\frac{N_A \cdot z_i \cdot e}{\varepsilon_o \varepsilon_r} \cdot \exp(-\,z_i \cdot e \cdot \Phi/kT) \qquad A1$$

with the boundary conditions

$$\Phi(R) = \frac{d\Phi}{dr}(R) = 0 \qquad A2$$

and

$$\frac{d\Phi}{dr}(b) = -\,\frac{\sigma}{\varepsilon_o \varepsilon_r} \qquad A3$$

A solution to eq. A1 is

$$\exp(z_i \cdot e \cdot \Phi/kT) = R^2 \cdot \alpha / \{r^2 \cdot \cos^2(s \cdot \ln(r/R) + \beta)\} \qquad A4$$

where α, β and s are constants to be determined from the boundary conditions A2 and A3.

A4 and A2 gives

$$\cos^2(\beta) = \alpha \qquad \text{A5}$$

and

$$s \cdot \tan(\beta) = 1 \qquad \text{A6}$$

The equation for c_{i0} may be obtained from equations A1 and A4

$$c_{i0} = \frac{2 \cdot kT \cdot \varepsilon_o \varepsilon_r}{N_A \cdot z_i^2 \cdot e^2} \cdot (1 + s^2) \cdot \frac{1}{R^2} \qquad \text{A7}$$

The boundary condition A3 is fulfilled if

$$s \cdot \tan(s \cdot \ln(R/b)) - \beta) = - \frac{\sigma \cdot z_i \cdot e \cdot b}{2 \cdot kT \cdot \varepsilon_o \varepsilon_r} - 1 \qquad \text{A8}$$

But since $s \cdot \tan(\beta) = 1$, eq. A8 becomes

$$\{s + \frac{1}{s} (\frac{\sigma \cdot z_i \cdot e \cdot b}{2 \cdot kT \cdot \varepsilon_o \varepsilon_r} + 1)\} \cdot \tan(s \cdot \ln(R/b)) = - \frac{\sigma \cdot z_i \cdot e \cdot b}{2 \cdot kT \cdot \varepsilon_o \varepsilon_r} \qquad \text{A9}$$

It is also possible to rewrite A4 to only depend on r, R and s.

$$\exp(- z_i \cdot e \cdot \Phi / kT) = (r^2/R^2) \cdot \{\cos(s \cdot \ln(r/R)) - \frac{1}{s} \sin(s \cdot \ln(r/R))\}^2 \qquad \text{A10}$$

From eq. A7 it can be seen that s for some values of $c_{io} \cdot R^2$ must be complex. The condition that determines if s is complex or not is obtained from A9. s is complex if

$$- \sigma \cdot e \cdot z_i \cdot b / \{2 \cdot kT \cdot \varepsilon_o \varepsilon_r\} < \{\ln(R/b)\} / \{1 + \ln(R/b)\} \qquad \text{A11}$$

It is most easy to calculate E_{el} for this type of system if using eq. A12.

$$E_{el} = \frac{1}{2} \cdot \varepsilon_o \varepsilon_r \int (\nabla\Phi)^2 \, dV \qquad \text{A12}$$

The derivative of Φ from eq. A10 may be used and the equation for E_{el} becomes

$$E_{el}/A = kT \cdot \{ - \frac{\sigma}{z_i \cdot e} - N_A \cdot \frac{R^2}{b} \cdot c_{i0} \cdot \ln(R/b) + \frac{2 \cdot \varepsilon_o \varepsilon_r}{z_i \cdot e \cdot b} \cdot \Phi_A \} \qquad \text{A13}$$

where Φ_A according to eq. A4 is

$$\Phi_A = \frac{kT}{z_i \cdot e} \cdot \ln\{(\frac{R}{b})^2 + \frac{\sigma \cdot (\sigma \cdot z_i \cdot e \cdot b + 4 \cdot kT \cdot \varepsilon_o \varepsilon_r)}{2 \cdot kT \cdot \varepsilon_o \varepsilon_r \cdot z_i \cdot e \cdot b \cdot N_A \cdot c_{i0}} \} \qquad \text{A14}$$

Appendix V

Energy calculations for reversed systems.

The surface area A(L) and the derivative $\partial H/\partial n_p$ will in this appendix be estimated for the reversed systems in the same manner as corresponding values where estimated in appendix III for normal systems.

If the "hydrophobic" volume per monomer defined by the hydrocarbon volume V_a^- as in appendix III is independent of aggregate geometry, the area A(L) is located a distance b_1 out in the water part. From this definition A(L) becomes

$$A(L) = \frac{d}{L} \cdot (1 + b_1/L)^{-d} \cdot V_{aq} \qquad A1$$

where the summation is over all components in the water part and

$$V_{aq} = \sum_i n_i \cdot V_i + n_a \cdot (V_a - V_a^-) \qquad A2$$

$(1/H)\cdot(\partial H/\partial n_p)$ may then be written

$$\frac{1}{H}\frac{\partial H}{\partial n_p} = -\frac{d}{L + b_1} \cdot \frac{dL}{dn_p} + \frac{d}{A\cdot L}\cdot\left(\frac{L}{L + b_1}\right)^d \cdot \frac{d}{dn_p}\{\sum n_i V_i + n_a(V_a - V_a^-)\} \qquad A3$$

and eq. (73) becomes

$$\frac{\partial}{\partial n_p}(E_{el}-TS) = A\cdot N_A \cdot \frac{dL}{dn_p}\cdot\{\sum_j (kT\cdot c_{jL}\cdot(\ln c_{jL} - 1) + \lambda_j \cdot c_{jL}) + f(L)\} -$$

$$- \{\frac{d}{L+b_1}\frac{dL}{dn_p} - \frac{d}{A\cdot L}\cdot\left(\frac{L}{L+b_1}\right)^d \cdot \frac{d}{dn_p}(\sum n_i\cdot V_i + n_a\cdot(V_a - V_a^-))\} \cdot$$

$$\cdot (E_{el} - TS + \sum \lambda_i \cdot n_i) - \sum \lambda_i \frac{dn_i}{dn_p} + \frac{A\cdot\sigma^2}{2\cdot\varepsilon_o\varepsilon_r} \cdot \frac{dL}{dn_p} \qquad A4$$

But according to eq. (52)

$$\lambda_i = - kT \cdot \ln c_{iL} - \frac{\partial f}{\partial c_i}(L) \qquad \text{A5}$$

where $\Phi(L)$ has been assumed equal to zero.

Equation A4 may together with A5 and equation A6 in appendix III be converted to

$$\frac{\partial}{\partial n_p}(E_{el}-TS) = A \cdot N_A \cdot \frac{dL}{dn_p} \{\sum_j (- c_{jL} - c_{jL} \frac{\partial f}{\partial c_j}(L)) + f(L)\} + \{ \frac{d}{L+b_1} \frac{dL}{dn_p} -$$

$$- \frac{d}{A \cdot L} \cdot (\frac{L}{L+b_1})^d \cdot \frac{d}{dn_p}(\sum n_j \cdot V_j + n_a \cdot (V_a - V_a')) \} \cdot N_A \cdot \int \{\sum_j (kT \cdot c_j +$$

$$+ \frac{1}{2} c_j \cdot z_j \cdot e \cdot \Phi + c_j \frac{\partial f}{\partial c_j}) - f\} \, dV + \sum_j \frac{\partial n_i}{\partial n_p} \{kT \cdot \ln c_{iL} + \frac{\partial f}{\partial c_i}(L)\} +$$

$$+ \frac{A \cdot \sigma^2}{2 \cdot \varepsilon_o \varepsilon_r} \cdot \frac{dL}{dn_p} \qquad \text{A6}$$

Introducing U(r) according to A13 in appendix III gives

$$\frac{\partial}{\partial n_p}(E_{el}-TS) = \sum_i \frac{\partial n_i}{\partial n_p} \cdot \{kT \cdot \ln c_{iL} + \frac{\partial f}{\partial c_i}(L) - \frac{V_i}{V_{aq}} \cdot (E_{el}^o + \int U(r) \, dV)\} -$$

$$- \frac{V_a - V_a'}{V_{aq}} \cdot \frac{\partial n_a}{\partial n_p} \cdot (E_{el}^o + \int U(r) \, dV) + A \frac{dL}{dn_p} \{- U(L) + \frac{d}{L+b_1} \cdot \frac{1}{A} \cdot$$

$$\cdot (E_{el}^o + \int U(r) \, dV) + \frac{\sigma^2}{2 \cdot \varepsilon_o \varepsilon_r}\} \qquad \text{A7}$$

From the modified Poisson-Boltzmann equation the following equation may be obtained (concerning the calculations, see appendix III).

$$- \frac{L^{d-1}}{A} \cdot \{(2-d) \cdot E_{el}^{o} - d \cdot \int U(r)\, dV\} + \frac{\sigma^2 \cdot L^d}{2 \cdot \varepsilon_o \varepsilon_r} = L^d \cdot U(L) \qquad A8$$

and eq. A7 becomes

$$\frac{\partial}{\partial n_p}(E_{el} - TS) = \sum_i \frac{\partial n_i}{\partial n_p} \cdot \{kT \cdot \ln c_{iL} + \frac{\partial f}{\partial c_i}(L) - \frac{V_i}{V_{aq}} \cdot (E_{el}^{o} + \int U(r)\, dV)\} -$$

$$- \frac{\partial n_a}{\partial n_p} \cdot \frac{V_a - V_a'}{V_{aq}} \cdot (E_{el}^{o} + \int U(r)\, dV) + \frac{A}{L} \cdot \frac{dL}{dn_p} \cdot \{2 \cdot E_{el}^{o}/A -$$

$$- \frac{b_1 \cdot d}{L + b_1} \cdot (E_{el}^{o}/A + \frac{1}{A} \cdot \int U(r)\, dV)\} \qquad A9$$

The derivative $(A/L) \cdot (dl/dn_p)$ may if $d \cdot b_1 << L$ be written as

$$\frac{A}{L} \cdot \frac{dL}{dn_p} = \frac{d}{L} \cdot \frac{dV_{aq}}{dn_p} - (1 + \frac{b_1 \cdot d}{L + b_1}) \cdot \frac{dA}{dn_p} \qquad A10$$

If the area A is divided into two parts

$$A = n_a \cdot A_{a,min} + A' \qquad A11$$

where $A_{a,min}$ is the minimum area of the amphiphilic molecule a, eq. A10 may be written

$$\frac{A}{L} \cdot \frac{dL}{dn_p} = \frac{d}{L} \cdot \sum \frac{dn_i}{dn_p} \cdot V_i + \frac{dn_a}{dn_p} \cdot \{\frac{d}{L} \cdot (V_a - V_a') - (1 + \frac{b_1 \cdot d}{L + b_1}) \cdot$$

$$\cdot A_{a,min}\} - (1 + \frac{b_1 \cdot d}{L + b_1}) \cdot \frac{dA'}{dn_p} \qquad A12$$

and eq. A9 becomes

$$\frac{\partial}{\partial n_p}(E_{el}-TS) = \Sigma \frac{dn_i}{dn_p} \cdot \{kT \cdot \ln c_{iL} + \frac{\partial f}{\partial c_i}(L) - \frac{V_i}{V_{aq}} \cdot (E^o_{el} + \int U(r)\, dV) +$$

$$+ \frac{d}{L} \cdot V_i \cdot (2 \cdot E^o_{el}/A - \frac{b_1 \cdot d}{L + b_1} \cdot (E^o_{el}/A + \frac{1}{A} \cdot \int U(r)\, dV))\} -$$

$$- \frac{\partial n_a}{\partial n_p} \cdot \{ \frac{V_a - V_a'}{V_{aq}} \cdot (E^o_{el} + \int U(r)\, dV) - (\frac{d}{L} \cdot (V_a - V_a') -$$

$$- (1 + \frac{b_1 \cdot d}{L + b_1}) \cdot A_{a,min}) \cdot (2 \cdot E^o_{el}/A - \frac{b_1 \cdot d}{L + b_1} \cdot (E^o_{el}/A +$$

$$+ \frac{1}{A} \cdot \int U(r)\, dV))\} - (1 + \frac{b_1 \cdot d}{L + b_1}) \cdot \frac{dA'}{dn_p} \cdot \{2 \cdot E^o_{el}/A -$$

$$- \frac{b_1 \cdot d}{L + b_1} \cdot (E^o_{el}/A + \frac{1}{A} \cdot \int U(r)\, dV)\} \qquad \text{A13}$$

Appendix VI

The solution to the Poisson-Boltzmann equation for the reversed cylindrical system, when no salt is present.

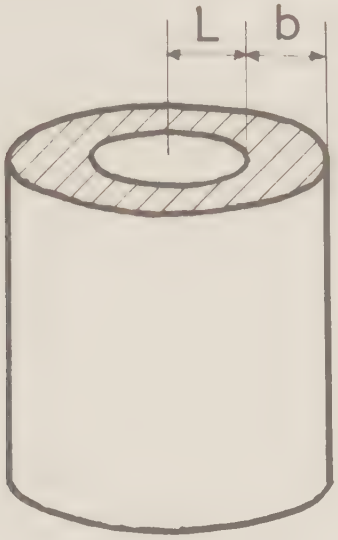

Figure A1. The reversed cylindrical system.

The PB-equation becomes for this type of system

$$\frac{1}{r}\frac{d}{dr}\left(r\,\frac{d\Phi}{dr}\right) = -\frac{N_A \cdot c_{i0} \cdot z_i \cdot e}{\varepsilon_o \varepsilon_r} \cdot \exp(-z_i \cdot e \cdot \Phi/kT) \qquad A1$$

with the boundary conditions

$$\Phi(L) = \frac{d\Phi}{dr}(0) = 0 \qquad A2$$

and

$$\frac{d\Phi}{dr}(L) = \frac{\sigma}{\varepsilon_o \varepsilon_r} \qquad A3$$

A solution to eq. A1 is

$$\exp(z_i \cdot e \cdot \Phi/kT) = (\alpha + \beta \cdot r^2)^2 \qquad A4$$

where α and β are constants, to be determined from eq. A2 and A3. The form of eq. A4 always gives $d\Phi(0)/dr = 0$, therefore only two constants α and β have to be determined.

The boundary condition $\Phi(L) = 0$ gives

$$1 = \alpha + \beta \cdot L^2 \qquad A5$$

and from eq. A3

$$\beta = \sigma \cdot z \cdot e/\{4 \cdot L \cdot \varepsilon_o \varepsilon_r \cdot kT\} \qquad A6$$

The potential becomes

$$\Phi(r) = \frac{2 \cdot kT}{z_i \cdot e} \cdot \ln(1 - \sigma \cdot z_i \cdot e \cdot b/\{4 \cdot \varepsilon_o \varepsilon_r \cdot kT\} \cdot \{1 - r^2/L^2\}) \qquad A7$$

The equation for c_{iL} may be obtained from A1 and A7.

$$c_{iL} = - \frac{2 \cdot \sigma}{N_A \cdot z_i \cdot e \cdot L} \cdot (1 - \sigma \cdot z_i \cdot e \cdot L/\{4 \cdot \varepsilon_o \varepsilon_r \cdot kT\}) \qquad A8$$

and E_{el}/A becomes

$$E_{el}/A = \frac{kT}{z_i \cdot e} \cdot \{- \sigma - \frac{4 \cdot \varepsilon_o \varepsilon_r \cdot kT}{z_i \cdot e \cdot L} \cdot \ln(1 - \sigma \cdot z_i \cdot e \cdot L/\{4 \cdot \varepsilon_o \varepsilon_r \cdot kT\})\} \qquad A9$$